UNIVERSITÉ DU QUÉBEC À MONTRÉAL

FACTEURS DÉVELOPPEMENTAUX ET DE L'ENVIRONNEMENT DÉTERMINANT L'ANATOMIE ET LES VARIATIONS DE DENSITÉ DU BOIS D'ÉPINETTE NOIRE À L'ÉCHELLE INTRA-ANNUELLE

THÈSE
PRÉSENTÉE
COMME EXIGENCE PARTIELLE
DU DOCTORAT EN SCIENCES DE L'ENVIRONNEMENT EXTENSIONNÉ DE
L'UNIVERSITÉ DU QUÉBEC À CHICOUTIMI

PAR
VALENTINA BUTTÓ

FÉVRIER 2021

REMERCIEMENTS

Je n’ai pas assez des mots pour remercier mon directeur, Hubert, et mes co-directeurs, Annie et Sergio, pour m’avoir appris tout ce que je sais aujourd'hui sur le plus beau métier de l’univers (pas seulement du monde!), le scientifique! Ils ont été des modèles à suivre, chacun avec sa personnalité et ses particularités uniques et indispensables pour ma formation comme chercheuse, mais aussi pour ma croissance personnelle. J’espère qu’ils vont continuer à me partager leur savoir, car il y a encore de nombreuses questions qui attendent d’être posées et de choses que je ne sais pas encore. Un gros merci à tous ces qui ont travaillé sur la base de données du gradient, une très précieuse source d’information qui a été nourrie par beaucoup de braves chercheurs, techniciens et étudiants au cours des ans et qui m’ont permis de réaliser cette thèse du doctorat.

Je voudrais également remercier toutes les collègues et les professeurs du laboratoire, qui ont contribué à construire un environnement agréable dans lequel il a été très plaisant travailler. Je remercie les amis qui ont partagé ma quotidienneté au travers d’activités de loisir mais aussi de partages, et qui m’ont permis de vivre de très beaux moments au-delà de l’environnement de travail.

I had the chance to have two committee members in my project thesis, Philippe and Vlad, who gave me the opportunity to visit their labs, stay in their countries and work with them on two beautiful manuscripts. They fed me with food (my Sicilian legacy accords to this aspect the highest value), new ideas and interesting conversations. I borrowed their expertise, their students, and their technicians, who are also in my thoughts while I am writing: I always felt welcome and I am extremely grateful for the experiences that we shared.

In questi quattro anni ho avuto la fortuna di poter costruire una vita che sono contenta di vivere. Questo é stato possibile, e lo é ancora, grazie alle persone che ho incontrato ma anche a quelle che erano giá nella mia vita e che non mi hanno mai abbandonata qualunque decisione io abbia preso. Grazie a mia madre, mio padre, mio fratello ed alla mia famiglia, affetti lontani ma sempre nel mio cuore, ed agli amici che mi hanno sempre fatta sentire come se non fossi mai andata via.

Je voudrais remercier mon conjoint, Maxence, qui a toujours été à mes côtés avec une patience infinie. Apparemment, il y a des rumeurs sur sa béatification imminente. Merci à mon petit chat, Errol, qui a été avec moi tout le long de mon doctorat. Il y a un beau cheval qui m’a accompagné lui aussi pendant ses années: merci à Tango et aux

propriétaires du centre équestre Élysée, où j’ai appris plen de choses sur les cheveaux, mais aussi que le dressage, ce n’est pas plate! Très clairement, merci à Cassy de m’avoir ramenée avec elle à son écurie, en partageant avec moi cette petite île de bonheur.

Un gros merci à tous.

DÉDICACE

“Qui se sait profond, s'efforce à la clarté : qui veut paraître profond aux yeux de la foule, s'efforce à l'obscurité. Car la foule tient pour profond tout ce dont elle ne peut voir le fond : elle a si peur de se noyer.”

— Friedrich Nietzsche, Le Gai Savoir

AVANT-PROPOS

Les modèles climatiques ont prévu un réchauffement de l'hémisphère Nord qui modifiera probablement l'aire de répartition des espèces boréales et influencera leur mortalité. Plongé dans cet environnement en constante évolution, les arbres offrent des informations très précieuses, gravées dans leurs cernes de croissance. En effet, depuis des décennies, les cernes annuels ont été utilisés pour étudier les fluctuations climatiques sur une large échelle temporelle. Néanmoins, les processus menant à la formation des cernes annuels et à la variation de leurs caractéristiques pendant la saison de croissance sont encore mal connus. Ce manque de connaissance limite fortement le pouvoir prédictif des modèles de flux de carbone. De la même façon, cela restreint notre compréhension des mécanismes menant à la formation d'une ressource primaire telle que le bois, dont la densité, un important indicateur de la séquestration de carbone chez les arbres, varie au cours de la saison de croissance.

Cette thèse a comme objectif d'acquérir une compréhension générale de la manière dont le climat et la dynamique de croissance des arbres influencent les traits cellulaires (lumen et épaisseur de paroi) et déterminent la variation de la densité du bois le long du cerne de croissance. Pour ce faire, l'épinette noire a été sélectionnée comme espèce modèle, étant donnée sa dominance dans la forêt boréale canadienne et son importance pour l'industrie forestière.

TABLE DES MATIÈRES

LISTE DES FIGURES

LISTE DES TABLEAUX

RÉSUMÉ

La croissance radiale est le processus permettant aux arbres de constituer du bois, ressource renouvelable par excellence, et qui assure par conséquent l'un des services de séquestration du carbone les plus efficaces sur Terre. Dans les biomes tempérés et boréaux, la croissance radiale se produit périodiquement. Cette alternance des périodes d'activité et de dormance donne lieu aux cernes annuels de croissance, dont les caractéristiques sont le résultat de l'interaction entre les facteurs climatiques et les facteurs endogènes qui agissent pendant la vie d'un arbre. Parmi ces facteurs endogènes, le développement des plantes, qui intègre des facteurs génétiques et des pressions sélectives des facteurs climatiques sur le long terme, peut être surveillé grâce à l'étude de la temporalité des événements saisonniers représentés par la phénologie. Dans cette perspective, le suivi de la phénologie des bourgeons et du bois fourni des informations importantes sur la croissance des cernes annuels ainsi que sur l'influence des facteurs de développement et climatiques sur les caractéristiques du xylème, notamment sa densité. Cette thèse a pour but de démêler les composantes développementales et climatiques expliquant les variations de densité le long du cerne. Elle étudiera notamment comment la dynamique de la formation du bois et les facteurs environnementaux affectent l'anatomie cellulaire, représentée par la taille des traits cellulaires, c'est-à-dire le lumen de la cellule et l'épaisseur de la paroi cellulaire. Ensuite, ces information seront utilisées pour tester un model mécaniste largement utilisé pour modéliser la croissance de cernes et les dynamiques saisonnières de la croissance du bois, le modèle de Vaganov-Shashkin.

Pour cette étude, nous avons sélectionné cinq peuplements d'épinettes noires, l'espèce dominante de la forêt boréale canadienne, situés sur un gradient latitudinal. Sur ces sites, la xylogenèse a été suivie sur 10 individus par site pendant 15 ans (2002-2016). À l'été 2017, des échantillons de bois ont été prélevés pour mesurer les traits cellulaires et la micro-densité. Dans chacun des sites, les variations des facteurs environnementaux ont été enregistrées par des stations météorologiques in situ. Sur les cinq peuplements, un protocole existant basé sur des indices de télédétection calibrés avec des observations de terrain a été utilisé pour extrapoler la phénologie des bourgeons à partir de l'indice différentiel normalisé de végétation (NDVI de l'anglais normalized difference vegetation index). Pour l'application modèle de Vaganov-Shashkin, la largeur des cernes a été mesuré et le modèle a été calibré pour la période 2002-2016. La validation du modèle a été réalisé à travers la comparaison entre les

prédictions du modelés (croissance interannuelle et dynamiques de formation de la cerne) et les observations obtenues par le monitorage de xylogenèse.

Nos résultats démontrent que le carbone alloué dans les tissus ligneux est indirectement mais étroitement lié à la dynamique de formation du bois, qui englobe les signaux de croissance à court et à long terme. Cette stratégie conservatrice, explique la très large aire de distribution de l'épinette noire. Les effets des facteurs environnementaux sur l'anatomie et la micro-densité cellulaires ne sont pas additifs, ce qui soutient l'hypothèse selon laquelle la densité du bois et l'anatomie cellulaire présentent différents patrons de corrélations écologiques. L'action contrebalancée des différents facteurs environnementaux explique comment une micro-densité similaire peut être atteinte avec un rapport paroi/lumen différent. Nous avons observé que dans tous les sites, la dynamique de la formation du bois s'est ajustée autour d'une température moyenne de ~14 °C, ce qui suggère des réponses convergentes autours variations de température pendant la différenciation cellulaire. L'anatomie cellulaire, et indirectement la micro-densité, ont été modulées par la durée des différentes étapes de la différenciation cellulaire, qui ont été elles-mêmes influencées par la phénologie des bourgeons. En effet, nous avons observé que la formation du bois final se produit après la fin de l'élongation des jeunes pousses, ce qui suggère que les arbres font face à la forte demande de sucres dans les principaux tissus séquestrant du carbone, c'est-à-dire le bourgeon et le bois, en séparant ces processus dans deux moments différents de la saison de croissance. Alors que l'élongation des pousses est en cours, la disponibilité des sucres pour la croissance secondaire est limitée. En conséquence, les cellules passeraient proportionnellement plus de temps à s'élargir qu'à déposer leur paroi secondaire, ce qui donnerait lieu à des cellules de bois initial présentant un diamètre de lumen important mais une paroi secondaire mince. Une fois que l'élongation des pousses est atteinte, les sucres seront massivement utilisés pour la formation du bois final, ce qui permettra une plus longue durée de dépôt de la paroi secondaire. La proportion croissante de sucres disponibles à ce stade permet le développement de parois cellulaires plus épaisses, dont la rigidité limitera la durée de l'allongement des cellules du xylème, ce qui se traduira par des cellules plus petites. L'interaction des phases de différenciation sur chaque trait cellulaire, et leur dépendance susmentionnée par rapport aux autres événements survenant au cours de la croissance primaire, sont probablement à l'origine de la relation non linéaire que nous avons détectée entre la taille des traits cellulaires et leur durée de différenciation. Nous avons en effet observé que la taille des caractères cellulaires, c'est-à-dire le diamètre des cellules et l'épaisseur de la paroi cellulaire, augmentait proportionnellement à la durée de leurs phases de différenciation, c'est-à-dire la durée de l'élargissement, du dépôt de la paroi secondaire et de la lignification, jusqu'à ce qu'ils atteignent un plateau.

La croissance interannuelle simulée avec le modèle de Vaganov-Shashkin était très corrélée avec celle qui a été observée dans les cinq sites, mais le modèle s’est avéré

peu adapté à modéliser les dynamiques des croissances intra-annuelle de nos sites, en étant donné que sa paramétrisation a été originairement basé sur de sites froids mais sèches. Cependant, une meilleure adaptation du modèle de Vaganov-Shashkin comme modèle prédictif des dynamiques de croissance intra-annuelle de l'épinette noire serait souhaitable afin d'extrapoler des informations sur des zones plus difficiles à échantillonner et sur la réponse de l'épinette noire aux changement climatiques.

Ces résultats couvrent d'importantes lacunes quant à nos connaissances sur les relations de cause à effet qui sous-tendent les variations de micro-densité chez les conifères. Nous avons démontré que les réponses à court terme aux variations environnementales peuvent être remplacées par des réponses plastiques qui modulent la différenciation cellulaire, ce qui indique que la dynamique de formation du bois est un puissant prédicteur de l'allocation de carbone dans les arbres. De plus, en fournissant des informations basées sur un suivi exceptionnellement long de la xylogenèse, ces résultats constituent une contribution précieuse pour augmenter les performances des modèles mécanistes existants en termes de temps de croissance des arbres et en termes de biomasse produite par l'épinette noire.

Mots clés : *Picea mariana* (Mill.) B.S.P., croissance secondaire, differéntiation cellulaire, déposition de paroi secondaire et lignification, micro-densité , modèle de Vaganov-Shashkin

ABSTRACT

Radial tree-growth is the process whereby trees build new wood, one of the most important renewable resource, which ensures efficient carbon sequestration services on Earth. In temperate and boreal climates, radial growth occurs periodically, and the alternation of periods of activity and dormancy results in tree rings, whose features are the result of the interaction between climatic and endogenous factors. Among the endogenous factors, plant development, which encompasses genetic attributes and selective pressures of long-term climatic signalling, can be monitored through the study of the timing of seasonal events represented by plant phenology. In this perspective, monitoring bud and wood phenology provides important information about tree-ring growth and the way in which developmental and climatic factors affect tree-ring cell features and then, wood density. This thesis aims to unravel the developmental and climatic components of density variations within the tree-ring, by studying how wood formation dynamics affect wood anatomy, represented by cell traits i.e. cell diameter and cell wall thickness, which are in turn influenced by the environmental factors. Then, this information have been used to test a mechanical model widely used to model tree ring growth and seasonal wood growth dynamics, the Vaganov-Shashkin model.

In this study, samples were collected from five sites in the coniferous boreal forest of Quebec, (Canada) along a latitudinal gradient stretching between 48°N and 53°N. On these sites, xylogenesis was monitored on 10 individuals × site for 15 years (2002-2016), and in the summer of 2017, additional microcores and cores were collected to measure cell traits i.e. lumen diameter, cell wall thickness; and micro-density. Weather information was recorded using weather stations at each site. Normalized Difference Vegetation Index (NDVI) was used to extrapolate bud phenology from each of the five sites. For the Vaganov-Shashkin model application, dark circles were measured and the model was calibrated for the period 2002-2016. The validation of the model was carried out through the comparison between the predictions of the model (interannual growth and dynamics of ring formation) and the observations obtained by the monitoring of xylogenesis.

Our results demonstrate that carbon allocated into woody tissues is indirectly but tightly linked to short and long-term growth signalling, in part explaining black spruce's conservative growth strategy and widespread distribution. The effects of environmental factors on cell traits and micro-density were not additive, supporting the hypothesis that wood density and cell anatomy display distinct patterns of ecological

correlations. The diverse effects of the environmental factors explain how similar micro-densities can be reached with different wall/lumen ratio. We observed that at all sites, wood formation dynamics adjusted around a mean temperature of ~14 °C, suggesting converging responses to temperature signalling during cell differentiation. Wood anatomy, and indirectly micro-density, were modulated by the duration of the different stages of cell differentiation i.e. duration of enlargement and secondary wall deposition, which were influenced by bud phenology. Indeed, we observed that latewood formation occurs once shoot elongation has ended, suggesting that trees cope with the high demand of sugars in the main C-sink tissues i.e. bud and wood by separating these processes in time. While shoot elongation is ongoing, sugar availability for secondary growth is limited. Accordingly, cells would proportionally spend more time in enlarging rather than undergoing secondary wall deposition, resulting in earlywood-cells with large diameter but thin secondary wall. Once shoot elongation is complete, sugars are massively conveyed into the stem, allowing for latewood formation. The increasing supply of sugars to the stem during latewood formation allows for the development of thicker cell walls limiting the capacity of cells to enlarge, resulting in smaller cells. The interplay between cell differentiation phases on each cell trait, and their above-mentioned dependence from the other events occurring during primary growth, are likely at the origin of the non-linear relationship we detected between cell traits and their duration of differentiation. Indeed, we observed that cell wall thickness and cell wall diameter, proportionally increased with the duration of their differentiation phases, until they reached a plateau.

Predicted inter-annual tree ring growth was highly correlated with the simulated time series from the Vaganov-Shashkin model, but simulations of the intra-annual growth dynamics highlighted that the model performances are limited in wet climates, given that its parameterization was originally based on drier sites. However, a better adaptation of the Vaganov-Shashkin model as a predictive model of the intra-annual growth dynamics of black spruce would allow to extrapolate information on more remote areas and on the growth-responses of black spruce to climate change.

These results cover important gaps on the causal relationships underlying micro-density variations in conifers. We demonstrated that in species characterized by a wide geographical distribution, plastic adjustments in wood formation dynamics can override climate responses. These adjustments are not directly detectable in wood trait size variations because of their pronounced dependency on developmental control. Furthermore, by providing information based on an exceptionally long xylogenesis monitoring period, these results are a valuable contribution to increase the performance of the existing mechanistic models in terms of predicting the onset of the growing season and the amount of biomass stocked in cold environments.

Keywords : black spruce, secondary growth, cell differentiation, secondary wall deposition and lignification, micro-density, Vaganov-shaskin model

INTRODUCTION

1.1 The boreal forest provides essential services for Earth

If during the COVID-19 outbreak the definitions range of "essential services and goods" has assumed many gradations, there's little doubt that boreal forest provides many of them. Boreal forests are indeed source of a multitude of renewable goods and services, and their existence supports a wide range of fundamental environmental dynamics (Brandt et al. 2013). The effects of climate change on boreal forests are already ongoing (Soja et al. 2007); however it is still challenging to make clear statements about the impacts of climate change on boreal forests long-term survival. Climate change on trees growing in boreal forests might have indeed an ambivalent effects, as the release of growth restrictions linked to rising temperatures may be accompanied by site-specific and species-specific conditions that could increase trees mortality or reduce tree growth (D'Orangeville et al. 2018, Luo et al. 2020). In this context, the development of reliable global models to understand and predict how climatic change could affect forest ecosystems is tightly linked to a deep knowledge of the processes underlying tree-growth.

The effects of global warming is expected to be most pronounced in Northern ecosystems relative to other ecosystems of the Boreal Hemisphere, with annual mean temperature across the north American boreal zone being 4–5 °C warmer by 2100 (Price et al. 2013, D'Orangeville et al. 2016). The forecasted variations would lead to alterations of the C cycle and of energy exchange, giving rise to modifications that will affect the distribution of species, the productivity of boreal forests, finally affecting the role of the boreal forest as regulator of global warming (Lloyd and Bunn 2007). Indeed, boreal forests stock 22% of the total forest carbon on the planet, (Bradshaw and Warkentin 2015, Gauthier et al. 2015). Only in Quebec, carbon forest, encompassing stem, living biomass and roots, range from 2 to 4 Kg C m^{-2} (Thurner et al. 2013). However, these estimations of carbon density are linked to high uncertainty, probably due to the poor spatial resolutions when upscaling biomass information collected at a regional level (Thurner et al. 2013). Furthermore, carbon balance in forestry ecosystems is based on seasonal variations, meaning that the capacity of trees to permanently stock carbon in their organs changes during the growing season (Kuptz et al., 2011).

By studying tree-growth phenology it is possible to investigate the seasonal patterns underlying all the growth-related physiological processes occurring within the tree, and that are finely-tuned to environmental conditions (Cleland et al., 2007). Being carbon mainly stocked in the stem (Kuptz et al., 2011), a greater understanding of radial tree-growth phenology at high temporal and spatial resolution becomes

necessary to increase accuracy in carbon biomass estimation in the boreal forest. Furthermore, once stem biomass is known, it is possible to estimate root and living biomass by means of allometric coefficients, adding further precision to carbon balance within the tree (Ma et al., 2020).

1.2 Looking at the missing link between inter- and intra-annual tree-ring growth

Due to the strong relationship between wood production and carbon sequestration, there is an increasing interest in intra-annual wood-growth processes and in their integration into larger vegetation models (Friend et al. 2019). The climatic signal captured by tree-rings has long been used in dendrochronology to study how exogenous factors influence tree-growth (Douglass 1919, McLean and Smith 1973). However, knowledge of the intrinsic mechanisms driving the formation of wood, the tree's primary carbon sink, is still incomplete (Vaganov et al. 2006).

Knowledge gaps in our understanding of intra-annual tree-ring growth dynamics and their drivers prevent from building models that can be generalized and applied at large scale, since our current modelling framework are based on the accumulation of empirical experiences that simulate the results of the processes, instead of the process itself. In this context, predictive and explanatory power do not coexist within the same model, making the downscaling of information from tree-ring to cell level poorly reliable. Many models such as MAIDENiso, TreeRing2000, and the Vaganov–Shashkin (VS), can be used to predict tree growth and productivity

while accounting for the many influential factors that come into play during the life of a plant (Vaganov et al. 2006, Danis et al. 2012). The generalization of their prediction is tightly linked to the integration of the fundamental processes that shapes woody tissues, starting from their cell traits variation across the tree ring. Such integration is needed to switch from an empirical to a mechanistic view of tree-growth processes. Furthermore, based on the triad —realism, accuracy, generality— the construction of a predictive models requires the implementation of causal relationships meant to provide a description of real-life phenomena, which cannot disregard experimental data (Hänninen 2016). Unluckily, long chronologies of intra-annual growth observations to validate, build, and improve these models are scarce, and time-series are not always available over large geographical areas, hampering mechanistic knowledge of the relationship between tree growth and carbon allocation in the tree tissues.

Wood developmental dynamics has been recognized as determinant factors for earlywood-latewood formation (Cuny et al 2016), and being affected by carbon allocation (Cartení et al 2018) seems promising endogenous factors that could be integrated in model general frameworks to better explain tree-ring growth. In conifers, carbon storage and allocation patterns during the growing season reflect multiple trade-offs between respiration, assimilation, storage, and wood formation (Skomarkova et al. 2006). Buds and wood are strong competing carbon sinks with their prioritization varying over the course of the growing season (Skomarkova et al. 2006, Deslauriers et al. 2016). According to the pioneer study of Gordon and Larson

(1968), at the beginning of the growing season, carbon is primarily allocated to the buds. All photosynthates of the current year are thus invested in height growth, while earlywood formation relies on reserves of the previous year. Only once primary growth has finished, a greater amount of carbon become available for stem growth, leading to the formation of latewood (Gordon and Larson 1968). Earlywood-latewood transition would then be explain by the modulatory activity of sugars, as well supported by the mechanistic framework proposed by Cartení et al 2018, these processes underlying a modification of the carbon accumulation within the stem, which is higher in latewood than in earlywood. Non-structural carbohydrate availability for radial growth increases once shoot elongation ceases, allowing for the formation of the thick-walled latewood cells by increasing the duration of secondary wall deposition (Cartenì et al. 2018). The different stages of bud and wood growth occur at different times which are reflected by the carbon allocation patterns in the tree tissues defining different phenological stages of tree growth (Antonucci et al. 2015, Deslauriers et al. 2017).

Sugars constitute an endogenous signal that, along with environmental factors as water, temperature and photoperiod, modulate the different phenological stages of wood formation, which is the result of the transition of cells through different developmental or differentiation stages (Savidge 2001, Deslauriers et al. 2016). Once differentiation begins, the timing of cell differentiation and subsequent residence time of xylem cells in each developmental zone determines cell size and cell wall thickness (Deslauriers et al. 2003). As the growing season progresses, the duration of

cell enlargement decreases favouring the formation of progressively smaller cells that, undergoing longer duration of secondary wall deposition and lignification, grow thicker cell walls. Therefore, earlywood-latewood transition depends on the interplay between wood formation dynamics i.e. duration of both enlargement and secondary wall deposition (Cuny et al. 2014). Cell enlargement and cell wall thickening fulfill different physiological needs and can be influenced by different environmental factors (Cuny and Rathgeber 2016, Balducci et al. 2016). For example, during cell distention, cell enlargement is driven by water, where exponential increases in cell volume are possible by the filling of the vacuole (Guerriero et al. 2014). In turn, secondary wall deposition has been observed to depend mostly on temperature, since warmer conditions allow for a longer growing season, during which trees have more time to assimilate carbon (Deslauriers et al. 2008, Fonti et al. 2013, Castagneri et al. 2017).

Within the tree-ring, the ratio between cell diameter and wall thickness reflects variations in wood density, whose intra-annual pattern is called *micro-density* (Denne 1989, Rathgeber et al. 2006). Being the product of carbon allocation for structural growth, wood density represents the trade-off between mechanical support i.e. cell wall thickness and water conductivity i.e. cell diameter (Preston et al. 2006, Chave et al. 2009). Wood density provides thus an assessment of carbon sequestration that can be transposed over wide areas and long-time resolutions to benefit predictive models at regional scales (Giroud et al. 2017). By studying micro-density, it is possible to observe variability in wood density at a high resolution and

ultimately assess the seasonal variation in carbon sequestration (Decoux et al. 2004, Rathgeber et al. 2006).

A better understanding of the processes underlying micro-density variation within the tree-ring and during wood formation could potentially yield a useful quantitative relationship and provide insights into modelling carbon sequestration in forest ecosystems and test existing predictions.

1.3 Objectives and hypothesis

In my thesis, I aimed to: 1) assess the relationship between the timing of both bud and wood formation, and the influence of both wood formation dynamics and environmental factors on cell anatomy and micro-density variation at the tree-ring scale and 2) validate the existing tools to predict tree growth and the intra-annual wood formation dynamics.

The first objective consisted of three distinct sub-aims with hypotheses that corresponded to three different chapters

1.1. Assessing the timing of both bud and wood formation, and comparing their spatial patterns in relation to annual mean temperature for black spruce across the coniferous boreal forest in Quebec, Canada. I test the hypothesis of a temporal separation in carbon allocation between bud and wood formation. Buds and wood

represent the main carbon sinks, and a trade-off between the resources invested in their growth is expected in order to maintain photosynthetic activity and to fulfil plant hydraulic and mechanical needs (Chapter I);

1.2 Determining how the timing of cell enlargement and secondary wall thickness deposition affect cell diameter and cell wall thickness variation within the tree-ring. I test the hypothesis that there exists a positive linear correlation between cell traits (i.e. cell diameter and cell wall thickness) and the duration of cell differentiation (i.e. enlargement and wall formation) (Chapter II);

1.3 Testing a conceptual framework designed to quantify direct and indirect effects of environmental factors, wood formation dynamics and cell traits i.e. cell diameter, wall thickness on micro-density variations. My hypothesis assumed that micro-density depends on endogenous and exogenous factors i.e. cell trait differentiation dynamics, and environmental conditions during cell formation (Chapter III).

For the second objective, one specific aim was developed corresponding to one last chapter:

2.1 Testing the Vaganov-Shaskin (VS) model predictions with long-term chronologies of black spruce cambial growth. I aim to compare the predicted and

observed timing of wood formation at both a tree-ring and xylem-cell resolution (Chapter IV).

1.4 Experimental approach

The study area covers a latitudinal gradient from 48°N to 53°N, representing the entire closed boreal forest of Quebec, Canada. Five sites were selected in even-aged adult black spruce stands in an effort to encompass a variety of black spruce populations in Quebec (Figure 1.1). All sites lie in the eastern part of the black spruce distribution, where black spruce is the dominant species (Figure 1.1). Two sites (SIM and BER) are situated in the balsam fir (*Abies balsamea* L. Mill.)–white birch (*Betula papyrifera* Marsh.) bioclimatic domain. MIS and DAN lie in the black spruce–moss bioclimatic domain. The northernmost site (MIR) is located in the spruce–lichen domain and is characterized by a lower tree density (Rossi et al. 2015). Long-term temperature and precipitation climate statistics were calculated from 1950–2016 data using the ANUSPLIN algorithm (Hutchinson et al. 2009, Hopkinson et al. 2011, McKenney et al. 2011). Average temperatures within the study area range from 1.9 to -3.4 °C, with the southernmost and northernmost sites being respectively the warmest and the coldest. Precipitation for all sites ranges between 626- and 906-mm. SIM and MIR are the wettest and the driest sites along the gradient, respectively.

The different timing of bud and wood formation were extracted by remote sensing imagery and by field observations (Figure 1.2). For wood formation, a 15 year-long weekly monitoring of xylogenesis (2002-2016) was performed across the gradient, sampling 10 individuals from each of the five sites. Microcores were collected at least 10 cm apart from each other to avoid the development of resin ducts, (Deslauriers et al., 2003). Individuals for xylogenesis monitoring has been changed each 5 years in order to avoid stress responses linked to a long-lasting weekly sampling.

Over 2002-2006, the photosynthetic and bud formation periods were derived from NDVI data that was extracted from atmospherically corrected bi-directional surface reflectance imagery using terra Moderate Resolution Imaging Spectroradiometer (MODIS) Vegetation Indices (Khare et al., 2019). The different stages of bud formation were computed using the methodological approach proposed by Khare et al. (2019) as they corresponded to different proportions of the double-logistic curve describing the standardized NDVI pattern.

Wood anatomy was measured by microcore sampling in 10 individuals from each site on the latitudinal gradient (Figure 1.2). From the same individuals, I collected 10 woody cores and performed X-ray scanning to obtain micro-density measurements (Millier et al. 2006).

Precipitation, temperature, and soil water content at 30 cm soil depth were collected

by automatic weather stations equipped with CR10X data loggers (Campbell Scientific Corporation, Canada); these stations were installed in a forest gap at each site and provided hourly measurements.

1.5 Structure of the thesis

This thesis is composed of four chapters, each one corresponding to one of the above-mentioned specific objectives. Each of the four chapters is written as a scientific paper for submission to a peer-reviewed journal. A citation for each chapter will be available upon publication of the respective chapters.

1.6 Figures

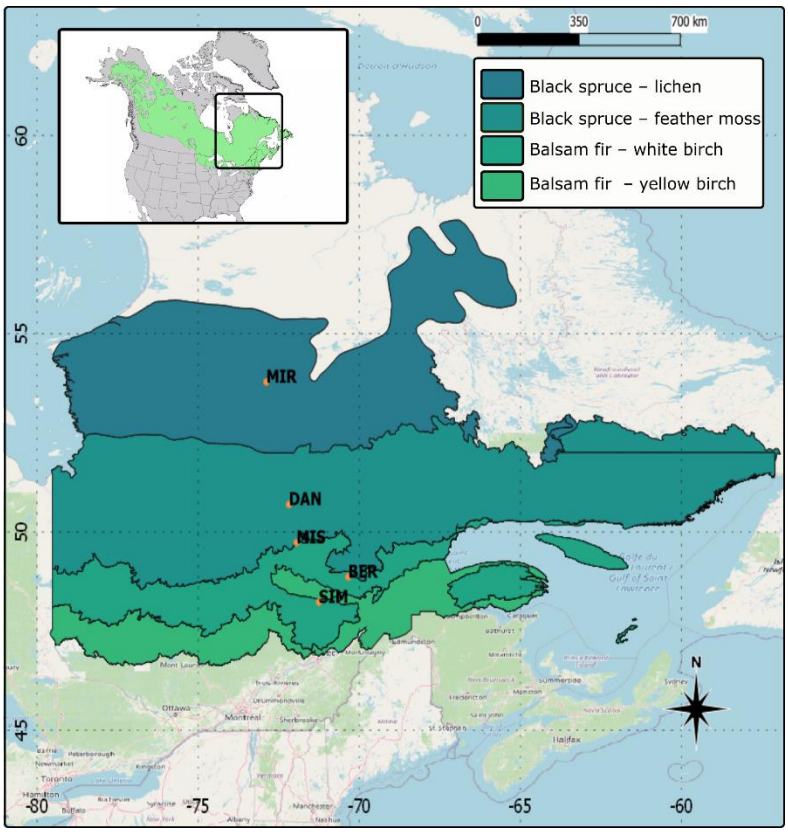

Figure 1.1 Spatial distribution of the five sites across the latitudinal gradient (bigger map) and spatial distribution of black spruce in north America (inset map modified from U.S. Geological Survey - Digital representation of "Atlas of United States Trees" by Elbert L. Little, Jr.). The different colours represent the bioclimatic domains as described by ecological classification of Québec (data downloaded by donneesquebec.ca)

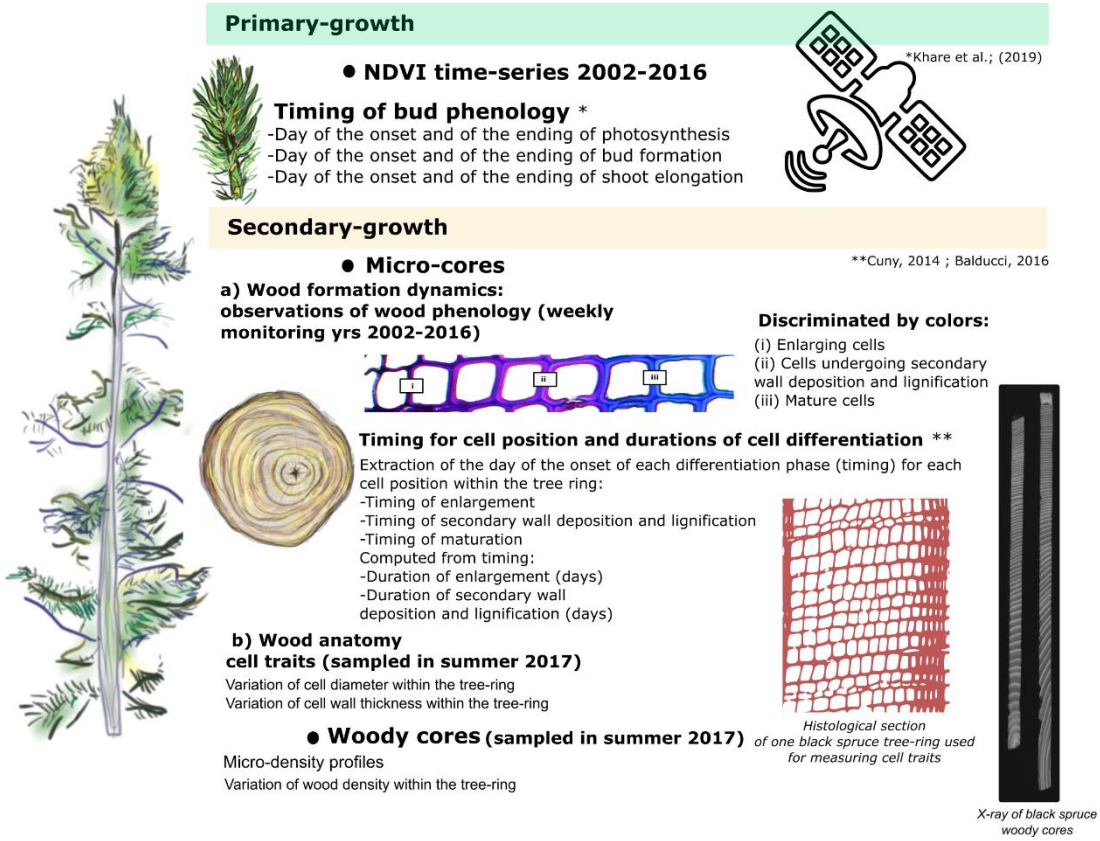

Figure 1.2 Dataset description with all the variables computed for the four chapters of this thesis

1.7 References

Antonucci S, Rossi S, Deslauriers A, Lombardi F, Marchetti M, Tognetti R (2015) Synchronisms and correlations of spring phenology between apical and lateral meristems in two boreal conifers. Tree Physiol 35:1086–1094.

Balducci L, Cuny HE, Rathgeber CBK, Deslauriers A, Giovannelli A, Rossi S (2016) Compensatory mechanisms mitigate the effect of warming and drought on wood formation. Plant, Cell Environ 39:1338–1352. http://doi.wiley.com/10.1111/pce.12689 (8 December 2016, date last accessed).

Björklund J, Seftigen K, Schweingruber F, Fonti P, Arx G, Bryukhanova M V, Cuny HE, Carrer M, Castagneri D, Frank DC (2017) Cell size and wall dimensions drive distinct variability of earlywood and latewood density in Northern Hemisphere conifers. New Phytol 216:728–740.

Bradshaw CJA, Warkentin IG (2015) Global estimates of boreal forest carbon stocks and flux. Glob Planet Change 128:24–30. https://linkinghub.elsevier.com/retrieve/pii/S0921818115000429 (27 July 2020, date last accessed).

Buttò V, Rossi S, Deslauriers A, Morin H (2019) Is size an issue of time? Relationship between the duration of xylem development and cell traits. Ann Bot 123:1257–1265. https://academic.oup.com/aob/advance-article/doi/10.1093/aob/mcz032/5381073 (22 May 2019, date last accessed).

Cartenì F, Deslauriers A, Rossi S, Morin H, De Micco V, Mazzoleni S, Giannino F (2018) The physiological mechanisms behind the earlywood-to-latewood transition: a process-based modelling approach. Front Plant Sci 9:1053.

Castagneri D, Fonti P, Von Arx G, Carrer M (2017) How does climate influence xylem morphogenesis over the growing season? Insights from long-Term intra-ring anatomy in Picea abies. Ann Bot 119:1011–1020. https://www.ncbi.nlm.nih.gov/pmc/articles/PMC5604563/ (29 June 2020, date last accessed).

Chave J, Coomes D, Jansen S, Lewis SL, Swenson NG, Zanne AE (2009) Towards a worldwide wood economics spectrum. Ecol Lett 12:351–366.

Cuny HE, Rathgeber CBK (2016) Xylogenesis: Coniferous Trees of Temperate Forests Are Listening to the Climate Tale during the Growing Season But Only Remember the Last Words! Plant Physiol 171:306–317. http://www.plantphysiol.org/lookup/doi/10.1104/pp.16.00037 (1 January 2017, date last accessed).

Cuny HE, Rathgeber CBKBK, Frank D, Fonti P, Fournier M (2014) Kinetics of tracheid development explain conifer tree-ring structure. New Phytol 203:1231–1241. http://doi.wiley.com/10.1111/nph.12871 (8 January 2017, date last accessed).

Cuny HE, Rathgeber CBKK, Kiessé TS, Hartmann FP, Barbeito I, Fournier M (2013) Generalized additive models reveal the intrinsic complexity of wood formation dynamics. J Exp Bot 64:1983–94. http://www.ncbi.nlm.nih.gov/pubmed/23530132 (12 December 2016, date last accessed).

D'Orangeville L, Duchesne L, Houle D, Kneeshaw D, Côté B, Pederson N (2016) Northeastern North America as a potential refugium for boreal forests in a warming climate. Science (80-) 352

D’Orangeville L, Houle D, Duchesne L, Phillips RP, Bergeron Y, Kneeshaw D (2018) Beneficial effects of climate warming on boreal tree growth may be transitory. Nat Commun 9:3213. http://www.nature.com/articles/s41467-018-05705-4 (23 July 2019, date last accessed).

Danis P-A, Hatté C, Misson L, Guiot J (2012) MAIDENiso: a multiproxy biophysical model of tree-ring width and oxygen and carbon isotopes. Can J For Res 42:1697–1713. www.nrcresearchpress.com/cjfr (4 February 2020, date last accessed).

Decoux V, Varcin É, Leban JM (2004) Relationships between the intra-ring wood density assessed by X-ray densitometry and optical anatomical measurements in conifers. Consequences for the cell wall apparent density determination. Ann For Sci 61:251–262. https://www.afs-journal.org/articles/forest/pdf/2004/03/F4307.pdf (27 July 2020, date last accessed).

Denne MP (1989) Definition of Latewood According to Mork (1928). IAWA J 10:59–62. http://booksandjournals.brillonline.com/content/journals/10.1163/22941932-90001112 (27 September 2017, date last accessed).

Deslauriers A, Fonti P, Rossi S, Rathgeber CBK, Gričar J (2017) Ecophysiology and Plasticity of Wood and Phloem Formation. In: Springer, Cham, pp 13–33. https://link.springer.com/chapter/10.1007/978-3-319-61669-8_2 (27 July 2020, date last accessed).

Deslauriers A, Huang J-G, Balducci L, Beaulieu M, Rossi S (2016) The contribution of carbon and water in modulating wood formation in black spruce saplings. Plant Physiol:pp--01525.

Deslauriers A, Morin H, Begin Y (2003) Cellular phenology of annual ring formation of Abies balsamea in the Quebec boreal forest (Canada). Can J For Res 33:190–200. http://www.nrcresearchpress.com/doi/abs/10.1139/x02-178 (12 January 2017, date last accessed).

Deslauriers A, Rossi S, Anfodillo T, Saracino A (2008) Cambial phenology, wood formation and temperature thresholds in two contrasting years at high altitude in southern Italy. Tree Physiol 28:863–871.

Douglass AE (1919) Climatic Cycles and Tree Growth....: A study of the annual rings of trees in relation to climated and solar activity. Carnegie Institution of Washington.

Fonti P, Bryukhanova M V., Myglan VS, Kirdyanov A V., Naumova O V., Vaganov EA (2013) Temperature-induced responses of xylem structure of Larix sibirica (Pinaceae) from the Russian Altay. Am J Bot 100:1332–1343. http://doi.wiley.com/10.3732/ajb.1200484 (3 October 2017, date last accessed).

Friend AD, Eckes-Shephard AH, Fonti P, Rademacher TT, Rathgeber CBK, Richardson AD, Turton RH (2019) On the need to consider wood formation processes in global vegetation models and a suggested approach. Ann For Sci 76

Gauthier S, Bernier P, Kuuluvainen T, Shvidenko AZ, Schepaschenko DG (2015) Boreal forest health and global change. Science (80-) 349:819–822.

Girardin MP, Hogg EH, Bernier PY, Kurz WA, Guo XJ, Cyr G (2016) Negative impacts of high temperatures on growth of black spruce forests intensify with the anticipated climate warming. Glob Chang Biol 22:627–643.

Giroud G, Bégin J, Defo M, Ung CH (2017) Regional variation in wood density and modulus of elasticity of Quebec's main boreal tree species. For Ecol Manage 400:289–299.

Gordon JC, Larson PR (1968) Seasonal Course of Photosynthesis, Respiration, and Distribution of 14 C in Young Pinus resinosa Trees as Related to Wood Formation . Plant Physiol 43:1617–1624.

Gricar J, Prislan P, De Luis M, Gryc V, Hacurová J, Vavrč\'\ik H, Čufar K (2015) Plasticity in variation of xylem and phloem cell characteristics of Norway spruce under different local conditions. Front Plant Sci 6:730.

Guerriero G, Hausman J-F, Cai G (2014) No stress! Relax! Mechanisms governing growth and shape in plant cells. Int J Mol Sci 15:5094–5114.

Hänninen H (2016) Boreal and Temperate Trees in a Changing Climate. Springer, Dordrecht, Dordrecht.

Hopkinson RF, Mckenney DW, Milewska EJ, Hutchinson MF, Papadopol P, Vincent ALA (2011) Impact of aligning climatological day on gridding daily maximum-minimum temperature and precipitation over Canada. J Appl Meteorol Climatol 50:1654–1665.

Hutchinson MF, McKenney DW, Lawrence K, Pedlar JH, Hopkinson RF, Milewska E, Papadopol P (2009) Development and testing of Canada-wide interpolated spatial models of daily minimum-maximum temperature and precipitation for 1961-2003. J Appl Meteorol Climatol 48:725–741.

Khare S, Drolet G, Sylvain JD, Paré MC, Rossi S (2019) Assessment of spatio-temporal patterns of black spruce bud phenology across Quebec based on MODIS-NDVI time series and field observations. Remote Sens 11

Kong D, Zhang Y, Wang D, Chen J, Gu X (2020) Photoperiod explains the asynchronization between vegetation carbon phenology and vegetation greenness phenology. J Geophys Res Biogeosciences

Lloyd AH, Bunn AG (2007) Responses of the circumpolar boreal forest to 20th century climate variability. Environ Res Lett 2:045013. http://stacks.iop.org/1748-9326/2/i=4/a=045013?key=crossref.ad319da31c2f72c4543475daeac041a5 (17 December 2016, date last accessed).

Luo Y, McIntire EJB, Boisvenue C, Nikiema PP, Chen HYH (2020) Climatic change only stimulated growth for trees under weak competition in central boreal forests Bellingham P (ed). J Ecol 108:36–46. https://onlinelibrary.wiley.com/doi/abs/10.1111/1365-2745.13228 (22 July 2020, date last accessed).

Ma, S.H., Eziz, A., Tian, D., Yan, Z.B., Cai, Q., Jiang, M.W., Ji, C.J. and Fang, J.Y., 2020. Size-and age-dependent increases in tree stem carbon concentration: implications for forest carbon stock estimations. Journal of Plant Ecology, 13(2), pp.233-240.

McKenney DW, Hutchinson Michael F, Papadopol P, Lawrence K, Pedlar J, Campbell K, Milewska E, Hopkinson RF, Price D, Owen T (2011) Customized spatial climate models for North America. Bull Am Meteorol Soc 12:1611–22.

McLean A, Smith JHG (1973) Effects of climate on forage yields and tree-ring widths in British Columbia. J Range Manag:416–419.

Millier F, Verger M, Rozenberg P (2006) Microdensitométrie sur arbres forestiers. Les Cah des Tech l'INRA:87–91.

Preston KA, Cornwell WK, DeNoyer JL (2006) Wood density and vessel traits as distinct correlates of ecological strategy in 51 California coast range angiosperms. New Phytol 170:807–818.

Price DT, Alfaro RI, Brown KJ, Flannigan MD, Fleming RA, Hogg EH, Girardin MP, Lakusta T, Johnston M, McKenney DW, Pedlar JH, Stratton T, Sturrock RN, Thompson ID, Trofymow JA, Venier LA (2013) Anticipating the consequences of climate change for Canada's boreal forest ecosystems 1. Environ Rev 21:322–365. http://www.nrcresearchpress.com/doi/abs/10.1139/er-2013-0042 (30 December 2016, date last accessed).

Rathgeber CBK (2017) Conifer tree-ring density inter-annual variability - anatomical, physiological and environmental determinants. New Phytol 216:621–625. http://doi.wiley.com/10.1111/nph.14763

Rathgeber CBK, Decoux V, Leban J-M (2006) Linking intra-tree-ring wood density variations and tracheid anatomical characteristics in Douglas fir (Pseudotsuga menziesii (Mirb.) Franco). Ann For Sci 63:699–706. http://www.edpsciences.org/10.1051/forest:2006050 (26 September 2017, date last accessed).

Rossi S (2015) Local adaptations and climate change: converging sensitivity of bud break in black spruce provenances. Int J Biometeorol 59:827–835.

http://link.springer.com/10.1007/s00484-014-0900-y (11 July 2019, date last accessed).

Rossi S, Cairo E, Krause C, Deslauriers A (2015) Growth and basic wood properties of black spruce along an alti-latitudinal gradient in Quebec, Canada. Ann For Sci 72:77–87. http://link.springer.com/10.1007/s13595-014-0399-8 (12 December 2016, date last accessed).

Rossi S, Deslauriers A, Morin H (2003) Application of the Gompertz equation for the study of xylem cell development. Dendrochronologia 21:33–39.

Savidge R (2001) Intrinsic regulation of cambial growth. J Plant Growth Regul 20:52–77.

Skomarkova M V., Vaganov EA, Mund M, Knohl A, Linke P, Boerner A, Schulze ED (2006) Inter-annual and seasonal variability of radial growth, wood density and carbon isotope ratios in tree rings of beech (Fagus sylvatica) growing in Germany and Italy. Trees - Struct Funct 20:571–586. http://carbodat.ei.jrc.it (29 July 2020, date last accessed).

Soja, A.J., Tchebakova, N.M., French, N.H., Flannigan, M.D., Shugart, H.H., Stocks, B.J., Sukhinin, A.I., Parfenova, E.I., Chapin III, F.S. and Stackhouse Jr, P.W., 2007. Climate-induced boreal forest change: predictions versus current observations. Global and Planetary Change, 56(3-4), pp.274-296.

Thurner, M., Beer, C., Santoro, M., Carvalhais, N., Wutzler, T., Schepaschenko, D., Shvidenko, A., Kompter, E., Ahrens, B., Levick, S.R. and Schmullius, C., 2014. Carbon stock and density of northern boreal and temperate forests. Global Ecology and Biogeography, 23(3), pp.297-310.

Vaganov EA (Evgeniĭ A, Hughes MK, Shashkin AV (Aleksandr V, Hughes MK (2006) Growth Dynamics of Conifer Tree Rings: Images of Past and Future Environments Springer-Verlag (ed), Ecological. Springer, Berlin. https://www.journals.uchicago.edu/doi/10.1086/586955 (16 March 2017, date last accessed).

Zhao M, He Z, Du J, Chen L, Lin P, Fang S (2019) Assessing the effects of ecological engineering on carbon storage by linking the CA-Markov and InVEST models. Ecol Indic 98:29–38.

Ziaco E (2020) A phenology-based approach to the analysis of conifers intra-annual xylem anatomy in water-limited environments. Dendrochronologia 59:125662. https://doi.org/10.1016/j.dendro.2019.125662

CHAPTER I

REGIONWIDE TEMPORAL GRADIENTS OF CARBON ALLOCATION ALLOW FOR SHOOT GROWTH AND LATEWOOD FORMATION IN BOREAL TREES

Rejected, Invited to Resubmit in Global ecology and biogeography

RESEARCH ARTICLE

Regionwide temporal gradients of carbon allocation allow for shoot growth and latewood formation in boreal trees

Valentina Buttò*[1], Siddhartha Khare[1], Guillaume Drolet[2], Jean-Daniel Sylvain[2], Fabio Gennaretti[3], Annie Deslauriers[1], Hubert Morin[1] Sergio Rossi[1,4]

1 Département des Sciences fondamentales, Université du Québec à Chicoutimi, Chicoutimi, QC, Canada

2 Direction de la recherche forestière, Ministère des Forêts, de la Faune et des Parcs, Québec,
QC, Canada

3 Institut de recherche sur les forêts (IRF), Université du Québec en Abitibi-Témiscamingue, Amos, QC, Canada

4 Key Laboratory of Vegetation Restoration and Management of Degraded Ecosystems, Guangdong Provincial Key Laboratory of Applied Botany, South China Botanical Garden, Chinese Academy of Sciences, Guangzhou, China

*Corresponding author: Valentina Buttò (orcid:0000-0003-1595-6745),
Département des Sciences fondamentales,Université du Québec à Chicoutimi, 555, boulevard de l'Université, Chicoutimi (Québec), Canada G7H 2B1.
Phone number: +1-418-545-5011 ext. 2330
Email: valentina.butto1@uqac.ca

2.1 Abstract

Aim: In boreal ecosystems, phenological events display seasonal patterns to support the developing tissues during the short time window available for growth in cold climates. Primary and secondary growth, two expensive processes for plants, are then expected to be modulated in time to allocate carbon efficiently to bud and woody tissues. We aimed to assess the phenology of primary and secondary meristems, testing their predictability on the base of the mean annual temperature, a widespread spatial index.

Location: *Quebec, Canada*

Time period: *2002-2015*

Major taxa studied: Gymnospermae

Methods: We combined weekly scaled field observations with Moderate Resolution Imaging Spectroradiometer (MODIS) time-series of the Normalized Difference Vegetation Index (NDVI) to extract timings of photosynthesis and meristem growth in five black spruce [*Picea mariana* (Mill.) B.S.P.] stands located along a latitudinal gradient. Using the relationship between meristems growth and mean annual temperature on the latitudinal gradient, we predicted their timings on a larger study area, covering the entire black spruce-stand distribution in Quebec.

Results: Photosynthesis started at the beginning of May, three weeks before bud reactivation and the onset of wood growth. Latewood formation started in mid-July, after shoot elongation was completed. Mean annual temperature was correlated with the onset of bud and wood phenology in spring, but not with the phenological events that occur in summer and autumn. Growth dynamics spatialized across the boreal forest of Quebec varied with the transition between the subarctic and humid continental climate.

Main conclusions: We observed that shoot elongation and latewood formation were temporally separated, providing evidence of a trade-off in structural carbon allocation between primary and secondary growth. Within a context of climate change, a warming could advance the onset of photosynthesis and meristem activity, thus anticipating carbon allocation, but the effects on the phenological events in summer and autumn could be marginal.

Keywords: black spruce, carbon sequestration, mean annual temperature, meristem activity, NDVI, *Picea mariana* (Mill.) B.S.P., phenology, photosynthesis, remote sensing, spatial analysis

2.2 Introduction

The timings of growth-related physiological processes occurring during the growing season of plants are finely tuned to the seasonal patterns of environmental conditions, which suggest that predicted environmental changes could affect the survival of trees and forest productivity (Cleland *et al.*, 2007). In temperate and boreal ecosystems, temperature is an important driver of bud and wood phenology, and tree growth responses to temperature variations are raising interest because of the forthcoming changes linked to global warming (Rossi & Isabel, 2017). *In situ* and common garden experiments have both shown that air temperature explains most of the variation in the phenology of black spruce (*Picea mariana* (Miller) B.S.P), one of the most important species in the boreal forest (Rossi & Bousquet, 2014). Black spruce grows from Alaska to Newfoundland and forms closed and dense stands in northeastern North America, with a distribution that reaches the 58th parallel over different hydric and thermal conditions (Walker & Johnstone, 2014).

During the growing season, the relative growth investment in height and stem volume must be balanced to sustain all plant processes (Franceschini *et al.*, 2016). The seasonal cycle of carbohydrates within the cambium and developing xylem i.e. the plant vascular tissue originating wood, is linked to wood phenology (Deslauriers *et al.*, 2016). In different environments, Carbone et al. (2013) indeed observed that the concentration of non-soluble carbohydrates increases during xylem differentiation, peaking when the number of cells in secondary wall formation reaches its maximum.

Experimental evidence shows that bud burst matches the onset of xylem differentiation, which relies, at least in the early growing season, on starch reserves (Deslauriers *et al.*, 2019; Fajstavr *et al.*, 2019). Later in the summer, latewood formation requires a strong and continuous supply of carbohydrates to the cambium, which is supposed to occur once shoot elongation is completed (Cartenì *et al.*, 2018). However, an improved detection of the chronological sequence of the phenological events of primary and secondary growth is required for a better understanding of carbon sequestration in plant tissues (Antonucci *et al.*, 2017).

The broad latitudinal distribution of the boreal forest provides a unique opportunity to study how environmental conditions influence seasonal carbon allocation to primary and secondary meristems at wide spatial scale. Changes in plant phenology can be monitored at varying scales, from single sites (Balzarolo *et al.*, 2016) to large regions with the help of satellite data (Hmimina *et al.*, 2013). Spectral vegetation indices derived from optical remote sensing data are able to provide time series of phenological parameters, which can be used to study species or ecosystem growing season dynamics (White *et al.*, 2005). The Normalized Difference Vegetation Index (NDVI) is the most used spectral tool in phenological studies as it provides the contrast between absorption of red light by pigments in the leaf chloroplasts and the strong scattering of near-infrared radiation due to leaf internal structure (Piao *et al.*, 2015)

The aim of our study was to assess the phenology of primary and secondary

meristems and compare the spatial patterns of the timings of sinks and sources in the boreal forest. We hypothesized a temporal separation in carbon allocation between primary and secondary meristems. Indeed, primary and secondary growth represent the two main carbon sinks during early summer, and a trade-off between the resources invested by trees is expected in order to maintain the optimal carbon balance and architectural development. To test our hypothesis, we assessed primary meristems phenology, i.e. bud development, using Moderate Resolution Imaging Spectroradiometer (MODIS) NDVI time series and the protocol proposed by Khare et al. (2019). The phenology of secondary meristems, i.e. wood phenology, was assessed by monitoring 15 years of xylogenesis at five permanent plots along a latitudinal gradient in the coniferous boreal forest. The spatial patterns of relationships between annual mean temperature and timings of bud and wood phenology in black spruce were projected on an area covering the entire distribution of the species in Quebec, Canada.

2.3 Materials and Methods

2.3.1 Study area and site selection

The study area covers nearly 800,000 km^2 of the northern temperate and boreal zone of Quebec, Canada (Figure 1). The area belongs to the boreal forest with a snowy climate, with a mean temperature of the warmest month exceeding 10.0° C and a mean temperature of the coldest month being below 3 °C (Beck *et al.*, 2018). The study area falls in two different climatic regions, humid continental, with mild summer conditions, and subarctic, with cool summers (Beck *et al.*, 2018). The former is located in the south and eastern parts of the study area, the latter covers the rest (Figure 1).

Field observations of xylogenesis and air temperature were collected at five permanent plots along a latitudinal gradient between the 48th and 53rd parallels north: Simoncouche (abbreviated as SIM), Bernatchez (BER), Mistassibi (MIS), Camp Daniel (DAN) and Mirage (MIR) (Figure 1). In addition, we selected 5,000 forest polygons extracted from the 1:20k Quebec forest map (MRNF, 2015) (Figure 1). Selected polygons corresponded to forest stands dominated by black spruce (black spruce cover >75%) that had remained undisturbed for the past 30 years.

2.3.2 Wood phenology and xylem cell size

The timings of wood phenology and anatomical attributes were assessed by microcores sampled on adult trees in the five permanent plots (Buttò *et al.*, 2019). Microcores were collected weekly or fortnightly during April-October 2002-2016

(except at MIR: 2012-2016) from 10 trees per permanent plot using surgical bone needles or Trephor. Microcores were embedded in paraffin, cut into transversal sections, and stained with cresyl violet acetate (0.16% in water). Wood phenology was assessed by classifying xylem cells under visible and polarized light at magnifications of × 400-500. Xylem cells were classified as (1) enlarging, (2) wall thickening and lignifying, or (3) mature (Deslauriers *et al.*, 2003). The daily sequence of cell production and maturation was estimated using the protocol proposed by Cuny et al. (2013). Accordingly, we fitted generalized additive models (GAM) with splines over the number of cells for each sampling day, thus estimating cell production and the timings of division and differentiation of each cell of the tree ring at daily scale (Cuny *et al.*, 2013). The timings represented the day of the year (DOY) of entry of the cells into each phenological event (Buttò *et al.*, 2019). Wood phenology was represented by the overall period of xylem cells production and maturation.

We determined the earlywood-latewood transition on the tree-rings and its timings from anatomical measurements made on additional microcores collected in 2017 on 10 individuals per plot. These samples were prepared using the abovementioned procedure, stained in safranin (1% in water) and permanently fixed on slides using Permount™. We measured lumen diameter and cell-wall thickness (single wall) on all sections using Wincell (Regent Instruments, Canada) on images collected by a camera fixed on an optical microscope at magnifications of ×20. Tracheids with lumen smaller than twice cell-wall thickness were considered as latewood. We

matched the anatomical measurements with the estimated daily timings of xylem formation to estimate the date of earlywood-latewood transition (Buttò *et al.*, 2019).

2.3.3 NDVI and bud phenology

Timings of photosynthesis and bud phenology were derived from NDVI time series extracted from the Terra Earth-orbiting platform's MODIS Vegetation Indices (MOD13Q1, version 6). We used 16 days temporal NDVI composite imagery on ISIN tiles h13 v03 and h13 v04 with a spatial resolution of 250 m. We used a total of 460 NDVI granules (a granule is a raster image; 230 for each ISIN tile) (https://earthdata.nasa.gov/). We extracted mean NDVI values for each permanent plot and black spruce polygon for the period 2009-2018. NDVI was fitted with double-logistic curves and the onset and ending of photosynthesis was estimated at the two inflection points (Antonucci *et al.*, 2017). The activity of the primary meristem was estimated on the same curves based on the thresholds defined in Khare et al. (2019), thus assessing bud phenology (i.e. the period from reactivation of the bud until bud set, going through winter bud, which is observed once shoot elongation is finished), and shoot elongation (i.e. the period of apical growth) (Dhont *et al.*, 2010).

2.3.4 ***Temperature data***

Hourly temperatures were recorded in the five permanent plots by weather stations equipped with CR10X dataloggers (Campbell Scientific Corporation, Canada) and averaged to obtain monthly time series. Monthly climate data were extracted for the

whole study area from Canadian Climate Data Archive of Environment Canada (Environment Canada, 1994). Temperatures were generated using thin-plate smoothing splines to develop elevation dependent spatially continuous climate surfaces from noisy weather station data, as implemented in the ANUSPLIN climate software (McKenney *et al.*, 2011).The monthly temperatures recorded by ANUSPLIN are highly correlated with those measured at the field plots (R=0.99). Annual temperatures were calculated from the monthly time series for both permanent plots and the whole study area.

2.3.5 Statistical analysis and spatial patterns

Differences between the timings of phenological events were tested by Kruskal–Wallis test, combined with a Dunn test for multiple comparisons for groups with unbalanced observations. Dunn test was performed using the Benjamini-Hochberg adjustment. The timings of phenological events were modelled by fitting general linear models (GLM) using Day Of the Year (DOY) as a dependent variable and mean annual temperature as a predictor. The phenological event was used as a categorical predictor in interaction with the temperature. Model performance was tested by comparing predictions and observations using Pearson correlations. Models displaying coefficient correlations >0.5 between observations and predictions were applied to assess the spatial patterns of timings of phenological events over the whole study area. GLM and all statistical analyses were performed in R (R Core Team,

2019). Kruskal-Wallis and multiple comparisons tests were performed with the packages “FSA” (Mevik *et al.*, 2019).

2.4 Results

2.4.1 Patterns of mean annual temperature

Across the permanent plots, mean annual temperature ranged from -2.6 °C to 2.1 °C, decreasing with latitude (Figure 2). In the coldest plots, MIR and DAN, mean annual temperatures during 2002-2016 ranged from -2.0 °C to 0.5 °C and from -2.5 °C to -1.5 °C, respectively. Warmer conditions were recorded in MIS and BER, with mean annual temperatures in 2002-2016 ranging from 0 °C to 0.5 °C. During 2002-2016, mean annual temperature was higher in SIM, the southernmost plot, ranging from 1 °C to 3.5 °C.

Across the whole study area, mean annual temperature ranged from -2.6 °C to 4.9 °C, with the warmer and colder regions being located in the southeastern and north and northeastern parts, respectively (Figure 2). On average, the temperature decreased by 1 °C per degree of latitude. The warmest temperatures were recorded close to large water masses.

2.4.2 Phenology across the latitudinal gradient

The different phenological events showed clear and distinct temporal dynamics along the latitudinal gradient (Figure 3). The Kruskal-Wallis test was significant ($p<0.001$), and multiple comparisons revealed different degree of similarity between the successive phenological events (Table 1). The similarities detected depended on the dates of different phenological events. Photosynthesis was the first process detected on DOY 125 ± 10 days, and was different from all the other phenological events. The

onsets of bud formation (147 ± 9 days) and wood phenology (DOY 151 ± 7 days) were similar and were observed within the same week (Table 1, Figure 3). Shoot elongation lasted 18 days, ranging from mid-June (DOY 174 ± 10 days) to the beginning of July (DOY 192 ± 11 days). Timings of the end of shoot elongation (DOY 192 ± 11 days) and start of latewood formation (DOY 196 ± 8 days) were similar. The end of latewood formation (DOY 196 ± 8 days) was similar to the ending of bud phenology (DOY 254 ± 15 days). Photosynthetic activity lasted 172 days, ending in October (DOY 297 ± 13 days) (Figure 3). Like its onset, the ending of photosynthesis was different from the other phenological events (Table 1).

Timings of photosynthesis and growth showed distinct spatial patterns along the latitudinal gradient, with an earlier and longer meristem activity in the southernmost permanent plots. Delay and anticipation in onset and ending of phenology, respectively, were observed in BER, possibly due to effects of the altitude of the site (Figure 4). SIM and MIS were the earlier permanent plots starting photosynthesis on DOY 118, and 119, respectively. Photosynthesis was resumed one week later in BER, and two weeks later in DAN and MIR (Figure 4). Bud phenology started earlier in the southernmost permanent plot (DOY 143 in SIM) and later in the northernmost one (DOY 154 in MIR), matching with the beginning of wood phenology. Shoot elongation had similar durations along the latitude, ranging from 20 days in BER to 16 days in DAN and MIR, ending when latewood formation started. Winter bud was

formed earlier in SIM on DOY 247 and later in MIS on DOY 248. Latewood formation ended at the latest in SIM on DOY 266 (Figure 4).

2.4.3 Phenology vs mean annual temperature

When correlated with mean annual temperature, all phenological events related to bud and wood phenology showed decreasing and similar slopes. Consequently, a higher mean annual temperature corresponded to earlier onset of bud and wood formation, but also to an earlier ending of these processes (Figure 5a). GLM explained 96% of the variance (Table 2). The most significant amount of variance was explained by the phenological events and their interaction with mean annual temperature. As shown by the changing slopes of our regressions, the effect of mean annual temperature changed according to the phenological event (Figure 5a). The onset of photosynthesis was well predicted by annual mean temperature, as shown by the strong correlations between predictions and observations ($R \geq 0.5$) (Figure 5b). Predictions were also satisfactory for the onset of bud and wood phenology, indicating that these phenological events are well represented by the mean annual temperature of the sites (Figure 5b). The correlation between observations and predictions was moderate (R between 0.3 and 0.5) for the onset and ending of shoot elongation. Mean annual temperature was weakly correlated with the onset of latewood formation and ending of bud and wood phenology, as indicated by the small correlation values between predictions and observations ($R \leq 0.2$).

MAE for the onset of photosynthesis and bud phenology was 6.1 and 5.8 days, respectively, and decreased to 4.4 days for the onset of wood phenology (Figure 5b). Prediction error for the onset and ending of shoot elongation was 7.1 and 8.1 days, respectively, increasing to 9.1 and 11.6 days for the ending of wood formation and ending of bud phenology. Prediction error for the ending of photosynthesis was 10.6 days (Figure 5b). The onset of photosynthesis, bud phenology and wood phenology were anticipated by 3 days per additional degree Celsius in mean annual temperature, with regressions showing similar slopes (Figure 5b).

The spatial patterns based on the predictions of the GLM models between temperature and phenological events demonstrated synchronous responses to the thermal gradients in meristems reactivations across the extended study area (Figure 6). The spatial patterns in mean annual temperature defined regions with earlier meristems phenology in the south and southeastern part of the study area, while colder regions showed proportional delays in meristems reactivation (Figure 2). Accordingly, the onset of photosynthesis occurred earlier in the southeast (DOY 110) and later in the north and northeast (DOY 130). Bud phenology started earlier in the southeast regions (DOY 135) and 20 days later in the north and northeast regions, the coldest parts of the study area. The onset of bud and wood phenology occurred within the same week and had the same spatial patterns, with wood phenology starting on average 3.5 days after bud phenology. An increase of 1 °C in mean annual

temperature resulted in an anticipation of 3.6 days in the onset of photosynthesis and 3 days in the onset of bud and wood phenology.

2.5 Discussion

In this study, we combined chronologies of xylogenesis with remote sensing data to extract the phenological timings of primary and secondary growth along a gradient covering the latitudinal distribution of black spruce in Quebec, Canada. The timings of the main phenological events were spatialized across our study area based on their relationship with mean annual temperature. Our findings provide a clear and comprehensive description of the phenological synchronisms among meristems accounting for the different phases of both bud (bud formation, shoot elongation) and wood (earlywood, latewood formation) phenology. In agreement with other reconstructions of the spatiotemporal patterns of plant phenology performed over large areas (Piao *et al.*, 2015), we identified the relationships between onset and ending of the growing season and mean annual temperatures occurring across the study area. Our results provide a spatial reconstruction at wide scale of the timings of plant sinks and sources in a boreal species of ecological and commercial importance for North America.

2.5.1 Synchronism between bud and wood phenology

We observed similar spatiotemporal patterns of the onset of bud and wood phenology, which occurred within the same week, demonstrating the synchronism

between primary and secondary meristems. Similar results were observed in conifer species, but in single plots (Fajstavr *et al.*, 2019). Within the tree, the balance between source (canopy assimilation) and sink (growth) lies in the temporal dynamics of non-structural carbohydrates, which is related to plant phenology (Oleksyn *et al.*, 2000). During spring, bud and wood growth represent the strongest sinks in trees, competing for carbon allocation (Deslauriers *et al.*, 2016). At the beginning of the growing season, xylem production is expected to depend on the influx of auxin coming from buds primordia and young leaves, where this hormone is massively produced to be conveyed into polar auxin transport (Schrader *et al.*, 2003). As shown by experimental evidence, cambial reactivation artificially triggered by winter warming is not sufficient to push the cambium into vigorous xylem cells production, which would support the hypothesis of a link between cambial activity and the supply of auxin from the young leaves and primordials (Oribe *et al.*, 2003). Activation of the apical meristems would then be necessary for the onset of wood phenology, which could explain their synchronism.

Our results demonstrate that latewood formation starts when shoot elongation has ceased, pointing to a temporal segregation of these two important growth processes, both of them being highly demanding in terms of carbon supply. This temporal segregation mirrors different investments in carbon allocation between primary and secondary growth, which is considered crucial for the initiation of latewood formation. At the beginning of the growing season, the developing buds are mainly supported by photosynthates produced by the old needles, while wood formation

mostly relies on reserves stored in the stem rather than the carbon translocated from the leaves (Hansen & Beck, 1990). Consistently, experimental evidence obtained by $^{13}CO_2$ pulse-labeling of photo-assimilates demonstrated that earlywood contains carbon assimilated from the previous summer and autumn, while latewood is prevalently composed of carbon assimilated during the current growing season (Hansen & Beck, 1990; Kagawa *et al.*, 2006). As proposed by Cartenì et al. (2018), as long as the early stages of bud formation and shoot elongation are ongoing, a smaller amount of carbon is available for xylem formation and in particular, for cell wall thickening, resulting in larger xylem cells with thin cell walls. Later during the growing season, the end of shoot elongation makes more sugars available for wood formation, allowing for a greater deposition of secondary wall, which lasts longer than cell enlargement and entails the formation of smaller cells and thick cell walls (Cartenì *et al.*, 2018). Our results represent suitable bases for ecophysiological models by providing reliable relationships that combine carbon sinks and sources in trees based on meristem phenology, which is still poorly integrated into the current mechanistic frameworks (Friend *et al.*, 2019).

Some studies have analyzed time series that included CO_2 flux data and phenology derived from remote sensing imagery in evergreen conifers (Gonsamo *et al.*, 2012; Kong *et al.*, 2020). During spring, the greenness displays a good synchronism with carbon dynamics in the canopy, as demonstrated by the comparison between NDVI and measurements from eddy covariance flux towers (Kong *et al.*, 2020). However, estimations of net ecosystem production do not allow to quantify where and how the

carbon calculated in the total carbon balance is used (Lovett *et al.*, 2006), thus preventing assessment of the timings of carbon allocation when using NDVI as an indicator of carbon phenology. Furthermore, Kong et al. (2020) have recently observed that estimations of the carbon patterns inferred from NDVI are less reliable in autumn compared to spring, due to the mismatch between NDVI index and photosynthetic capacity occurring at the end of the growing season. With our results, we provide a complete framework of the timings of carbon allocation in the main C-sinks of the plants i.e. primary and secondary growth, at a large geographical scale, improving the carbon patterns inferred from NDVI.

As expected, photosynthesis occurs during a longer time window, i.e. several weeks, than meristem activity. The mismatch between photosynthetic and meristems activity is linked to the different ecological requirements of these processes (Körner, 2012). In conifers of cold environments, temperature is a major driver of photosynthesis downregulation (Hansen & Beck, 1990). During winter, photosynthesis can occur when leaf temperature is above freezing point and water is available in the soil in liquid form (Blechschmidt-Schneider, 1990). Even under earlier reactivation, photosynthesis can stop and reactivate in the case of changing environmental conditions. According to current knowledge, such a flexibility is prevented for the growth of buds and cambium in cold climate species, where only one growing season is actually reported in the literature. Indeed, growth reactivation of buds in black spruce avoids late frost events as much as possible, explaining the different timings of

photosynthetic activity and meristems phenology (Silvestro *et al.*, 2019; Marquis *et al.*, 2020).

Proportional changes in shoot elongation and latewood formation could arise from a series of interlocking events, linked to the timings of the previous phenological phases and to endogenous factors (Hänninen, 2016). The steady proportions between timings of the intermediate stages of bud and xylem formation during the growing season could then be linked to resource partitioning, which is influenced by allometric ratios, under which the number of vegetative and reproductive elements influence phenology and growth (Weiner, 2004). In plants, the number of buds is pre-established, and has been showed to interact with carbon allocation and bud phenology (Fournier *et al.*, 2020). In conifers, it has been observed that the number of internodes set during the previous growing season explained the differences in height growth among regions and provenances better than phenology (Chuine *et al.*, 2001). Indeed, Chuine et al. (2001) observed that a greater number of internodes is correlated with a higher growth rate, which allows for greater heights to be reached.

2.5.2 Mean annual temperature and black spruce phenology

We tested the use of mean annual temperature as an indicator of photosynthesis and meristems phenology at wide geographical scale. We observed that it is well correlated with the phenological events in spring, i.e. onset of photosynthesis, and bud and xylem reactivation. The onset of bud and wood growth depends on chilling and forcing requirements: their fulfillment releases dormancy (Delpierre *et al.*, 2018).

Although simple and simplistic, mean annual temperature characterizes a representative, intuitive and largely-used statistic, whose variations can be easily integrated into spatial model scenarios to assess climate change impacts at the geographical scale of species distribution. The ability of annual temperature to describe the patterns of xylem cell production and development was also demonstrated for conifer species across the northern hemisphere (Rossi *et al.*, 2016). Annual mean temperature is not related to the timings of bud set, suggesting that other factors are involved in the autumnal processes of meristems phenology (Deslauriers & Rossi, 2019).

Phenological events exhibited the same spatial pattern, occurring earlier in the southern and southeastern regions and later in the northern, and north-eastern regions of the study area. Regions with earlier phenology were closer to the ocean, suggesting that the thermal variation along the latitude is not the only factor discriminating phenology across our study area, which is also influenced by the effect of water bodies. The spatial patterns of phenological events in spring matched with the location of the two different climatic zones of the boreal forest of Quebec described by Beck et al. (2018) and reported in Fig. 1. The humid continental climate in the east is characterized by warm summers, earlier spring snowmelt and constant precipitation, which produce favorable conditions for an earlier and faster growth resumption in spring (Rossi *et al.*, 2011). On the long-term, the date of snowmelt also affects the duration of wood formation, with a determinant role on nutrient cycling in the soil (Rossi *et al.*, 2011). On a larger scale, it has been observed that precipitation

regime can change plants thermal sensitivity, with important consequences for spring phenology (Shen *et al.*, 2015; Du *et al.*, 2019). In wetter areas, the lower risk of drought triggers a greater temperature sensitivity of the start of the growing season, allowing plants to maximize thermal benefit, which entails an anticipation of spring phenology (Shen *et al.*, 2015).

2.6 Conclusions

In this study, we combined MODIS derived time series of NDVI with *in situ* measurements to assess the timings of bud and wood phenology in five permanent plots distributed across a latitudinal gradient in Quebec, Canada. We assessed the time window of carbon allocation in black spruce, here represented by the periods of activity of the two main sinks, i.e. primary and secondary growth. The beginning of bud and wood formation, which are the main growth processes in trees, occur within the same week, but shoot elongation and latewood formation are temporally separated. Estimations of the timings of photosynthetic activity and carbon allocation at the biome level are crucial for understanding the carbon budget of trees and assessing how they allocate carbon into the canopy (apical growth) and wood (radial growth). We demonstrate that mean annual temperature can be a good predictor of phenology at a large scale, but only for spring events. Our results have major consequences on the understanding of the effects of climate change on terrestrial ecosystems. In the boreal forest, where winter chilling requirement is always fulfilled, warmings occurring in springtime could advance the onset of photosynthesis and meristem activity, thus anticipating carbon allocation in trees. On the other hand, phenological events occurring in summer and autumn are generally less sensitive to the temperature because they rely on the interaction with other environmental or endogenous factors (Gallinat *et al.*, 2015; Chen *et al.*, 2020). As a consequence, the effects of a warming on plant phenology during or at the end of the growing season

could be marginal or less important. Within a scenario of homogenous warming during the year and an abundant precipitation regime, we can expect a lengthening of the growing season for boreal black spruce, which would enable a longer time window for carbon allocation in the growing tissues (Chen *et al.*, 2020).

2.7 Figures

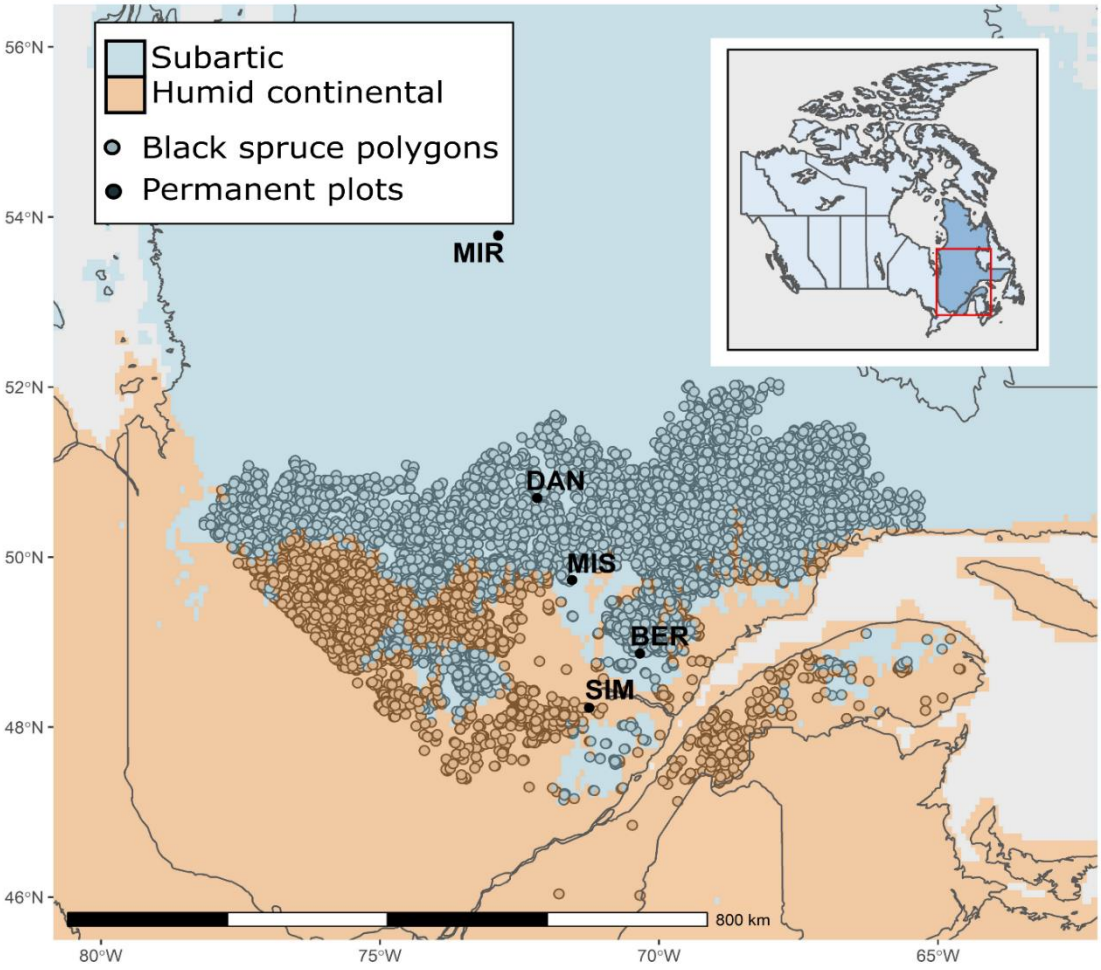

Figure 2.1 Representation of the study area and permanent plots. Grey and black dots indicate the coordinates of the 5,000 polygons extracted from the Quebec Government 1:20k forest map (MRNF, 2015) and the five permanent plots of the latitudinal gradient. Orange and blue background colors represent the two different climates i.e. humid continental and subarctic according to the Köppen-Geiger classification identified by Beck et al. (2018).

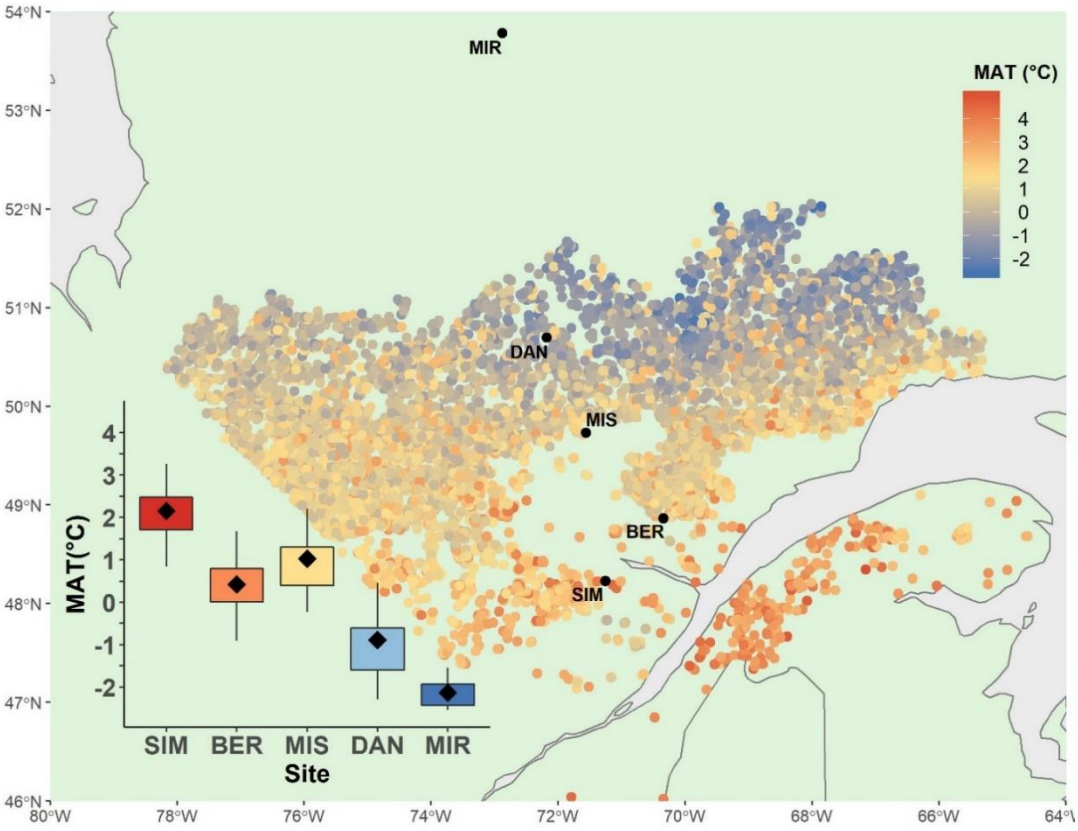

Figure 2.2 Spatial representation of mean annual temperature (MAT) for the extended study area and for the sites of the permanent plots located across the latitudinal gradient. In the inset plot, black diamonds represent mean values; lower and upper box limits represent the first and third quartiles, the whiskers extend to the most extreme data point that is no more than 1.5 times the interquartile range from the box.

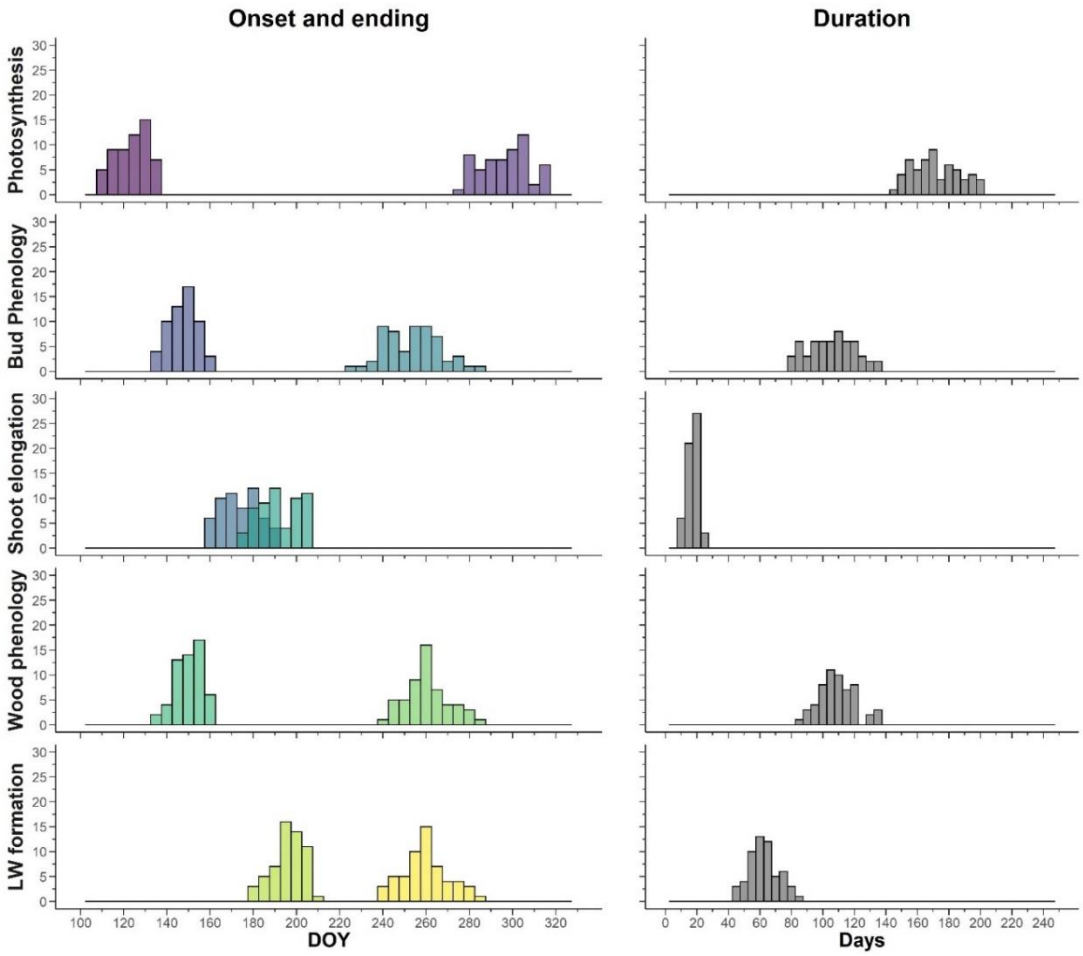

Figure 2.3 Frequency distributions of the timings of all phenological events during 2002-2016 for the five permanent plots across the latitudinal gradient. Bud phenology was extracted from NDVI data while timings of xylogenesis were derived from field observations. Shoot elongation and latewood (LW) formation are events of bud and wood phenology, respectively. The end of wood phenology matches with the end of latewood formation.

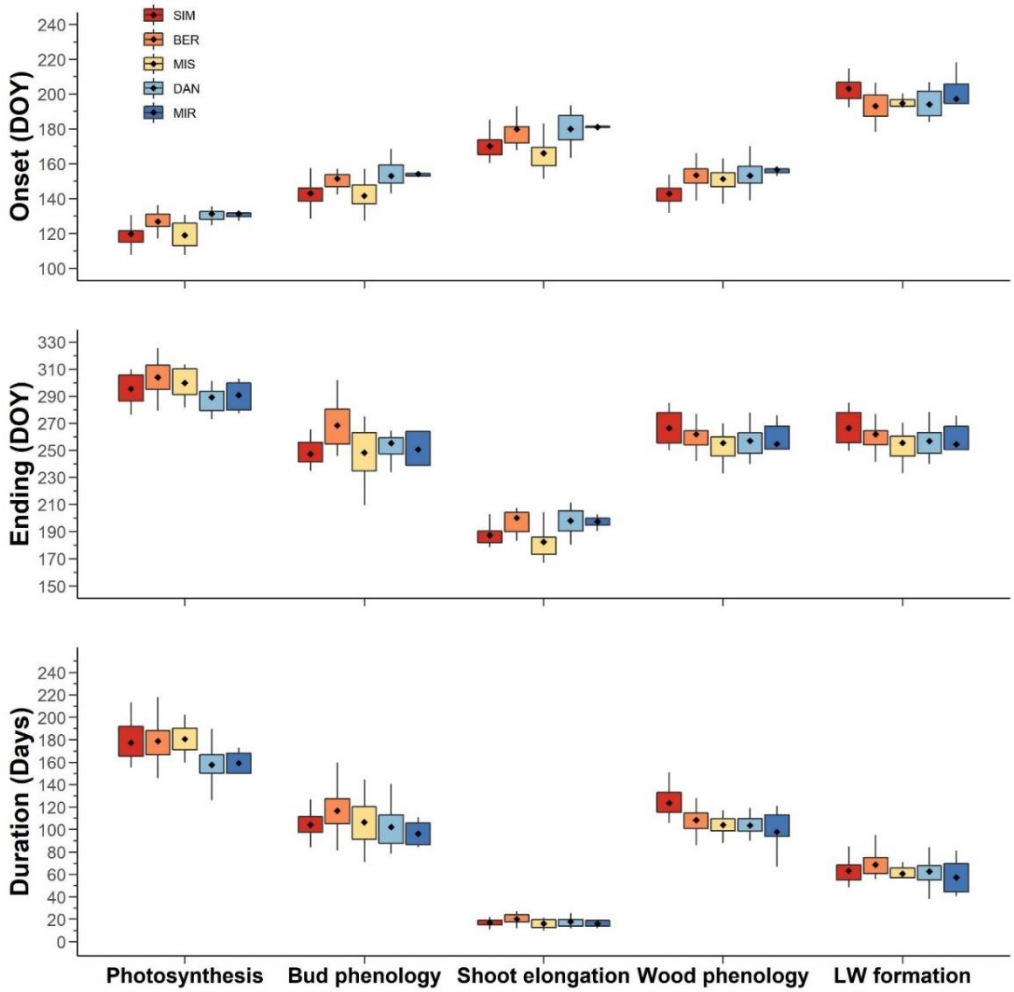

Figure 2.4 Box and whisker diagram of the timings of all phenological events during 2002-2016 for the five permanent plots of the latitudinal gradient. Permanent plots are ordered according to their latitude, from the warmest and southernmost site (SIM) to the coldest and northernmost one (MIR). Black diamonds represent mean values. Lower and upper box limits represent the first and third quartiles, which are subtracted or added, respectively, to the 1.5 × inter-quartile range to obtain upper and lower whisker lengths. Shoot elongation and latewood (LW) formation are events within bud and wood phenology, respectively.

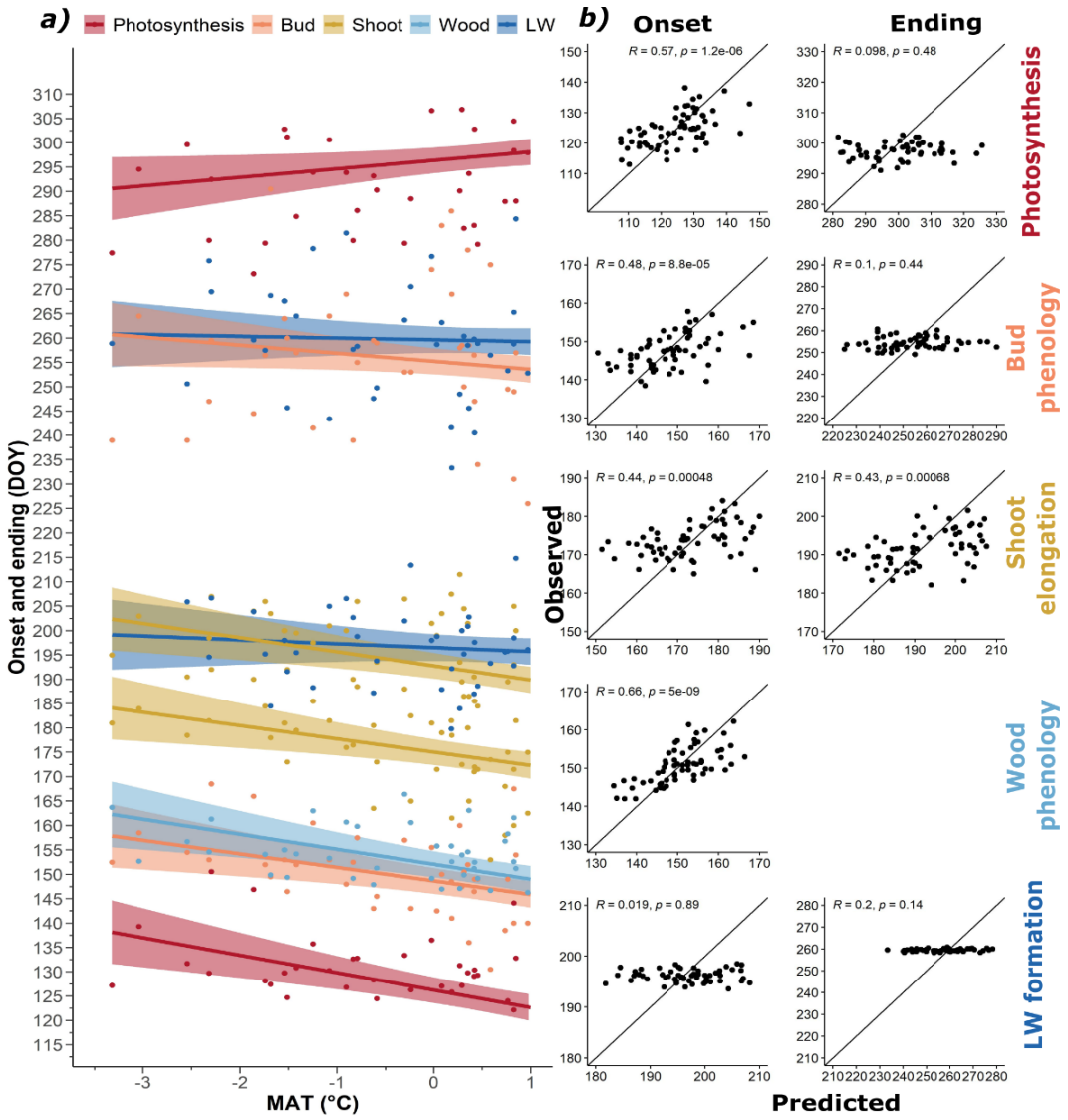

Figure 2.5 **a)** Relationships between mean annual temperature (MAT) and photosynthesis, bud and wood phenology, shoot elongation and latewood (LW) formation for the permanent plots of the latitudinal gradient (2002-2016). Dots represent the raw data. Colored lines and shading represent the fitted models and 0.95 confidence intervals, respectively; **b)** Correlations between observed and predicted timings of phenological events for the permanent plots of the latitudinal gradient (2002-2016) with the 1:1 bisector

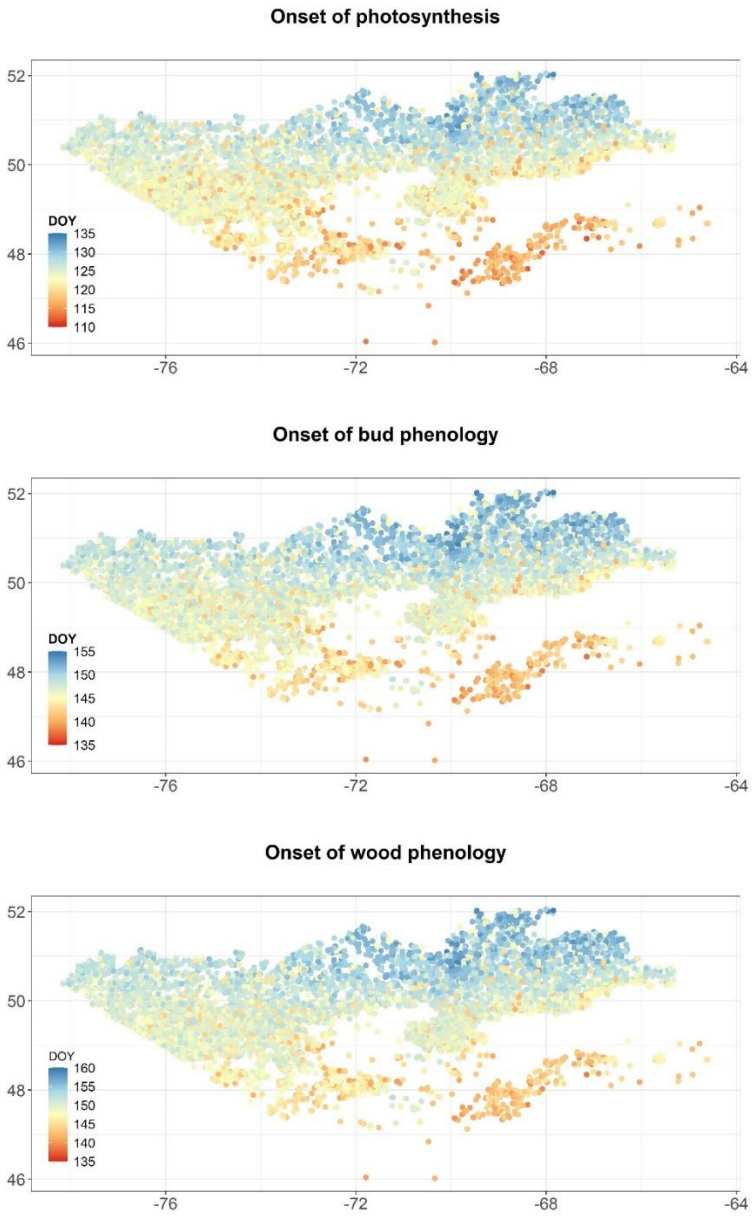

Figure 2.6 Predictions of phenological events as a function of mean annual temperature obtained from GLM, for the onset of photosynthesis, bud phenology and wood formation for the extended study area

2.8 Tables

Table 2.1 Average timing and standard deviation of all phenological events across the plots of the latitudinal gradient, with multiple comparison results (Dunn test). Events sharing the same letters are not significantly different.

Phenological event	DOY ± SD	Comparison
Onset of photosynthesis	125 ± 10	e
Onset of bud phenology	147 ± 9	a
Onset of wood phenology	151 ± 7	a
Onset of shoot elongation	174± 10	b
End of shoot elongation	192 ± 11	d
Onset of latewood formation	196 ± 8	d
End of bud phenology	254 ± 15	c
End of latewood formation	259 ± 12	c
End of photosynthesis	297 ± 13	f

Table 2.2 Results of the generalized linear model (GLM) relating photosynthesis, bud (with shoot elongation) and wood phenology with mean annual temperature (MAT) in the permanent plots of the latitudinal gradient from 2002-2016. Phenological events and mean annual temperature are used as covariates

Source of variation	Regressors			Model		
	Type I SS	**F-value**	**P**	**F-value**	**P**	**R^2**
Phenological event (PE)	1761357	1831.2	<0.001	871.6	<0.001	0.96
Mean annual temperature (MAT)	3665	35.0	<0.001			
Interaction (PE x MAT)	4874	5.1	<0.001			

Authors' contributions

VB and SR conceived the manuscript;

SK and SR extracted NDVI time series, historical climate data for the extended study area and bud phenology stages for both site of latitudinal gradient and extended study area;

VB processed the data of wood formation and historical climate for the latitudinal gradient, performed the statistical analysis, designed the figures and wrote the manuscript;

All authors discussed the results, and SK, GD, JDS, FG, AD, HM, SR commented on the manuscript;

All authors approved the final version of the manuscript.

2.9 References

Antonucci, S., Rossi, S., Deslauriers, A., Morin, H., Lombardi, F., Marchetti, M. & Tognetti, R. (2017) Large-scale estimation of xylem phenology in black spruce through remote sensing. Agricultural and Forest Meteorology, 233, 92–100.

Balzarolo, M., Vicca, S., Nguy-Robertson, A.L., Bonal, D., Elbers, J.A., Fu, Y.H., Grünwald, T., Horemans, J.A., Papale, D., Peñuelas, J., Suyker, A. & Veroustraete, F. (2016) Matching the phenology of Net Ecosystem Exchange and vegetation indices estimated with MODIS and FLUXNET in-situ observations. Remote Sensing of Environment, 174, 290–300.

Beck, H.E., Zimmermann, N.E., McVicar, T.R., Vergopolan, N., Berg, A. & Wood, E.F. (2018) Present and future köppen-geiger climate classification maps at 1-km resolution. Scientific Data, 5, 1–12.

Blechschmidt-Schneider, S. (1990) Phloem transport in Picea abies (L.) Karst. in mid-winter - I Microautoradiographic studies on 14C-assimilate translocation in shoots. Trees, 4, 179–186.

Buttò, V., Rossi, S., Deslauriers, A. & Morin, H. (2019) Is size an issue of time? Relationship between the duration of xylem development and cell traits. Annals of Botany, 123, 1257–1265.

Carbone, M.S., Czimczik, C.I., Keenan, T.F., Murakami, P.F., Pederson, N., Schaberg, P.G., Xu, X. & Richardson, A.D. (2013) Age, allocation and availability of nonstructural carbon in mature red maple trees. New Phytologist, 200, 1145–1155.

Cartenì, F., Deslauriers, A., Rossi, S., Morin, H., De Micco, V., Mazzoleni, S. & Giannino, F. (2018) The physiological mechanisms behind the earlywood-to-latewood transition: a process-based modelling approach. Frontiers in Plant Science, 9, 1053.

Chen, L., Hänninen, H., Rossi, S., Smith, N.G., Pau, S., Liu, Z., Feng, G., Gao, J. & Liu, J. (2020) Leaf senescence exhibits stronger climatic responses during warm than during cold autumns. Nature Climate Change, 10, 777–780.

Chuine, I., Aitken, S.N. & Ying, C.C. (2001) Temperature thresholds of shoot elongation in provenances of Pinus contorta. Canadian Journal of Forest Research, 31, 1444–1455.

Cleland, E.E., Chuine, I., Menzel, A., Mooney, H.A. & Schwartz, M.D. (2007) Shifting plant phenology in response to global change. Trends in Ecology and Evolution, 22, 357–365.

Cuny, H.E., Rathgeber, C.B.K.K., Kiessé, T.S., Hartmann, F.P., Barbeito, I. & Fournier, M. (2013) Generalized additive models reveal the intrinsic complexity of wood formation dynamics. Journal of experimental botany, 64, 1983–94.

Delpierre, N., Lireux, S., Hartig, F., Camarero, J.J., Cheaib, A., Čufar, K., Cuny, H., Deslauriers, A., Fonti, P., Gričar, J. & others (2018) Chilling and forcing temperatures interact to predict the onset of wood formation in Northern Hemisphere conifers. Global change biology, 25, 1089--1105.

Deslauriers, A., Fournier, M.P., Cartenì, F. & Mackay, J. (2019) Phenological shifts in conifer species stressed by spruce budworm defoliation. Tree Physiology, 39, 590–605.

Deslauriers, A., Huang, J.-G., Balducci, L., Beaulieu, M. & Rossi, S. (2016) The contribution of carbon and water in modulating wood formation in black spruce saplings. Plant Physiology, pp--01525.

Deslauriers, A., Morin, H. & Begin, Y. (2003) Cellular phenology of annual ring formation of Abies balsamea in the Quebec boreal forest (Canada). Canadian Journal of Forest Research, 33, 190–200.

Deslauriers, A. & Rossi, S. (2019) Metabolic memory in the phenological events of plants: Looking beyond climatic factors. Tree Physiology, 39, 1272–1276.

Dhont, P., Sylvestre, P., Gros-Louis, M.-C. & Isabel, N. (2010) Field Guide for Identifying Apical Bud Break and Bud Formation Stages in White Spruce. 17.

Du, J., He, Z., Piatek, K.B., Chen, L., Lin, P. & Zhu, X. (2019) Interacting effects of temperature and precipitation on climatic sensitivity of spring vegetation green-up in arid mountains of China. Agricultural and Forest Meteorology, 269–270, 71–77.

Fajstavr, M., Bednářová, E., Nezval, O., Giagli, K., Gryc, V., Vavrčík, H., Horáček, P. & Urban, J. (2019) How needle phenology indicates the changes of xylem cell formation during drought stress in Pinus sylvestris L. Dendrochronologia, 56, 125600.

Fournier, M.-P., Paré, M.C., Buttò, V., Delagrange, S., Lafond, J. & Deslauriers, A. (2020) How plant allometry influences bud phenology and fruit yield in two Vaccinium species. Annals of Botany.

Franceschini, T., Martin-Ducup, O. & Schneider, R. (2016) Allometric exponents as a tool to study the influence of climate on the trade-off between primary and secondary growth in major north-eastern American tree species. Annals of Botany, 117, 551–563.

Friend, A.D., Eckes-Shephard, A.H., Fonti, P., Rademacher, T.T., Rathgeber, C.B.K., Richardson, A.D. & Turton, R.H. (2019) On the need to consider wood formation processes in global vegetation models and a suggested approach. Annals of Forest Science, 76, 49.

Gallinat, A.S., Primack, R.B. & Wagner, D.L. (2015) Autumn, the neglected season in climate change research. Trends in Ecology and Evolution, 30, 169–176.

Gonsamo, A., Chen, J.M., David, T.P., Kurz, W.A. & Wu, C. (2012) Land surface phenology from optical satellite measurement and CO 2 eddy covariance technique. Journal of Geophysical Research: Biogeosciences, 117.

Hänninen, H. (2016) Boreal and Temperate Trees in a Changing Climate, Springer, Dordrecht, Dordrecht.

Hansen, J. & Beck, E. (1990) The fate and path of assimilation products in the stem of 8-year-old Scots pine (Pinus sylvestris L.) trees. Trees, 4, 16–21.

Hmimina, G., Dufrêne, E., Pontailler, J.Y., Delpierre, N., Aubinet, M., Caquet, B., de Grandcourt, A., Burban, B., Flechard, C., Granier, A., Gross, P., Heinesch, B.,

Longdoz, B., Moureaux, C., Ourcival, J.M., Rambal, S., Saint André, L. & Soudani, K. (2013) Evaluation of the potential of MODIS satellite data to predict vegetation phenology in different biomes: An investigation using ground-based NDVI measurements. Remote Sensing of Environment, 132, 145–158.

Kagawa, A., Sugimoto, A. & Maximov, T.C. (2006) 13CO2 pulse-labelling of photoassimilates reveals carbon allocation within and between tree rings. Plant, Cell and Environment, 29, 1571–1584.

Khare, S., Drolet, G., Sylvain, J.D., Paré, M.C. & Rossi, S. (2019) Assessment of spatio-temporal patterns of black spruce bud phenology across Quebec based on MODIS-NDVI time series and field observations. Remote Sensing, 11, 2745.

Kong, D., Zhang, Y., Wang, D., Chen, J. & Gu, X. (2020) Photoperiod explains the asynchronization between vegetation carbon phenology and vegetation greenness phenology. Journal of Geophysical Research: Biogeosciences.

Körner, C. (2012) Alpine treelines: functional ecology of the global high elevation tree limits,.

Lovett, G.M., Cole, J.J. & Pace, M.L. (2006) Is net ecosystem production equal to ecosystem carbon accumulation? Ecosystems, 9, 152–155.

Marquis, B., Bergeron, Y., Simard, M. & Tremblay, F. (2020) Probability of spring frosts, not growing degree-days, drives onset of spruce bud burst in plantations at the boreal-temperate forest ecotone. Frontiers in Plant Science, 11, 1031.

McKenney, D.W., Hutchinson, M.F., Papadopol, P., Lawrence, K., Pedlar, J., Campbell, K., Milewska, E., Hopkinson, R., Price, D. & Owen, T. (2011)

Customized spatial climate models for Canada. Bulletin of the American Meteorological Society, 92, 1611–1622.

Mevik, B.-H., Wehrens, R. & Liland, K.H. (2019) pls: Partial Least Squares and Principal Component Regression.

MRNF (2015) Norme de stratification écoforestière - Quatrième inventaire écoforestier du Québec méridional. Ministère des Forêts, de la Faune et des Parcs, Secteur des forêts.,.

Oleksyn, J., Zytkowiak, R., Karolewski, P., Reich, P.B. & Tjoelker, M.G. (2000) Genetic and environmental control of seasonal carbohydrate dynamics in trees of diverse Pinus sylvestris populations. Tree Physiology, 20, 837–847.

Oribe, Y., Funada, R. & Kubo, T. (2003) Relationships between cambial activity, cell differentiation and the localization of starch in storage tissues around the cambium in locally heated stems of Abies sachalinensis (Schmidt) Masters. Trees, 17, 185–192.

Piao, S., Tan, J., Chen, A., Fu, Y.H., Ciais, P., Liu, Q., Janssens, I.A., Vicca, S., Zeng, Z., Jeong, S.J., Li, Y., Myneni, R.B., Peng, S., Shen, M. & Peñuelas, J. (2015) Leaf onset in the northern hemisphere triggered by daytime temperature. Nature Communications, 6, 1--8.

R Core Team (2019) R: A Language and Environment for Statistical Computing.

Rossi, S., Anfodillo, T., Čufar, K., Cuny, H.E., Deslauriers, A., Fonti, P., Frank, D., Gričar, J., Gruber, A., Huang, J.-G.G., Jyske, T., Kašpar, J., King, G., Krause, C., Liang, E., Mäkinen, H., Morin, H., Nöjd, P., Oberhuber, W., Prislan, P., Rathgeber, C.B.K., Saracino, A., Swidrak, I. & Treml, V. (2016) Pattern of xylem phenology in

conifers of cold ecosystems in the Northern Hemisphere. Global change biology, 22, 3804–3813.

Rossi, S. & Bousquet, J. (2014) The bud break process and its variation among local populations of boreal black spruce. Frontiers in Plant Science, 5, 1–9.

Rossi, S. & Isabel, N. (2017) Bud break responds more strongly to daytime than night-time temperature under asymmetric experimental warming. Global Change Biology, 23, 446–454.

Rossi, S., Morin, H. & Deslauriers, A. (2011) Multi-scale influence of snowmelt on xylogenesis of black spruce. Arctic, Antarctic, and Alpine Research, 43, 457–464.

Schrader, J., Baba, K., May, S.T., Palme, K., Bennett, M., Bhalerao, R.P. & Sandberg, G. (2003) Polar auxin transport in the wood-forming tissues of hybrid aspen is under simultaneous control of developmental and environmental signals. Proceedings of the National Academy of Sciences, 100, 10096–10101.

Shen, M., Piao, S., Cong, N., Zhang, G. & Jassens, I.A. (2015) Precipitation impacts on vegetation spring phenology on the Tibetan Plateau. Global Change Biology, 21, 3647–3656.

Silvestro, R., Rossi, S., Zhang, S., Froment, I., Huang, J.G. & Saracino, A. (2019) From phenology to forest management: Ecotypes selection can avoid early or late frosts, but not both. Forest Ecology and Management, 436, 21–26.

Walker, X. & Johnstone, J.F. (2014) Widespread negative correlations between black spruce growth and temperature across topographic moisture gradients in the boreal forest. Environmental Research Letters, 9, 064016.

Weiner, J. (2004) Allocation, plasticity and allometry in plants. Perspectives in Plant Ecology, Evolution and Systematics, 6, 207–215.

White, M.A., Hoffman, F., Hargrove, W.W. & Nemani, R.R. (2005) A global framework for monitoring phenological responses to climate change. Geophysical Research Letters, 32, 1–4.

2.10 Authors' contributions

VB and SR conceived the manuscript;

SK and SR extracted NDVI time series, historical climate data for the extended study area and bud phenology stages for both site of latitudinal gradient and extended study area;

VB processed the data of wood formation and historical climate for the latitudinal gradient, performed the statistical analysis, designed the figures and wrote the manuscript;

All authors discussed the results, and SK, GD, JDS, FG, AD, HM, SR commented on the manuscript;

All authors approved the final version of the manuscript.

2.11 Acknowledgements

This work was funded by the Ministère des Forêts, de la Faune et des Parcs du Québec, NSERC Industrial Research Chair on Black Spruce Growth and the Influence of Spruce Budworm on Landscape Variability in Boreal Forests, the Canada Foundation for Innovation, the Consortium de Recherche sur la Forêt Boréale Commerciale, the Fonds de Recherche sur la Nature et les Technologies du Québec, and the Forêt d'Enseignement et de Recherche Simoncouche. The authors thank A. Garside for editing the English text and Roberto Silvestro for his comments to a first draft of the manuscript.

CHAPITRE II

IS SIZE AN ISSUE OF TIME? RELATIONSHIP BETWEEN THE DURATION OF XYLEM DEVELOPMENT AND CELL TRAITS

Published in Annals of botany

Citation: Buttò, Valentina, Sergio Rossi, Annie Deslauriers, and Hubert Morin. "Is size an issue of time? Relationship between the duration of xylem development and cell traits." Annals of botany 123, no. 7 (2019): 1257-1265.

ORIGINAL ARTICLE

IS SIZE AN ISSUE OF TIME? RELATIONSHIP BETWEEN THE DURATION OF XYLEM DEVELOPMENT AND CELL TRAITS

Valentina Buttò *(1), Sergio Rossi (1) (2), Annie Deslauriers (1), Hubert Morin (1)

1 Département des Sciences fondamentales, Université du Québec à Chicoutimi, Chicoutimi, QC, Canada
2 Key Laboratory of Vegetation Restoration and Management of Degraded Ecosystems, Guangdong Provincial Key Laboratory of Applied Botany, South China Botanical Garden, Chinese Academy of Sciences, Guangzhou, China

Running title: Xylem development and cell traits

*Corresponding author: Département des Sciences fondamentales, Université du Québec à Chicoutimi, 555, boulevard de l'Université, Chicoutimi (Québec), Canada G7H 2B1 Phone number: +1-418 545-5011 ext. 2330

Email: valentina.butto1@uqac.ca

3.1 Abstract

Background and Aims Secondary growth is a process related to the formation of new cells that increase in size and wall thickness during xylogenesis. Temporal dynamics of wood formation influence cell traits, in turn affecting cell patterns across the tree ring. We verified the hypothesis that cell diameter and cell-wall thickness are positively correlated with the duration of their differentiation phases.

Methods Histological sections were produced by microcores to assess the periods of cell differentiation in black spruce (*Picea mariana* (Mill.) B.S.P). Samples were collected weekly between 2002 and 2016 from a total of 50 trees in five sites along a latitudinal gradient in Quebec (Canada). The intra-annual temporal dynamics of cell differentiation were estimated at a daily scale, and the relationships between cell traits and duration of differentiation were fitted using a modified von Bertalanffy growth equation.

Results At all sites, larger cell diameters and cell-wall thicknesses were observed in cells that experienced a longer period of differentiation. The relationship was a nonlinear, decreasing trend that occasionally resulted in a clear asymptote. Overall, secondary wall deposition lasted longer than cell enlargement. Earlywood cells underwent an enlargement phase that lasted for 12 days on average, while secondary wall thickness lasted 15 days. Enlargement in latewood cells averaged 7 days and secondary wall deposition occurred over an average of 27 days.

Key Message Cell size across the tree ring is closely connected to the temporal dynamics of cell formation. Similar relationships were observed among the five study sites, indicating shared xylem formation dynamics across the entire latitudinal distribution of the species.

Conclusions The duration of cell differentiation is a key factor involved in cell growth and wall thickening of xylem thereby determining the spatial variation of cell traits across the tree ring.

Keywords: Cell differentiation, cell diameter, cell-wall thickness, cell enlargement, modelling, growth, *Picea mariana*, temporal dynamics, timing, wall thickening, xylogenesis

3.2 Introduction

Secondary growth in trees is at the base of biomass production and forest productivity. In extratropical ecosystems, tree growth is the result of an annual process of xylem formation that engenders the production of new cells, and whose traits influence volume quantity and quality of the resulting wood. In conifers, cell traits change across the tree ring leading to the formation of larger thin-walled cells, followed by smaller thick-walled cells (Schweingruber 2012). This transition can occur more or less gradually, depending on the species and cell origin—as either earlywood or latewood (Denne 1989). Despite this arbitrary and simplistic categorization, the spatial pattern across the tree ring involves substantial changes in wood properties and the hydraulic capacity of the cells (Domec and Gartner 2002; Chave *et al.* 2009; Fonti *et al.* 2010). The mechanism underlying the gradual transition between earlywood and latewood can be strongly endogenous, involving complex developmental dynamics (Cuny and Rathgeber 2016; Cartenì *et al.* 2018).

During xylem formation, auxins are a major driver of vessel differentiation along the tree trunk and across its radial section (Aloni and Zimmermann 1983; Aloni 2013). However, recent experimental and modelling studies have questioned the major role of auxins in earlywood–latewood transition, as initially hypothesized by Larson (1960). In these studies, earlywood–latewood transition could not be explained by major changes in auxin concentrations; the concentrations were less

than the threshold of detectability during latewood formation, and auxins failed to rebuild the decreasing latewood cell sizes in model simulations (Uggla *et al.* 2001; Hartmann *et al.* 2017; Fajstavr *et al.* 2018). Developmental dynamics are thus suggested as the most direct drivers of changes to tracheid size across the tree ring, whereas auxins maintain a fundamental role in regulating cambial growth and cell enlargement.

Apart from some recent meta-analyses (Rossi *et al.* 2013; Cuny *et al.* 2014), there have been few studies investigating changes in the intra-annual secondary growth of a given species across a wide geographical scale (Rossi *et al.* 2015). Cell enlargement and wall thickening, the two main phases of tracheid differentiation, involve different physiological needs; these needs are fulfilled by developmental or environmental factors that change over the growing season (Deslauriers *et al.* 2016; Cuny and Rathgeber 2016; Balducci *et al.* 2016). The temporal dynamics of these two phases have long been known to be key factors in xylem formation (Skene 1969; Denne 1971; Wodzicki 1971), and, more recently, multiple studies have shown that the duration of these two differentiation phases influences cell size across the tree ring (See Deslauriers *et al.* 2017 for a review).

Anfodillo *et al.* (2011) observed a linear relationship between a cell trait and the duration of cell formation processes by noting that larger initial earlywood cells along the stem were coupled with a longer duration of cell enlargement. Cells

growing at the base of the stem were larger than ones at the treetop as cells lower in the stem had a longer duration of formation. In a three-year study, Cuny *et al.* (2014) found a linear relationship between the duration of enlargement and cell diameter for all cells in a tree ring; however, they did not find any relationship between duration and cell-wall thickness. Using a single-cell growth model, Cartenì *et al.* (2018) simulated the relationship between cell traits and the duration of their differentiation phases. They modelled a nonlinear trend where cell-trait size increased linearly with the duration of different phases but then reached a plateau beyond a certain point. This new insight vis-à-vis the temporal dynamics of cell-trait development illustrates that our understanding of wood formation remains incomplete. It also confirms that xylogenesis is a complex process depending on many factors that may result in nonlinear patterns, as has been observed for other biological processes (Cushing *et al.* 2002).

The nonlinear pattern observed by Cartenì *et al.* (2018) was, however, limited to single cells. Ideally, confirming this relationship between cell traits and the length of the differentiation phases requires a large number of observations at an intra-annual resolution. Since the monitoring of xylogenesis requires weekly sampling, longer time series are rare and difficult to obtain. Furthermore, a mathematical relationship explaining univocally the relationship between cell traits (i.e. dimension of lumen, cell wall, etc.) across the entire tree ring and their temporal dynamics has never been quantified. More specifically, the duration of cell enlargement and wall

formation varies over the growing season (Deslauriers *et al.* 2003; Rossi *et al.* 2006a; Moser *et al.* 2009), yet this relationship remains unclear (Cuny *et al.* 2014).

This study aims to determine the relationship between cell traits and the duration of their differentiation phases. We test the hypothesis of a positive linear correlation between cell traits (i.e. cell diameter and cell-wall thickness) and the duration of cell differentiation (i.e. enlargement and wall formation). For this, we monitored xylogenesis in individuals of black spruce (*Picea mariana* Mill. B.S.P.) from 2002–2016, sampled from five sites located across the species' entire latitudinal distribution across Quebec (Canada). To incorporate the complexity of the xylogenesis and its influence on cell traits, we applied a novel approach to the study of xylem formation (Cuny *et al.* 2013; Balducci *et al.* 2016). Our unique and lengthy dataset permits a robust analysis and allows for a deeper understanding of the influences of temporal dynamics on cell traits.

3.3 Materials and methods

3.3.1 Study sites and tree selection

The study area covers a latitudinal gradient stretching from 48°–53°N across the boreal forest of Quebec, Canada (Table 3.1). All sample sites are in even-aged, uniform, adult stands dominated by black spruce. Two sites (SIM and BER) are located in the balsam fir (*Abies balsamea* L. Mill.)–white birch (*Betula papyrifera*

Marsh.) bioclimatic domain. Two others (MIS and DAN) lie in the black spruce–moss bioclimatic domain. The most northern site (MIR) falls in the spruce–lichen domain and is characterized by a lower tree density (Rossi *et al.* 2015). Mean annual temperature along the gradient ranges between 1.6 and 4.1 °C; the sites are progressively cooler moving northward (Table 1). In summer, mean temperatures range from 11.1–14.6 °C, with a progressively shorter growing season toward the most northern site (Table 3.1). Annual precipitation decreases northward along the gradient from 1162 to 827 mm (Rossi *et al.* 2015).

3.3.2 Timing and duration

At each site, we selected ten dominant or co-dominant trees having upright stems and relatively larger diameters (Table 3.1). Trees with polycormic stems, partially dead crowns, reaction wood or evident damage due to parasites were avoided. In the four lower latitude sites of the latitudinal gradient, we collected one microcore per tree weekly, occasionally fortnightly, from April–October (2002–2016). Microcore sampling was done with surgical bone needles (2002–2007) or Trephor (2007–2016) (Rossi *et al.* 2006b). The northernmost site (MIR) was sampled following the same protocol but was sampled only from 2012–2016.

To avoid the development of resin ducts, samples were collected at least 10 cm apart from each other (Deslauriers *et al.* 2003). The microcores were dehydrated through successive series of immersions in ethanol and D-limonene. The microcores

were embedded in paraffin, cut into 8 μm cross sections (i.e. transversal sections) and stained with cresyl violet acetate (0.16 % in water) (Rossi *et al.* 2006b). We discriminated between developing and mature tracheids under visible and polarized light at magnifications of 400–500×. Cells were classified as i) enlarging, ii) thickening and lignifying or iii) mature. Cells were counted across three radial rows (Deslauriers *et al.* 2003). The enlargement zone was characterized by the absence of glistening under polarized light; this indicates the presence of only primary cell walls. Cells undergoing secondary cell-wall formation glistened under polarized light. Cresyl violet acetate reacts with lignin, turning from violet to blue in mature cells. Maturation was reached when the cell walls were entirely blue (Rossi *et al.* 2006a).

3.3.3 Xylem-cell anatomy

Two additional microcores per tree were collected in the summer of 2017. These samples were prepared following the above-mentioned protocol, stained with safranin (1 % in water) and fixed on slides with a mounting medium. Digital images of the tree ring cross sections were collected using a camera fixed on an optical microscope at a magnification of 20×. We measured lumen area, lumen diameter and cell-wall thickness (single wall) along at least 30 radial cell rows per tree ring using Wincell (Regent instruments, Canada). Tracheids having lumen smaller than 2 × cell-wall thickness were considered as latewood (Filion and Cournoyer 1995). A summary of

the performed measurements for the xylogenesis and wood anatomy datasets is provided in Table S1.

3.3.4 Statistical analysis

We applied generalized additive models (GAMs) for each site to assess the temporal dynamics of the differentiation phases and to produce the tracheidograms (Figure supplementaire 3.1). The assessment of the temporal dynamics was based on Cuny *et al.* (2014) and Balducci *et al.* (2016). The raw data provided the number of cells produced at each differentiation phase at the sampling times (Figure supplementaire 3.1). These data, computed for 10 individuals per site, were averaged by year and by site before modelling the temporal dynamics.

We fitted GAMs with splines to the xylogenesis data to obtain three curves that describe the daily sequence of cell production for the three differentiation phases, i.e. i) enlargement, ii) secondary wall deposition and iii) maturation. The timing (the onset for each phase) was extracted from the three curves as the day when each cell position underwent a differentiation phase. The duration of enlargement and wall formation was defined as the difference between the onset of one phase and the onset of the successive phase (Fig. S1).

The tracheidograms of lumen area, lumen diameter and cell-wall thickness were obtained based on the percentile position of the cells across the tree ring. Using

the GAMs, we measured cell traits along multiple radial cell rows. We then averaged the standardized percentiles of their horizontal position to provide average sizes (Figure supplementaire 3.1). We computed cell diameter as the sum of the lumen diameter and 2 × single cell-wall thicknesses.

The relationship between dynamics (duration of enlargement and cell-wall formation) and cell traits (cell diameter and cell-wall thickness) was described as a yearly average by applying a modified von Bertalanffy growth equation according to the formula:

$$y = a \times (1 - e^{-k(x-b)})$$

where *a*, *k* and *b* represent the asymptote, growth rate and horizontal intercept, respectively. The fit was validated visually using the distribution of the residuals, and, when required, parameters were adjusted with lower or upper bounds to improve the overall fit. Statistics were performed running the *mgcv* (Wood 2017), *nls* and *stats* packages in R (R Core Team 2017).

3.4 Results

3.4.1 Cell traits

GAMs described very well the changes in anatomical traits across the tree ring, summarizing the inter-annual variability in a single curve per site (Figure supplementaire 3.2). The lowest variability was observed at MIR due to fewer years of sampling (Figure supplementaire 3.2). Overall, lumen area ranged from 42–741 μm^2, gradually decreasing in size from 20% of the tree ring (Figure. 3.1). The largest and smallest lumen areas were measured at SIM and BER, the two southernmost sites. Cell diameter ranged from a minimum of 11 µm to a maximum of 34 µm. Cell diameter showed a similar pattern to lumen area; at most sites, maximum cell diameter occurred at ca. one fifth of the way across the tree ring. Cell-wall thickness increased through the tree ring, starting at an initial thickness of 1.91 µm and reaching a maximum thickness of 4.73 µm at about four fifths of the way across the tree ring. SIM showed a different pattern, as cell-wall thickness increased gradually throughout the tree ring.

3.4.2 Timing and duration of xylogenesis

The timing of the onset of the differentiation phases varied along the gradient. The earliest activities were in the southernmost site although the delays did not follow a linear pattern along the latitudinal gradient in relation to the latitude of the sample

sites (Figure. 3.3). The earliest onset of cell enlargement was observed at SIM at the end of May (DOY 145) and then ten days later in BER, DAN and MIR. At MIS, cells began enlarging on DOY 153. Similarly, cell-wall formation began earlier in SIM (DOY 157) and seven days later in MIR (DOY 164) with DAN being the last site to begin cell-wall deposition (DOY 169). Mature tracheids were also observed earlier in SIM (DOY 173) compared to DAN (DOY 184), which was the last site to achieve this stage. Xylem cells completed their maturation earliest on DOY 231 at MIR and 32 days later at SIM (DOY 263). The percentage of latewood also varied along the gradient, from 15–27 %. The lowest and highest latewood percentages were calculated for MIR and BER, respectively. The duration of cell differentiation showed a similar pattern between sites, with the exception of MIR (Fig. 3). Cell enlargement lasted 12–14 days for the first xylem cells, and it decreased to 4–5 days for the final cells of the tree ring. The duration of enlargement at MIR was strongly affected by the smaller period of observation (2012–2016) that amplified the effect of a different dynamic observed for one year, 2014, for which we had only nine days of observations. The duration of enlargement in MIR was eight days for the first cells. This peaked at 40 % of the tree ring, when cells enlarged for 12 days, then reached the minimum of four days over the last percentile of the tree ring. Cell-wall formation showed an opposite trend; its duration increased across the tree ring. The duration of wall formation varied across the tree ring, starting from a minimum of 17 days in earlywood and peaking at 32 days in latewood. Minimum and maximum total duration of xylem formation occurred at 50 % and 100 % of the tree ring,

respectively. The length of xylem formation in MIR was different, however, as the duration gradually decreased across the tree ring (Figure. 3.3). On average, the length of the growing season decreased with increasing latitude, ranging from 118 days at SIM to 76 days at MIR.

3.4.3 Relationship between cell traits and the duration of development

The modified von Bertalanffy equation represented very well the relationship between cell traits and the duration of cell differentiation at each site (Figure. 3.4). The pattern was clear: both cell traits increased along with a longer duration of development. Decreasing rates of growth were observed, which resulted in an asymptote. The standardized residuals were symmetrically distributed; this confirmed the good fit of the regressions. Overall, 97% of the standardized residuals were located within the -2 to 2 range, demonstrating that the model suitably represented the data (Figure supplementaire 3.3).

3.4.4 Cell diameter versus the duration of enlargement

The asymptote A ranged from 33.37–47.63, with the lowest and highest values being estimated for MIR and DAN, respectively (Table 2). This last value was slightly overestimated, as shown by the visual fitting and the larger error of the resulting parameter (Table 2). The growth rate K ranged from 0.09, detected at MIS and DAN, to 0.19 at MIR. The intercept B ranged from -1.77 to 1.64, for SIM and BER,

respectively (Table 2). Overall, cells enlarged 3 µm·day^{-1}. Earlywood cells averaged 29 µm in diameter; such a size was achieved in 11 days. Latewood cells required six days to reach a mean diameter of 24 µm (Figure 3.4). On average, the enlargement of earlywood cells required three more days than the enlargement of latewood cells. No latitudinal pattern was observed in the estimated parameters of the enlargement phase.

3.4.5 Cell-wall thickness versus the duration of wall formation

The asymptote A ranged from 3.98 for MIR to 4.87 for BER (Table 3.2). This parameter followed the latitudinal gradient, decreasing toward the north; BER, which showed the highest asymptote, was the exception to this pattern. In general, the growth rate K was lower than that estimated for cell diameter, with values ranging between 0.07—detected at BER and SIM—and 0.21, calculated for MIR. Compared to cell diameter, the horizontal intercept B was higher for cell-wall thickness, ranging from 5.78 to 10.40 for BER and MIR, respectively (Table 3.2). In the two southern sites, a cell-wall thickness of 3 µm was reached after 20 days, a longer duration than in the northern sites. For MIR, the model was adapted by using a higher limit for A. This limit improved the fit of the regression, but it generated a modest underestimation of cell-wall thicknesses, as revealed by the residuals (Figure supplementaire. 3.2). Earlywood cell walls had an average thickness of 2 µm after 15 days, while latewood cell walls averaged 3 µm thick after 22 days.

3.5 Discussion

This study assessed the intra-annual dynamics of xylem formation in adult black spruce trees across a wide latitudinal range. Based on 15 years of observations, our dataset tested the hypothesis that cell traits are positively and linearly correlated with the duration of their differentiation phases. The initial hypothesis was only partially accepted; longer differentiation phases (i.e. cell enlargement and cell-wall formation) resulted in larger sizes (i.e. cell diameter and cell-wall thickness). However, we found a nonlinear relationship.

3.5.1 The influence of the duration of enlargement on cell size changes across the tree ring

From the observed nonlinear relationship (i.e. modified von Bertalanffy), our analysis shows that the maximum size of growing tracheids is limited at longer durations. Until this study, there was only a partial understanding of the relationship between cell size and duration of cell developmental stages across a radial section of a tree trunk. Anfodillo *et al.* (2011) demonstrated that different durations of enlargement could explain the size decrease of the first earlywood cells—produced by cambial reactivation—downwards along the stem. Indeed, the larger cells located at the base of the tree stem grew for a longer period than the smaller treetop cells to form a tapering pattern. In addition, based on three years of observation, Cuny *et al.* (2014) assessed a species-specific linear relationship between cell size and the duration of their

enlargement across the radial pattern. Cells across the tree ring increased linearly in size as the duration of enlargement increased (i.e. a linear relationship) (Cuny *et al.* 2014). Our dataset, however, that involved cells that were heterogeneous in size allowed us to better describe this relationship. Indeed, by modelling the cell growth of a single cell, Cartenì *et al.* (2018) found a nonlinear relationship over which longer durations did not necessarily correspond to increasing cell sizes. Therefore, by considering all the cells that form a tree ring and relying on a dataset covering several years, it was possible to describe a nonlinear relationship between cell diameter and the duration of enlargement.

Our data shows that cells increase initially in size as the duration of enlargement is greater. After a given period, cell growth gradually slows down and then ceases. Cell diameter then remains unchanged even if cells could continue to grow. We hypothesize that cell size growth is constrained by physiological and biomechanical constraints. Cell enlargement results from a combination of DNA replication, i.e. endoreplication and cell expansion (Perrot-Rechenmann 2010). The latter process occurs when enough water is absorbed to exceed the wall-yielding threshold pressure (Genard *et al.* 2001). During cell differentiation, the deposition of several layers of secondary walls stiffens cell walls and progressively reduces the cell's capability to enlarge (Dünser and Kleine-Vehn 2015). The loss of flexibility, due to the deposition of secondary walls, stops cell expansion.

This ceasing of cell expansion arrives later in earlywood than in latewood, thereby explaining their different cell sizes (Cartenì *et al.* 2018). During the initial phase of the growing season, the priority of primary (leaf) growth over secondary (wood) growth along the stem results in a low availability of sugars for the xylogenesis (Cartenì *et al.* 2018). In our model, cell size increases as the period of differentiation lengthens; however, secondary walls are deposited slowly, eventually constraining cell enlargement after about 15 days. During the second part of the growing season, the deposition of secondary walls is faster as there is a higher quantity of sugars available for radial growth; this results in a more rapid loss of cell flexibility in latewood. For smaller cell sizes, the growth of the primary wall will constrain size only after five days of differentiation, resulting in latewood cells that are smaller than the earlywood cells. According to our model, the maximum duration of cell expansion, which corresponds to the mean theoretical asymptote, is 35 days (combining all sites together).

The relationship between the duration of enlargement and cell size may also play an important role in maintaining hydraulic safety. A shorter period of enlargement produces smaller cells that avoid cavitation more easily. We estimate that a maximum duration of enlargement of 16 days in black spruce will produce cells 30–36 µm in diameter. For temperate climates, Cuny *et al.* (2014) calculated that the largest cells of Norway spruce, Scots pine and silver fir had diameters of 50 µm after an average of 18 days. Therefore, two additional days of cell enlargement for these temperate species added 20 µm in cell diameter relative to our colder sites. We speculate that the duration

of enlargement and the resulting cell diameter is species-specific given that this trait is highly important in the trade-off between water transport efficiency and hydraulic safety. Larger conduits have a higher hydraulic efficiency, but they are more vulnerable to cavitation (Pitterman *et al.* 2006). In cold climates, bubbles generated by freezing-induced embolism are also more difficult to eliminate when conduits are larger (Pittermann and Sperry 2003). Consequently, as we observed in the boreal forest, early spring cells grow for less time than cells growing in a temperate climate, thereby avoiding the increased risk of cavitation linked to larger cell sizes. The smaller early spring cells of the cooler boreal forest are also less prone to damage from freeze-thaw events.

In our study, we assessed a relationship that fully represents the dynamics of both earlywood and latewood cells and that applies to a wide geographical area. Nevertheless, the latitudinal gradient did not appear to affect the distribution of cell sizes. Indeed, even if the northernmost site had the lowest asymptote along the latitudinal gradient (33 µm at MIR), the other sites showed similar asymptotic values (42 µm on average). Water availability should drive directly cell enlargement, but it affects cell growth significantly only when water becomes a limiting factor (Cuny and Rathgeber 2016; Prislan *et al.* 2018). We may not have observed climatic determinism in cell enlargement as water is not a limiting factor along our study's latitudinal gradient (Table 1). However, evidence provided by rain exclusion experiments performed at our study sites (except MIR) highlight a limited influence of water stress

on black spruce growth and tracheid anatomy (Belien *et al.* 2012). When comparing xylogenesis in black spruce growing in parcels having or lacking rain, Belien *et al.* (2012) observed that timing and xylem growth were not affected by induced water stress; this stress produced only slightly smaller cells. The high resilience of this cell trait is caused by adjustments in the duration and rate of cell enlargement and secondary wall deposition and lignification that mostly counterbalances any effect of water stress (Balducci *et al.* 2016).

The relationship we observed confirms many previous findings related to the quantitative aspects of xylogenesis in conifers. In Scots pine, the duration of enlargement was estimated at 21 days for the initial tree-ring cells, decreasing to 10 days for the final cells (Wodzicki 1971). Deslauriers *et al.* (2003) observed that cell enlargement in balsam fir lasted less than a week for earlywood cells, whereas it was more than a week for latewood cells. In three European species of the alpine timberline, European larch, stone pine and Norway spruce, Rossi *et al.* (2006)a found that cell enlargement occurred over an average of 20 days for the first earlywood cells, decreasing to a few days for the final latewood cells. More recently, a model of Cartenì *et al.* (2018)—calibrated using stone pine, Norway spruce, European larch and black spruce—estimated an average duration of 18.8 days for the first earlywood cells and 5.9 days for the final latewood cells.

3.5.2 Cell-wall size is linked to the duration of cell-wall deposition

In general, cell-wall deposition depends linearly on the duration of earlywood formation. However, during latewood cell formation, cell-wall thickness does not increase proportionally with duration. Across our latitudinal gradient, latewood cell differentiation begins when cell-wall deposition reaches 20–40 days. Uggla *et al.* (2001) observed that in latewood, cell formation was tightly linked to a longer period of wall material deposition, not its rate. Since carbohydrate availability did not change significantly during the growing season, Uggla *et al.* (2001) deduced that this could not be a trigger for latewood formation and proposed that latewood formation was under developmental control. Further studies found that the increase in cell-wall thickness was synchronous with the increasing availability of polysaccharides over the growing season, reassessing the role of sugars in the earlywood–latewood transition (Deslauriers *et al.* 2016; Cartenì *et al.* 2018). In our results, the duration of wall formation severely affects cell-wall thickness in the first part of the tree ring. This influence decreases across the tree ring, where other factors slow down cell-wall thickness deposition until bringing it to a complete halt.

The more abrupt decrease in cell-wall thickness at longer durations could be linked to cell maturation and cell death. Groover and Jones (1999) indicate that cell death is activated when a critical amount of secondary wall is attained. The joint action of secondary-wall precursors and protease induces calcium accumulation within a cell and generates vacuole collapse, occurring after about 6 h (Groover and Jones 1999).

As secondary cell-wall formation exerts a control on cell death, the deposition of cell-wall material abruptly slows down at longer durations. Interestingly, the maximum duration of secondary cell-wall formation predicted by our model averaged 45 days, a value that was always observed along our latitudinal gradient. We thus propose that programmed cell death is involved in the faster attainment of the asymptote, contrary to cell enlargement, where it is reached more slowly.

We observed that maximum cell-wall thickness, which is reached in latewood, follows a temperature gradient. Latewood cells, generally constituting the final portion of the annual tree ring, are more sensitive to temperature than earlywood cells (Cuny and Rathgeber 2016). Warmer conditions induce a thicker cell wall because they are linked to a longer growing season during which trees have more time to assimilate carbon (Fonti *et al.* 2013). Furthermore, warmer temperatures correspond to larger earlywood cells that allow a better assimilation of carbon due to their higher hydraulic efficiency (Fonti *et al.* 2013). Evidence of the link between temperature and cell traits was also found by Deslauriers *et al*. (2008) who observed that the high temperatures experienced by trees at treeline in 2003 induced a longer period of secondary-wall deposition, which resulted in thicker cell walls. In our results, the values achieved by the asymptotes suggest that the maximum cell-wall thickness reached at each site followed the latitudinal gradient. Trees growing at the southern sites produced thicker cell walls in latewood than trees growing at the more northern sites.

The observed duration for cell-wall deposition in our study also agrees with previous estimates for boreal species, with latewood requiring a longer period of cell-wall formation than earlywood (Wodzicki 1971; Deslauriers *et al.* 2008; Lupi *et al.* 2011). In three conifer species in France, the duration of secondary-wall formation increased from 20 to 55 days across the tree ring (Cuny *et al.* 2014). Compared to earlywood, Deslauriers *et al.* (2003) observed that the time required by balsam fir to complete cell-wall formation was 10–15 days longer in latewood. Cartenì *et al.* (2018) estimated an average duration of cell-wall formation ranging from 16–35 days, depending on the position of the cell within the tree ring. The duration of wall formation increases during the growing season with the final latewood cells requiring up to 40 days to complete this differentiation phase (Deslauriers *et al.* 2008; Lupi *et al.* 2011).

3.6 Conclusions

In this study, we demonstrated the relationship between temporal dynamics of cell differentiation and cell traits. We tested and confirmed the hypothesis that the intra-annual growth in cell traits increases in a nonlinear fashion with the duration of differentiation. Despite the wide geographical scale analysed, involving the broad latitudinal distribution of black spruce in Quebec, Canada, we were able to assess a general pattern that occurs independently of the variable site conditions. We found that cell growth and cell-wall thickening reach a plateau, beyond which cell traits remain stable, independent of the duration of differentiation. Even if the existence of

this nonlinear pattern confirms the complexity of xylogenesis, we found a relationship that emphasizes the different biological mechanisms between earlywood and latewood cells. These findings provide a more integrated knowledge of xylogenesis and its developmental dynamics. In particular, we demonstrated that duration of cell differentiation is a key factor that has a major role in establishing the final traits of xylem cells.

3.7 Tables

Table 3.1 Location, environmental conditions and average characteristics of the sampled trees at the five study sites, sites ordered in terms of latitude

Site	Latitude	Longitude	Altitude (m asl)	Annual temperature	May–September temperature	Tree height (m)	Tree DBH (cm)	Annual precipitation (mm)
SIM	48°13′	71°15′	338	1.9	13.3	16.1 ± 1.2	20.4 ± 2.4	1162
BER	48°51′	70°20′	611	0.2	11.4	17.3 ± 1.8	21.1 ± 3.7	1109
MIS	49°43′	71°56′	342	0.7	12.8	18.3 ± 1.1	19.6 ± 2.8	1009
DAN	50°41′	72°11′	487	−1.2	11.0	16.6 ± 2.2	18.5 ± 2.9	1006
MIR	53°47′	72°52′	384	1.6	11.1	13.1 ± 1.2	19.6 ± 3.0	827

DBH: diameter at breast height

Table 3.2 Parameters of the von Bertalanffy-modified equation for cell diameter versus duration of cell enlargement and cell-wall thickness versus duration of wall formation. The parameters *a*, *k* and *b* represent the asymptote, growth rate and horizontal intercept, respectively

Cell traits	**Sites**	***a***	***k***	***b***
Cell diameter	SIM	42.36 ± 4.28	0.11 ± 0.03	-1.77 ± 0.94
	BER	37.18 ± 3.79	0.17 ± 0.05	1.64 ± 0.65
	MIS	42.58 ± 9.78	0.09 ± 0.05	-0.99 ± 1.57
	DAN	47.63 ± 11.81	0.09 ± 0.05	0.37 ± 1.03
	MIR	33.37 ± 2.45	0.19 ± 0.07	-1.43 ± 1.34
Cell-wall thickness	SIM	4.85 ± 0.38	0.07 ± 0.01	6.08 ± 1.59
	BER	4.87 ± 0.43	0.07 ± 0.02	5.78 ± 1.88
	MIS	4.02 ± 0.17	0.17 ± 0.05	10.16 ± 1.64
	DAN	3.84 ± 0.15	0.15 ± 0.03	8.01 ± 1.25
	MIR	3.98 ± 0.61	0.21 ± 0.10	10.40 ± 0.82

Supplementary table 3.1 Summary of the xylogenesis and wood anatomy measurements with their respective years of sampling at each site. The average number of sampling weeks as well as the average number of microcores sampled by year constituting the dataset was calculated. With this number of microcore samples each year, the cumulative number of cells for each differentiation phase was counted annually. Fewer cells in the enlargement phase (i) are usually computed because of the early peak of enlargement activity that occurs at the beginning of the growing season when the most of cells have not yet been produced. In the dataset for cell anatomy, the average number of cells measured automatically ranged between 6/1000 and 13/1000 of all measured cells

Xylogenesis							**Wood anatomy**
Site	**Years of sampling**	**Avg. # Sampled weeks**	**Avg. # of microcores sampled**	**Cumulated Avg. # of cells manually computed in the differentiation phase/week**			**Avg. # cells measured/year**
				i	**ii**	**iii**	
SIM	2002–2016	23	230	63	215	627	13900
BER	2002–2016	19	190	33	256	1135	12290
MIS	2002–2016	20	200	82	92	532	7270
DAN	2002–2016	19	190	25	116	598	6090
MIR	2012-2016	20	200	61	107	832	13190

3.8 Figures

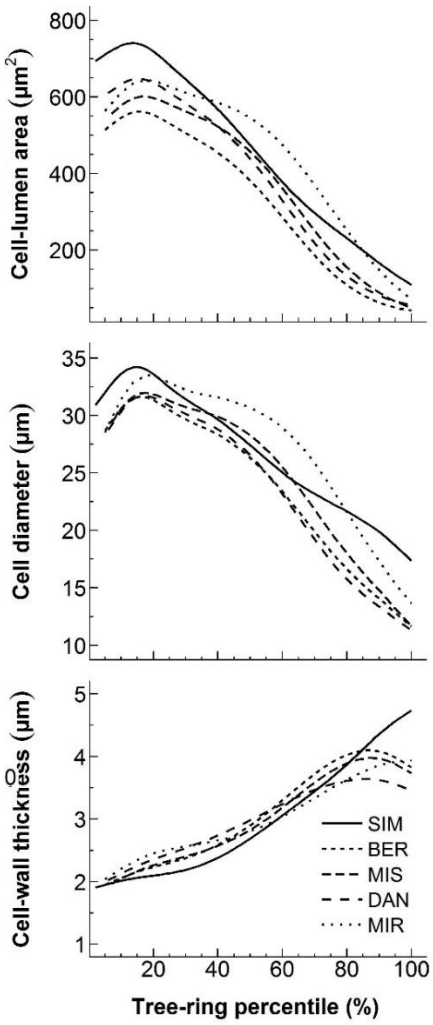

Figure 3.1 Tracheidograms of black spruce from five sites distributed along a latitudinal gradient across the closed boreal forest of Quebec, Canada. Each tracheidogram represents the average intra-annual variation of cell traits over the years of study for each site as described in Table 1.

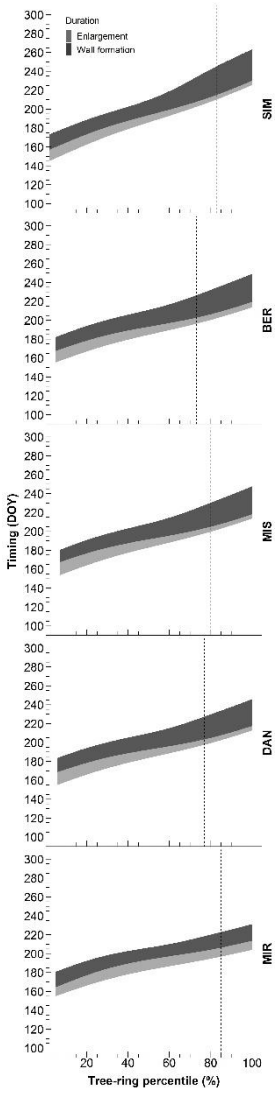

Figure 3.2 Cell-trait timings across the tree rings of black spruce collected from five sites distributed along a latitudinal gradient through the closed boreal forest of Quebec, Canada. Timings represent the day (day-of-year, DOY) at which a certain percentile of the tree ring was enlarging (light grey) or forming secondary walls (dark grey). The dashed line marks the percentage of latewood at each site.

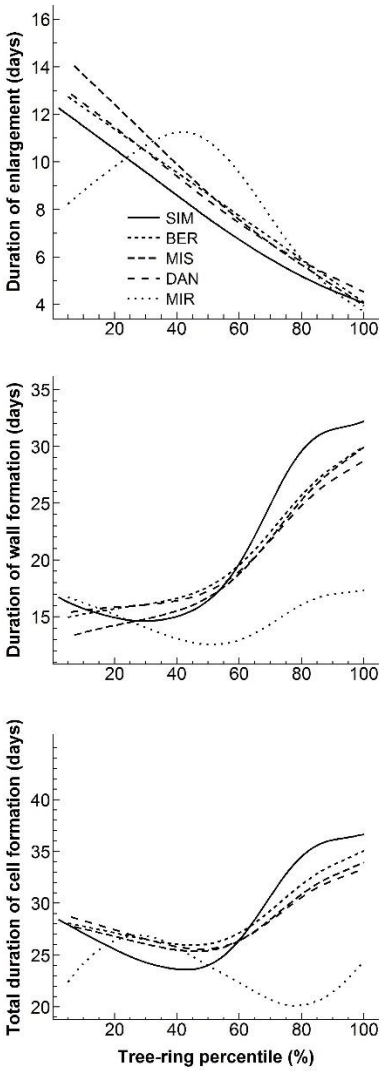

Figure 3.3 Variation in the duration of the various cell differentiation phases across a black spruce tree ring at five sites along a latitudinal gradient in Quebec, Canada. The modelling protocol proposed by Cuny *et al.* (2014) and Balducci *et al*. (2016) was used to assess the duration of each differentiation phase.

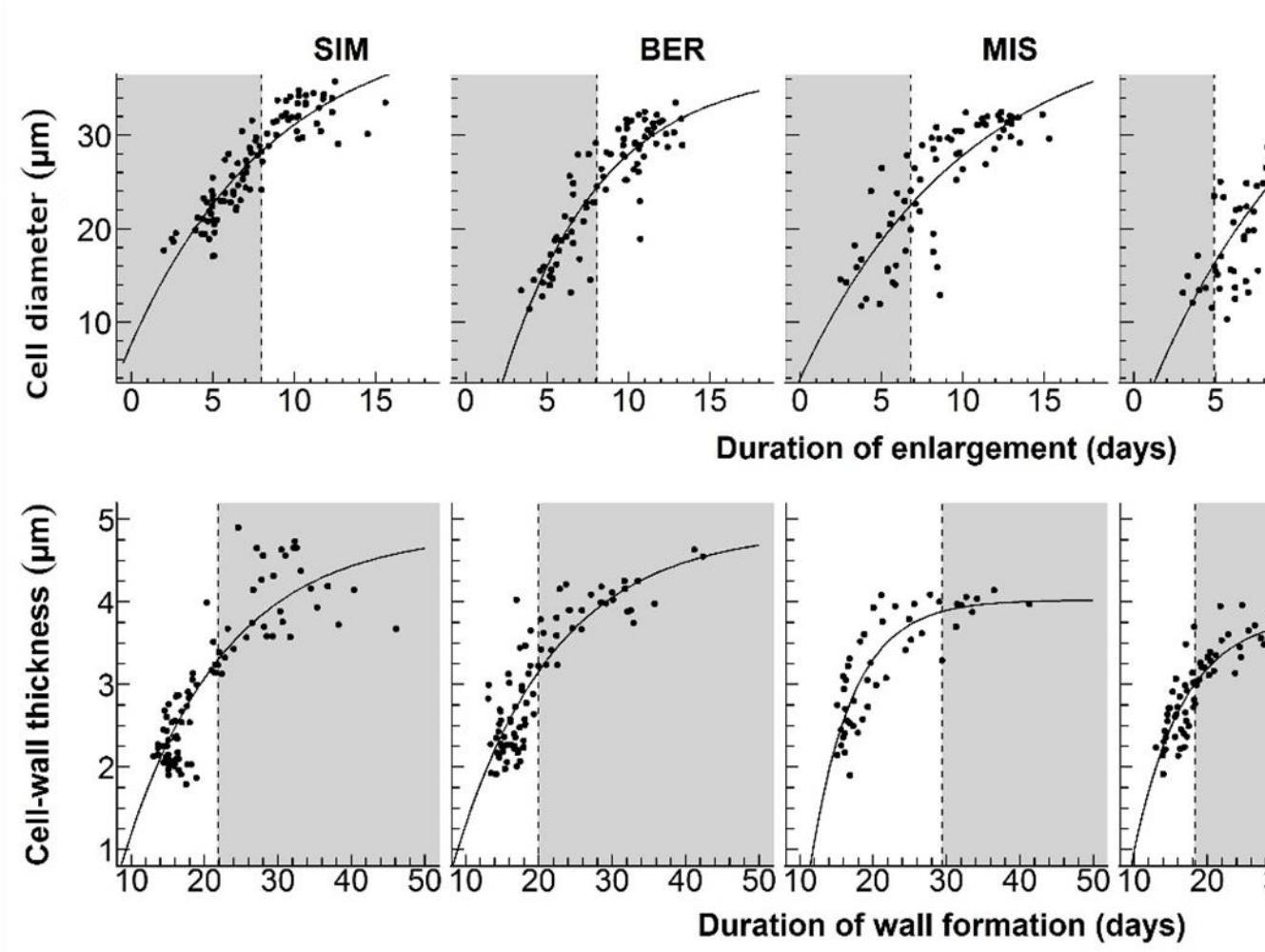

Figure 3.4 Cell traits versus the duration of their developmental phases plotted using the modified von Bertalanffy equation. The top row presents cell diameter versus the duration of enlargement. Cell-wall thickness versus the duration of lignification is presented in the bottom row. The dashed line represents the threshold between earlywood and latewood; the light-grey background represents the latewood portion. Each plot represents one of the five sites along a latitudinal gradient across the closed boreal forest of Quebec, Canada

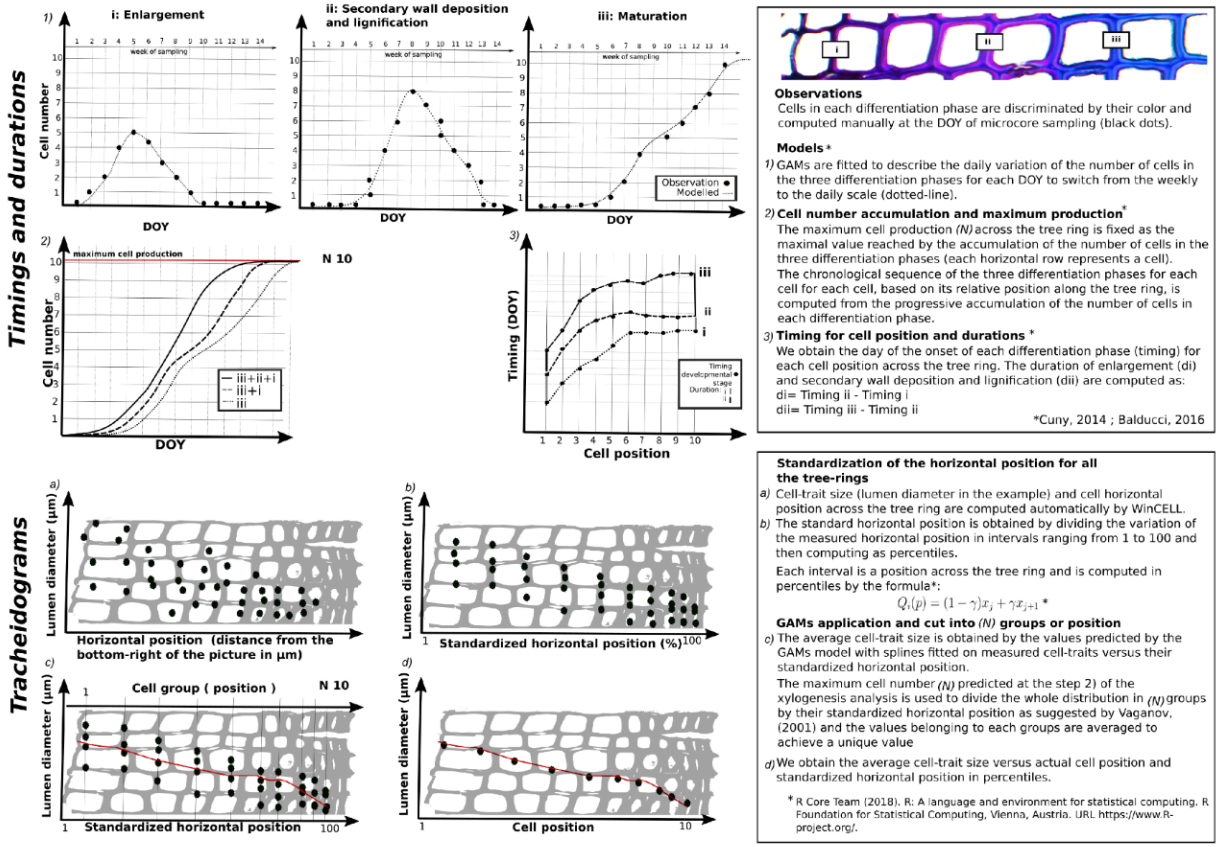

Supplementary figure 3.1 Schematic drawing summarizing the statistical analysis performed on the two datasets (xylogenesis and wood anatomy). In the example, the observations from a single tree ring are processed and modelled to obtain the temporal dynamics of xylogenesis and tracheidograms of the cell traits. In this example, we hypothesize a monitoring of xylogenesis over a growing season lasting 14 weeks after which time we conduct measurements of wood anatomy

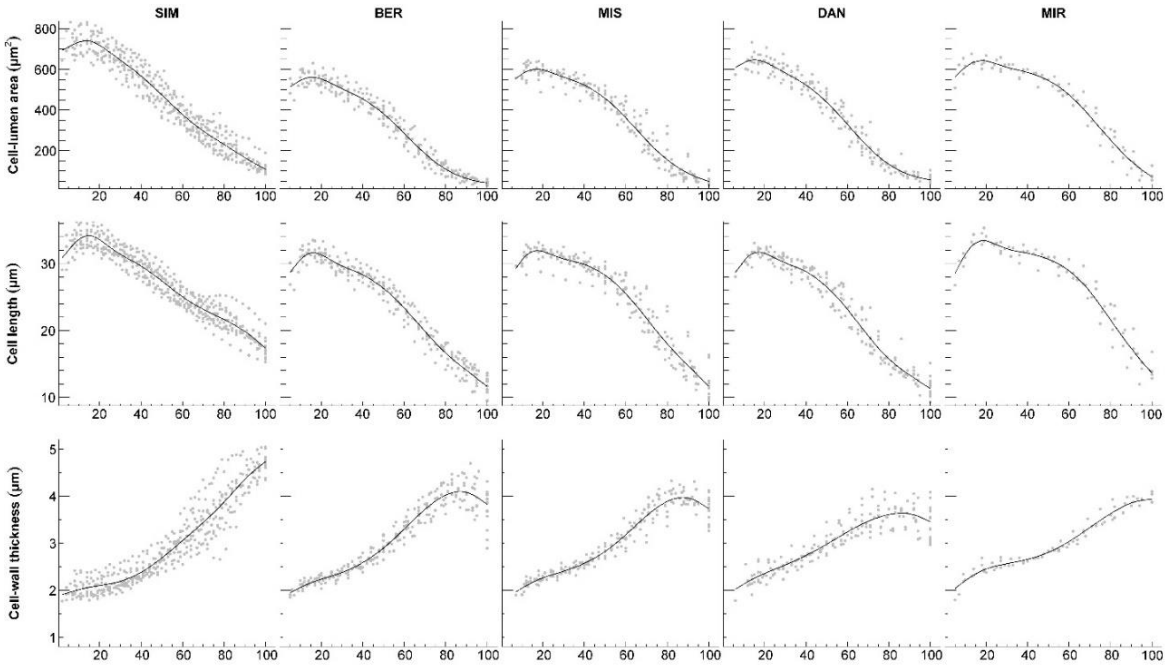

Supplementary figure 3.2 Tracheidograms of black spruce from five sites distributed along a latitudinal gradient across the closed boreal forest of Quebec, Canada. The black line is the fitting that summarizes the inter-annual variability (grey points). The number of points is proportional to the number of cells produced in each tree ring and to the number of years sampled for each site

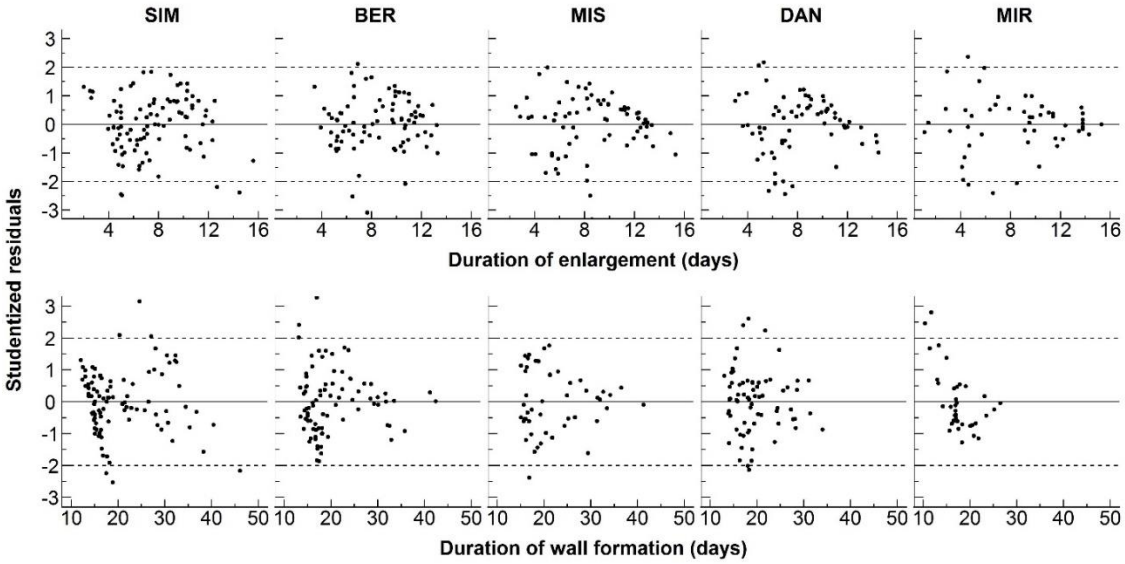

Supplementary figure 3.3 Distribution of residuals obtained by the fitting of the modified von Bertalanffy equation. Cell traits versus their differentiation phases are represented for each of the five sites along a latitudinal gradient across the closed boreal forest of Quebec, Canada

3.9 References

Aloni R. 2013. Role of hormones in controlling vascular differentiation and the mechanism of lateral root initiation. Planta 238: 819–830.

Aloni R, Zimmermann MH. 1983. The control of vessel size and density along the plant axis: A new hypothesis. Differentiation 24: 203–208.

Anfodillo T, Deslauriers A, Menardi R, Tedoldi L, Petit G, Rossi S. 2011. Widening of xylem conduits in a conifer tree depends on the longer time of cell expansion downwards along the stem. Journal of Experimental Botany 63: 837–845.

Balducci L, Cuny HE, Rathgeber CBK, Deslauriers A, Giovannelli A, Rossi S. 2016. Compensatory mechanisms mitigate the effect of warming and drought on wood formation. Plant, Cell and Environment 39: 1338–1352.

Belien E, Rossi S, Morin H, Deslauriers A. 2012. Xylogenesis in black spruce subjected to rain exclusion in the field. Canadian Journal of Forest Research 42: 1306–1315.

Carteni F, Deslauriers A, Rossi S, et al. 2018. The physiological mechanisms behind the earlywood-to-latewood transition: a process-based modelling approach. Frontiers in Plant Science 9: 1053.

Chave J, Coomes D, Jansen S, Lewis SL, Swenson NG, Zanne AE. 2009. Towards a worldwide wood economics spectrum. Ecology Letters 12: 351–366.

Cuny HE, Rathgeber CBK. 2016. Xylogenesis: coniferous trees of temperate forests are listening to the climate tale during the growing season but only remember the last words! Plant Physiology 171: 306–317.

Cuny HE, Rathgeber CBK, Frank D, Fonti P, Fournier M. 2014. Kinetics of tracheid development explain conifer tree-ring structure. New Phytologist 203: 1231–1241.

Cuny HE, Rathgeber CBK, Kiessé TS, Hartmann FP, Barbeito I, Fournier M. 2013. Generalized additive models reveal the intrinsic complexity of wood formation dynamics. Journal of Experimental Botany 64: 1983–94.

Cushing JM, Costantino RF, Dennis B, Desharnais R, Henson SM. 2002. Chaos in ecology: experimental nonlinear dynamics. Elsevier.

Denne MP. 1971. Temperature and tracheid development in Pinus sylvestris seedlings. Journal of Experimental Botany 22: 362–370.

Denne MP. 1989. Definition of latewood according to Mork (1928). IAWA Journal 10: 59–62.

Deslauriers A, Fonti P, Rossi S, Rathgeber CBK, Gričar J. 2017. Ecophysiology and plasticity of wood and phloem formation. In: Amoroso M., Daniels L., Baker P., Camarero J. (eds) Dendroecology. Ecological Studies (Analysis and Synthesis), Springer, vol 231. p. 13–33.

Deslauriers A, Huang J-G, Balducci L, Beaulieu M, Rossi S. 2016. The contribution of carbon and water in modulating wood formation in black spruce saplings. Plant Physiology 170: 2072–2084.

Deslauriers A, Morin H, Begin Y. 2003. Cellular phenology of annual ring formation of Abies balsamea in the Quebec boreal forest (Canada). Canadian Journal of Forest Research 33: 190–200.

Deslauriers A, Rossi S, Anfodillo T, Saracino A. 2008. Cambial phenology, wood formation and temperature thresholds in two contrasting years at high altitude in southern Italy. Tree Physiology 28: 863–871.

Domec J-C, Gartner BL. 2002. How do water transport and water storage differ in coniferous earlywood and latewood? Journal of Experimental Botany 53: 2369–2379.

Dünser K, Kleine-Vehn J. 2015. Differential growth regulation in plants—the acid growth balloon theory. Current Opinion in Plant Biology 28: 55–59.

Fajstavr M, Paschová Z, Giagli K, Vavrčik H, Gryc V, Urban J. 2018. Auxin (IAA) and soluble carbohydrate seasonal dynamics monitored during xylogenesis and phloemogenesis in Scots pine. iForest-Biogeosciences and Forestry 11: 553.

Filion L, Cournoyer L. 1995. Variation in wood structure of eastern larch defoliated by the larch sawfly in subarctic Quebec, Canada. Canadian Journal of Forest Research 25: 1263–1268.

Fonti P, Von Arx G, Garcia-González I, et al. 2010. Studying global change through investigation of the plastic responses of xylem anatomy in tree rings. New Phytologist 185: 42–53.

Fonti P, Bryukhanova MV, Myglan VS, Kirdyanov AV, Naumova OV, Vaganov EA. 2013. Temperature-induced responses of xylem structure of Larix sibirica (Pinaceae) from the Russian Altay. American Journal of Botany 100: 1332–1343.

Genard M, Fishman S, Vercambre G, et al. 2001. A biophysical analysis of stem and root diameter variations in woody plants. Plant Physiology 126: 188–202.

Groover A, Jones AM. 1999. Tracheary element differentiation uses a novel mechanism coordinating programmed cell death and secondary cell wall synthesis. Plant Physiology 119: 375–384.

Hartmann FP, Rathgeber CBK, Fournier M, Moulia B. 2017. Modelling wood formation and structure: power and limits of a morphogenetic gradient in controlling xylem cell proliferation and growth. Annals of Forest Science 74: 14.

Larson PR. 1960. A physiological consideration of the springwood summerwood transition in Red Pine [Pinus resinosa]. Forest Science 6: 110–122.

Lupi C, Morin H, Deslauriers A, Rossi S. 2011. Xylogenesis in black spruce: does soil temperature matter? Tree Physiology 32: 74–82.

Moser L, Fonti P, Büntgen U, et al. 2009. Timing and duration of European larch growing season along altitudinal gradients in the Swiss Alps. Tree Physiology 30: 225–233.

Perrot-Rechenmann C. 2010. Cellular responses to auxin: division versus expansion. Cold Spring Harbor Perspectives in Biology: a001446.

Pitterman J, Sperry JS, Wheeler J, Hacke UG, Sikkema EH. 2006. Mechanical reinforcement of tracheids compromises the hydraulic efficiency of conifer xylem. Plant, Cell and Environment 29: 1618–1628.

Pittermann J, Sperry J. 2003. Tracheid diameter is the key trait determining the extent of freezing-induced embolism in conifers. Tree Physiology 23: 907–914.

Prislan P, Čufar K, De Luis M, Gričar J. 2018. Precipitation is not limiting for xylem formation dynamics and vessel development in European beech from two temperate forest sites. Tree Physiology 38: 186–197.

R Core Team. 2017. R: A Language and Environment for Statistical Computing.

Rossi S, Anfodillo T, Čufar K, et al. 2013. A meta-analysis of cambium phenology and growth: linear and non-linear patterns in conifers of the northern hemisphere. Annals of Botany 112: 1911–1920.

Rossi S, Anfodillo T, Deslauriers A. 2006a. Assessment of cambial activity and xylogenesis by microsampling tree species: an example at the alpine timberline. IAWA Journal 27: 383–394.

Rossi S, Anfodillo T, Menardi R. 2006b. Trephor: a new tool for sampling microcores from tree stems. IAWA Journal 27: 89–97.

Rossi S, Cairo E, Krause C, Deslauriers A. 2015. Growth and basic wood properties of black spruce along an alti-latitudinal gradient in Quebec, Canada. Annals of Forest Science 72: 77–87.

Schweingruber FH. 2012. Tree rings: basics and applications of dendrochronology. Springer Science & Business Media.

Skene DS. 1969. The period of time taken by cambial derivatives to grow and differentiate into tracheids in Pinus radiata: D. Don. Annals of Botany 33: 253–262.

Uggla C, Magel E, Moritz T, Sundberg B. 2001. Function and dynamics of auxin and carbohydrates during earlywood/latewood transition in Scots pine. Plant Physiology 125: 2029–2039.

Wodzicki TJ. 1971. Mechanism of xylem differentiation in Pinus silvestris L. Journal of Experimental Botany 22: 670–687.

Wood SN. 2017. Generalized Additive Models: An Introduction with R. Chapman and Hall/CRC.

3.10 Acknolegements

The authors thank M. Boulianne, J. Boulouf, B. Dufour, G. Dumont-Frenette, F. Gionest, M.-J. Girard, A. Lemay, C. Lupi, V. Nèron, S. Pedneault, P.-Y. Plourde, G. Savard, M. Thibeault-Martel and M.-J. Tremblay for technical support. Murray Hay verified the English. This study was funded by the NSERC Industrial Research Chair, the Canada Foundation for Innovation, le Consortium de Recherche sur la Forêt Boréale Commerciale, les Fonds de Recherche sur la Nature et les Technologies du Québec and la Forêt d'Enseignement et de Recherche Simoncouche

CHAPITRE III

ENVIRONMENTAL AND DEVELOPMENTAL FACTORS DRIVING XYLEM ANATOMY AND MICRO-DENSITY IN BLACK SPRUCE

Accepted in New phytologist

ORIGINAL ARTICLE

Environmental and developmental factors driving xylem anatomy and micro-density in black spruce

Valentina Buttò*[1], Philippe Rozenberg[2], Annie Deslauriers [1], Sergio Rossi [1, 3], Hubert Morin[1]

1. Département des Sciences fondamentales, Université du Québec à Chicoutimi, Chicoutimi, QC, Canada
2. Institut National de la Recherche pour l'Agriculture, l'Alimentation et l'Environnement (INRAE), UMR 0588 BIOFORA Orléans Cedex 2 France
3. Key Laboratory of Vegetation Restoration and Management of Degraded Ecosystems, Guangdong Provincial Key Laboratory of Applied Botany, South China Botanical Garden, Chinese Academy of Sciences, Guangzhou, China

Running title: factors involved in wood formation

*Corresponding author: Département des Sciences fondamentales,

Université du Québec à Chicoutimi, 555, boulevard de l'Université, Chicoutimi (Québec), Canada G7H 2B1

Phone number: +1-418 545-5011 ext. 2330

Email: valentina.butto1@uqac.ca

4.1 Abstract

- Wood density is the product of carbon allocation for structural growth and reflects the trade-off between mechanical support and water conductivity. We tested a conceptual framework based on the assumption that micro-density depends on direct and indirect relationships with endogenous and exogenous factors.
- The dynamics of wood formation, including timings and rates of cell division, cell enlargement, and secondary wall deposition, were assessed from microcores collected weekly between 2002 and 2016 from five black spruce stands located along a latitudinal gradient in Quebec, Canada. Cell anatomy and micro-density were recorded by anatomical analyses and X-ray measurements.
- Our structural equation model explained 80% of micro-density variation within the tree-ring with direct effects of wall thickness ($\sigma = 0.61$), cell diameter ($\sigma = -0.51$), and photoperiod ($\sigma = -0.26$). Wood formation dynamics had an indirect effect on micro-density. Micro-density increased under longer periods of cell wall deposition and shorter durations of enlargement.

- Our results fill a critical gap in understanding the relationships underlying micro-density variation in conifers. We demonstrated that short-term responses to environmental variations could be overridden by plastic responses that modulate cell differentiation. Our results point to wood formation dynamics as a reliable predictor of carbon allocation in trees.

Keywords: cell diameter, cell wall thickness, cell enlargement, photoperiod, secondary wall deposition, soil water content, structural equation modelling, temperature

4.2 Introduction

The boreal forest biome stocks 22% of the total global forest carbon (Bradshaw & Warkentin, 2015). As they cover a large area of the Northern Hemisphere, boreal ecosystems play an important role in regulating climate (Pan *et al.*, 2011; Gauthier *et al.*, 2015). Models of future carbon sequestration within boreal ecosystems still present a high level of uncertainty because of a lack of observations required to validate estimates of carbon balance and a poor understanding of the processes underlying carbon sinks in northern regions (Boudreau *et al.*, 2008; Hayes *et al.*, 2012; Thurner *et al.*, 2014). In areas outside of the tropics, trees' carbon balance is subjected to seasonal variations, which affect the capacity of trees to permanently stock carbon in the woody tissue, the main carbon sink of trees (Kuptz *et al.*, 2011). Simulations of vegetation productivity at a large scale would benefit from a better understanding of the carbon sink processes in trees, which includes incorporating the effects of growth dynamics in wood and wood properties (Friend *et al.*, 2019). Therefore, wood density, a key factor for carbon sequestration, becomes a variable of interest in the perspective of improving model predictions of carbon sequestration at various spatial and temporal resolutions (Giroud *et al.*, 2017).

Wood density is the product of carbon allocation for structural growth, and its variability within the tree reflects the trade-off between mechanical support, represented by cell wall thickness, and water conductivity, represented by cell

diameter (Preston *et al.*, 2006; Chave *et al.*, 2009). Despite the importance of wood density for carbon sequestration and tree hydraulics, little is known about the factors controlling variations in wood density across the tree ring, i.e. micro-density, at the intra-annual scale (Balducci *et al.*, 2013, 2015). Indeed, wood density can be measured at two levels. The first is at the tree-ring level by recording values such as the minimum, mean, and maximum tree-ring wood density. The second is at the micro-density level, integrating density measurements at specific locations within a tree ring. The responsiveness of wood density to variations in environmental factors has long been exploited by dendroclimatologists to detect regional climatic signals (Wimmer & Grabner, 2000; Gagen *et al.*, 2006; Drew *et al.*, 2013) and to assess the effects of climate change along elevational gradients (Rozenberg *et al.*, 2020). These dendrochronological studies have unravelled complex response patterns at interannual scales. Nonetheless, given the processes of carbon sequestration operating at a finer scale, micro-density seems more suitable for the study of carbon allocation and sequestration during the growing season (Arzac *et al.*, 2018).

In conifers, tree-ring micro-density is highly correlated with xylem cell anatomy, in particular with cell diameter and cell-wall thickness (Rathgeber *et al.*, 2006). Variations in the ratio of cell diameter to cell wall thickness affect xylem density, which peaks during latewood formation when the greatest amount of cell wall is associated with a smaller cell diameter (Barnett & Jeronimidis, 2003; Cato *et al.*,

2006; Björklund *et al.*, 2017). Cell anatomy is shaped by the dynamics of wood formation; its intra-annual variability results in different rates of cell division and duration of differentiation. Differentiation occurs through the phases of cell enlargement and secondary wall deposition and lignification (Cuny *et al.*, 2014; Rathgeber *et al.*, 2017; Buttò *et al.*, 2019).

In temperate and boreal ecosystems, a reduced cell diameter across the tree ring is related to a shorter duration of enlargement, generally associated with an increase in cell wall thickening, which is linked to a longer duration of wall deposition and lignification (Deslauriers *et al.*, 2003; Rossi *et al.*, 2006a; Buttò *et al.*, 2019). However, the processes of cell enlargement and cell wall deposition interact to define cell size. Enlargement is eventually constrained by the stiffening of the cell wall because of the deposition and lignification of the secondary wall (Dünser & Kleine-Vehn, 2015; Cartenì *et al.*, 2018). At the same time, an increase in surface area, linked to a longer duration of cell expansion, affects cell wall thickness by limiting the deposition of the secondary wall. Thus, wood formation dynamics, via their influence on cell anatomy, are indirectly linked to micro-density, as wood production and xylem anatomical features are linked to the timing of cell differentiation (Rossi *et al.*, 2015).

Variations in temperature, water availability, and photoperiod during wood formation affect micro-density. This strong environmental influence permits determining the

relationship between environmental factors and carbon sequestration over a year. Increased temperatures and water content during wood formation both increase wood density in gymnosperms, whereas the role of photoperiod on wood density remains unclear (Roderick & Berry, 2002; Way & Montgomery, 2015). Photoperiod allows plants to perceive the progression of the seasons, and its timing differs between latitudes but remains unchanged between years for a given location (Way & Montgomery, 2015). During the early spring, growth reactivation is synchronized with a longer photoperiod, which provides the tree with a less variable signal for spring than the signal of daily temperature (Körner, 2012). In cold climates, trees synchronize their cambial activity with daylength, and peaks in wood production have been observed around the summer solstice (Rossi *et al.*, 2006b). Along with photoperiod, temperature is considered as the driving factor for tree growth in cold-limited climates; warmer conditions trigger additive effects during xylem formation by increasing cell production and cell diameter (Deslauriers & Morin, 2005; Fonti *et al.*, 2013). Larger cells allow increased hydraulic conductivity, which, during cell differentiation, positively affects cell wall deposition (Fonti *et al.*, 2013). During cell enlargement, water allows cells to extend their primary wall and increase in size. Water also enhances nutrient transport across the stem and, in turn, cellulose production within cell walls (Ericsson *et al.*, 1996; Guerriero *et al.*, 2014; Deslauriers *et al.*, 2016). Warmer temperatures directly promote cell division and cell wall

thickening by increasing microfibril deposition (Deslauriers *et al.*, 2008; Rossi *et al.*, 2008; Cuny & Rathgeber, 2016).

The scarce availability of long-term records of xylogenesis precludes a full understanding of the interactions of environmental factors and wood formation dynamics on xylem anatomy and micro-density. The main objective of this paper is to test a conceptual framework designed to quantify direct and indirect effects of environmental factors, cell differentiation temporal dynamics, and cell anatomy, i.e. cell diameter and wall thickness, on micro-density. Our hypothesis holds that micro-density depends on endogenous and exogenous signals linked to wood formation dynamics and environmental factors during cell differentiation. We tested our hypothesis by measuring cell size and micro-density within chronologies of wood formation collected over 15 years (2002–2016) from black spruce (*Picea mariana* Mill. B.S.P.) found within five permanent plots distributed along a wide latitudinal gradient.

4.3 Material and methods

4.3.1 Study area and tree selection

The study area covers a latitudinal gradient from 48°N to 53°N, representing the entire closed boreal forest of Quebec, Canada. Five sites were selected in even-aged and mature black spruce stands to represent the entire latitudinal extent of black

spruce populations in Quebec (Table 1, Figure S1). All sites lie in the eastern part of the black spruce distribution, where black spruce is the dominant species (Figure S1). Two sites (SIM and BER) are situated in the balsam fir (*Abies balsamea* L. Mill.)–white birch (*Betula papyrifera* Marsh.) bioclimatic domain. MIS and DAN lie in the black spruce–moss bioclimatic domain. The northernmost site (MIR) is located in the black spruce-lichen domain and is characterized by a lower tree density (Rossi *et al.*, 2015). All stands are of natural origin and are characterized by similar ages, approximately 100 years, with the exception of SIM, which is 80 years old (Rossi *et al.*, 2015). Average temperatures across the study region range from 1.9 to −3.4°C, with the southernmost and northernmost sites being respectively the warmest and the coldest (Figure S1). Annual precipitation for all sites ranges between 626 (MIR) and 906 (SIM) mm (Figure S1).

4.3.2 Xylem formation

Ten dominant or co-dominant trees were selected at each site, and we avoided sampling individuals having polycormic stems, evident parasite damage, reaction wood, or partially dead crowns (Table 1). Small microcores were collected with a surgical bone needle (2002–2007) or Trephor (2007–2016) (Rossi *et al*., 2006c) from 10 individuals per site. Sampling occurred weekly or fortnightly from April to October 2002–2016, except at MIR, which was sampled at the same frequency from 2012 to 2016. During sampling, the development of resin ducts was avoided by

collecting microcores 10 cm from each other (Deslauriers et al., 2003). Microcores were dehydrated in D-limonene, embedded in paraffin, cut in transversal sections with a rotary microtome, and stained with cresyl violet acetate (0.16% in water). The sections were observed at 400–500× magnification under visible and polarized light. Glistening and coloration discriminated between (i) cell enlargement, (ii) cell wall deposition and lignification, and (iii) mature cells (Deslauriers *et al*., 2003, Figure 1). In each tree ring, cells were counted along three radial rows and classified as enlarging when no glistening was detected—due to only the presence of a primary wall. Cells undergoing secondary wall deposition glistened under polarized light, while the beginning of lignification was marked by a different coloration with the cresyl turning from violet to blue (Rossi *et al*., 2006a). Mature cells exhibited blue cell walls.

4.3.3 Wood anatomy and micro-density

In summer 2017, we collected additional microcores from 10 individuals per site for measuring wood anatomy characteristics. These samples were prepared using the above-mentioned procedures but were stained in safranin (1% in water) and permanently fixed on slides using Permount™. We photographed the transversal sections using a camera fixed on an optical microscope at 20× magnification (Figure 1). Lumen diameter, cell diameter, and cell wall thickness (single wall) were measured on all sections using Wincell (Regent Instruments, Canada). We also

collected woody cores from the same trees for measuring micro-density; the samples were dried to a 12% moisture content and cut into 2-mm-thick sections (Polge & Nicholls, 1972; Millier *et al.*, 2006). The samples were X-rayed on three cellulose acetate films with a calibration wedge containing 12 grey levels; this calibration wedge allowed us to convert the images into optical density values. The X-ray films were scanned at 1000 dpi, providing a measurement resolution of 25 μm (Millier *et al.*, 2006, Figure 1). We used WinDendro (Regent Instruments, Canada) to measure intra-annual density profiles and tree-ring widths.

4.3.4 Assessing the dynamics of xylem formation

We assessed the dynamics of xylem formation following Cuny *et al.* (2013) and Balducci *et al*. (2016). The rate of cell division and the daily sequence of cell enlargement and cell wall thickening was estimated by fitting additive models (GAM) with splines over the number of cells counted for each sampling day. This procedure assessed the daily rate of cell production and the timing and duration of differentiation for each cell making up part of the tree ring. Timing represented the DOY of entry of each cell into a differentiation phase (Cuny *et al.*, 2014). The position of each measured variable along the tree ring, i.e. micro-density, cell diameter, and cell wall thickness, were divided into percentiles to study their variation against a relative tree-ring position (expressed in %). Therefore, for each site and year of sampling, we computed profiles of cell diameter, cell wall thickness,

and micro-density on the basis of their relative position within the tree ring by fitting a GAM (see Buttò *et al.* (2019) for further details).

4.3.5 Weather measurements during cell differentiation

Temperature and soil water content at 30-cm depth were obtained from automatic weather stations equipped with CR10X dataloggers (Campbell Scientific Corporation, Canada) and installed in a forest gap at each site. Data were collected hourly, and daily averages were calculated for the time windows corresponding to the timing of wood formation dynamics (i.e. beginning and end) of cell enlargement and cell wall formation for each relative tree-ring position, estimated by the above-mentioned procedures. Photoperiod was calculated as the difference between daily sunset and sunrise times, computed as proposed by Teets (2003).

4.3.6 Statistical analysis

We ran principal component analysis (PCA) to investigate the relationships between environmental parameters (photoperiod, mean temperature, soil water content), wood formation dynamics (rate of cell division, duration of enlargement, duration of secondary wall deposition and lignification), cell anatomy, and micro-density for each tree-ring percentile. Then, we used a structural equation model (SEM) to test the following framework based on our hypothesis (Figure 2):

I. Micro-density variation depends directly on both cell anatomy and environmental factors;

II. Micro-density variation depends indirectly on wood formation dynamics, i.e. rate of cell division, duration of enlargement, and duration of secondary wall deposition and lignification (henceforth labelled as secondary wall deposition).

Because of the strong relationship between cell anatomy and wood formation dynamics, micro-density depends indirectly on the duration of both cell enlargement and secondary wall deposition (Figure 2). To represent the dichotomy between endogenous (cell differentiation) and exogenous (weather) factors, we treated wood formation dynamics and environmental variables as independent causal variables in our model. To eliminate the effect of the environmental factors on wood formation dynamics, we used residual distributions, which were obtained by regressing the rate of cell division, the duration of enlargement, and the duration of secondary wall deposition with their respective most correlated environmental variable (Figure 2, Table S1).

The degree of multicollinearity between all variables selected for the model was assessed by the computation of the variance inflation factor (VIF). We adopted a VIF threshold value of <5 for variable selection, which excludes the possibility of estimating coefficients having a sign and strength that do not match those of their

respective correlations (Zuur *et al.*, 2010). For analysis of the SEM, we used lavaan r's package (Rosseel, 2012), running 10000 bootstrapped resamples with confidence intervals and *P*-values as determined using the Bollen–Stine bootstrapping method (Beaujean, 2014). Models were accepted when the Bollen–Stine bootstrapped *P*-value was >0.05. Finally, we used both a comparative fit index (CFI) score of >0.95 and a standardized root mean square residual (SRMR) score of <0.09 to confirm the goodness of fit (Hu & Bentler, 1999; Hooper *et al.*, 2008).

4.4 Results

4.4.1 Timings of cell differentiation and climate

Xylem differentiation began earlier at SIM, at the end of May (DOY 144) (Figure 3). At the other sites, xylem differentiation began in the first week of June, from DOY 152 at MIS to DOY 157 at MIR. Xylem completed its maturation earliest at MIR (DOY 253) and ten days later at SIM (DOY 269). Xylem differentiation lasted the longest at SIM (124 days) and the shortest at MIR (96 days). The average temperature during xylem differentiation was 14.0 ± 4.11°C; MIR and SIM were the coldest and the warmest sites, respectively (Figure 4). Soil water content during xylem differentiation was 0.29 $m^3 \cdot m^{-3}$, ranging from 0.17 $m^3 \cdot m^{-3}$ at DAN to 0.41 $m^3 \cdot m^{-3}$ at BER, the site located at the highest elevation (Figure 4, Table 1).

4.4.2 Micro-density, cell anatomy, and wood dynamics

Mean density showed values of 500 kg·m^{-3} at the southernmost sites of the gradient (SIM, BER, MIS), dropping to 450–470 kg·m^{-3} at the northernmost sites (DAN, MIR, Figure 5). The micro-density profiles gradually increased from 400 to 575 kg·m^{-3}, with a maximum value recorded at 80% of the tree-ring width.

In earlywood, intra-annual density varied between sites (350–425 kg·m^{-3}) without showing a clear climatic influence. Differences in micro-density between sites became more evident starting from 60% of the tree-ring width when the latewood at the southernmost sites became 150 kg·m^{-3} denser than that at the northernmost sites.

Mean cell diameter varied along the latitudinal gradient; the largest cells (27 μm) were produced at SIM and MIR, and the smallest cells (22.6 μm) were observed at DAN (Figure 5). All sites attained a maximum cell diameter (27.5–35 μm) at 20% of the tree-ring width. In general, cell wall thickness was 3 μm at all sites. The greatest variability of cell wall thickness was observed at SIM. Cell wall thickness increased across the tree ring and was 1.90–2.00 μm for the first cells produced during a year, culminating at values of 4.73 μm at 80–100% of the tree-ring width (Figure 5).

On average, the highest rate of cell division was observed at the southernmost site, SIM (0.3 cell·day^{-1}) and the lowest at the northernmost site, MIR (0.2 cell·day^{-1}). Rates of cell division during cell differentiation followed a bell-shaped pattern, with

values ranging from 0.15 to 0.30 cell day^{-1}, while the first percentile of the tree ring was developing. At the beginning of the growing season, cell division increased, culminating at 40% of the tree ring (except for MIR, where the culmination was reached at 20% of the tree ring), and dropped during latewood formation. The highest cell production rate corresponded to increased cell production across all sites of the latitudinal gradient, where average cell production varied from 30 (SIM) to 15 (DAN) cells per year (Figure S2).

The duration of enlargement of a xylem cell lasted on average 8–9 days. Longer cell enlargement (12–14 days) was observed for the first cells and decreased to 4 days for the final cells of the tree ring. The wide interannual variation observed at MIR, coupled with the shorter observation period (2012–2016), may be at the origin of the different patterns detected at this site. The duration of secondary wall deposition ranged from 22 days at SIM and BER to 19 days at MIR. Secondary wall deposition lasted 15 days for the initial cells of the tree ring and lengthened across the tree ring with different rates among sites. The final cells of latewood completed the formation of the secondary cell wall formation in 35 days, except at MIR where it lasted 23 days (Figure 5).

4.4.3 Micro-density variation, wood formation, and environment

The first two principal components of the PCA explained respectively 50.5% and 15.1% of the intra-ring variability of our variables (Figure 6). Data points were not clustered, indicating no site-specific responses in our variables (Figure 6). Micro-density, cell anatomy, and photoperiod were strongly correlated with principal component 1 (PCA_1), whereas the rate of cell division, mean temperature, and soil water content were strongly correlated with principal component 2 (PCA_2) (Figure 6, Table 2). Larger cells were produced with a longer photoperiod and duration of enlargement; these cells also had a positive and strong correlation with PCA_1 (r >0.8). In contrast, the longer duration of secondary wall deposition and warmer conditions resulted in smaller cells and a higher micro-density, corresponding to a strong and negative correlation with PCA_1 ($r < -0.8$). Rates of cell division showed the highest correlation with PCA_2 ($r = 0.74$), with faster dividing cells associated with warmer and wetter environmental conditions (Table 2). When cambial cells divided faster, differentiating cells experienced a longer duration of enlargement and a shorter duration of secondary wall deposition, which resulted in a low cell wall thickness and low micro-density (Figure 6).

Mean temperature and soil water content during cell differentiation were most correlated with PCA_2 (having respective correlation coefficients of 0.64 and 0.53). Therefore, larger cells were produced with longer photoperiods, longer durations of

enlargement, and when the soil was wetter. In contrast, smaller cells and a higher micro-density were observed when the duration of secondary wall deposition was longer and conditions were warm and wet.

To constrain multicollinearity between variables within a reasonable threshold (maximum VIF <5), the rate of cell division was removed from the SEM model, this also being the endogenous variable least correlated with micro-density in our data set ($r = -0.32$, Table 1S). The Bollen–Stine bootstrapped *P*-value could not reject the proposed SEM model ($P = 0.9$), and CFI and SRMR showed values of 1 and 0.003, respectively. Our model explained 80% of micro-density ($R^2 = 0.8$) variation and 70% of cell diameter and wall thickness variations across the tree ring ($R^2 = 0.7$). Cell wall thickness was the most important factor that directly explained micro-density, having a standard coefficient (σ) equal to 0.61 (Table 3, Figure 7). Therefore, any indirect effects on cell wall thickness contributed strongly to increasing micro-density. The direct effect of cell diameter was low and negative ($\sigma = -0.06$), indicating that micro-density decreased slightly with an increase in cell diameter. However, cell wall thickness was largely and negatively affected by cell diameter ($\sigma = -0.51$). The strong effect of cell diameter on micro-density, which we observed in the PCA, was therefore indirect and mediated by wall thickness.

Cell diameter was linked directly with wood formation dynamics, proportionally increasing with the duration of enlargement ($\sigma = 0.17$) and decreasing with the

duration of secondary wall deposition ($\sigma = -0.10$). In contrast, wall thickness increased with a shorter duration of enlargement ($\sigma = -0.11$) and a longer duration of secondary wall deposition ($\sigma = 0.13$). Wood formation dynamics therefore had indirect effects on micro-density via cell anatomy. When the duration of cell enlargement was longer, secondary wall deposition was shorter. This produced larger cells characterized by a thinner wall, which led to a low micro-density. In contrast, when the duration of enlargement was shorter and secondary wall deposition was longer, cells were smaller and showed a greater wall thickness. This produced a high micro-density.

Environmental factors during cell differentiation had a direct effect on micro-density and an indirect effect through cell anatomy (Table 3, Figure 7). Micro-density was directly and negatively affected by photoperiod ($\sigma = -0.26$); higher micro-density values occurred at shorter photoperiods. In contrast, the direct effects of mean temperature and soil water content were both positive, each having a similar influence ($\sigma = 0.10$, $\sigma = 0.09$, respectively). Environmental factors during the period of cell formation also directly influenced the anatomy of xylem. Cell wall thickness decreased with a longer photoperiod ($\sigma = -0.32$) and marginally decreased with a higher soil water content ($\sigma = -0.03$). Cell wall thickness increased with higher temperatures; however, the effect was limited ($\sigma = 0.09$). Cell diameter strongly

increased with a longer photoperiod (σ = 0.81), higher soil water content (σ= 0.20) and, marginally, a higher mean temperature (σ = 0.05) (Table 3, Figure 7).

Among the environmental factors, only photoperiod was strongly correlated with wood formation dynamics, i.e. the duration of enlargement (r = 0.64) and the duration of secondary wall deposition (r = −0.62) (Table S1). The residual distributions of wood formation dynamics used in the SEM were obtained through the regression of the duration of enlargement (or the duration of secondary wall deposition) and photoperiod only (Figure 7).

4.5 Discussion

4.5.1 Effect of wood formation dynamics on micro-density

Across the tree ring, the increasing proportion of cell wall per cell diameter describes the general pattern of tree-ring density, which culminates in latewood (Preston *et al.*, 2006; Björklund *et al.*, 2017). A higher micro-density, produced from an increasing wall/lumen ratio, mirrors changes in the proportion of carbon invested, on the one hand, to promote cell enlargement and primary wall expansion and, on the other, to synthesize secondary wall components (Deslauriers *et al.*, 2016; Lemay *et al.*, 2017). During tracheid differentiation, carbon is required primarily to sustain cell expansion, preventing cell lysis through the deposition of an extensible primary wall, which is able to contain the high amount of water needed to maintain turgor pressure for

enlargement (Steppe *et al.*, 2015; Zarra *et al.*, 2019). A higher amount of carbon is required for secondary wall formation (cellulose, hemi-cellulose, and lignin), which results in thicker-walled cells that will directly and strongly influence wood micro-density (Balducci *et al.*, 2015; Traversari *et al.*, 2018): the smaller the cell diameter, the thicker the walls, thus reducing the lumen. As the diameter of a cell greatly influences the thickness of the cell wall, the direct variability explained by cell diameter on micro-density is low; however, cell diameter influences micro-density indirectly by affecting the cell wall/lumen ratio.

Wood formation dynamics, i.e. the duration of cell enlargement and cell wall thickening, indirectly affect micro-density by modulating cell anatomy over the course of the growing season (Buttò *et al.*, 2019; Ziaco, 2020; Vieira *et al.*, 2020). In turn, wood formation dynamics are affected by many signals at the endogenous level, i.e. hormones (Hartmann *et al.*, 2017; Buttò *et al.*, 2020), transcriptions (Cato *et al.*, 2006), and carbon (Deslauriers *et al.*, 2016; Cartenì *et al.*, 2018), and at exogenous level, i.e. water (Cabon *et al.*, 2020; see the following sections on environmental factors). In agreement with previous studies (Anfodillo *et al.*, 2011; Cuny *et al.*, 2014), we observed that the duration of cell enlargement positively influences cell diameter, underlying the strong effect of the endogenous factors that control cell enlargement. A longer duration of enlargement can be promoted by high auxin levels, which causes the release of protons into the apoplast and a lowering of extracellular

pH (Buttò *et al.*, 2020). Acid extracellular conditions lead to the activation of pH-dependent proteins that increase wall loosening and promote cell enlargement (see Majda & Robert (2018) for a review). At the beginning of the growing season, the high levels of auxin produced by the young leaves, along with higher water availability, may then induce a longer cell enlargement duration, thereby forming larger xylem cells (Hacke *et al.*, 2017; Buttò *et al.*, 2020; Cabon *et al.*, 2020).

Numerous studies of black spruce and other conifer species (Cato *et al.*, 2006; Balducci *et al.*, 2016; Cuny *et al.*, 2019; Vieira *et al.*, 2020) have shown that cell wall thickness increases with the duration of cell wall deposition, a situation that enables a longer time window for carbon allocation into cell walls (Deslauriers *et al.*, 2016). Contrary to cell enlargement, wall thickening and secondary wall deposition are highly demanding processes in terms of resources, regulated mainly by C supply (Deslauriers *et al.*, 2008, 2016; Verbančič *et al.*, 2018). As for micro-density, the duration of cell deposition peaked during latewood formation, when carbon availability for secondary growth is highest because of the cessation of shoot elongation, which implies a resource trade-off between primary and secondary growth (Cartenì *et al.*, 2018). Accordingly, it has been observed that black spruce radial growth is strongly dependent on photo-assimilates of the current year; the sugars from the cambium and developing xylem are more important for sustaining wood growth than sugars from the inner part of the wood (Deslauriers *et al.*, 2016).

Starch reserves are mainly related to metabolic function and frost hardiness (Delpierre *et al*., 2019). When exposed to chilling temperatures, starch is indeed transformed into soluble sugars, which remain at a high concentration until spring dehardening and have metabolic and cryoprotectant functions (Delpierre *et al.*, 2019).

Because wood growth relies on current year photosynthates, the carbon pools available for wood formation can be markedly reduced if a stress were to occur, as observed in the case of defoliation by spruce budworm, one of the main disturbances occurring within Canadian boreal stands (Deslauriers *et al.,* 2019). Defoliated black spruce trees are characterized by a decreased cell production and a lower amount of secondary wall deposed during latewood formation, which leads to a decreased wood density (Paixao *et al.,* 2019). According to Deslauriers *et al*., (2019), underlying this reduction of carbon allocation to wood formation is the prioritization of primary growth by means of an anticipation of bud phenology. These phenological shifts, observed in balsam fir and black spruce, allow the tree to avoid a phenological synchrony between bud formation and spruce budworm emergence (Deslauriers *et al.*, 2019). Therefore, it is likely that, rather than adopting an active defensive strategy to develop resistance to stress events, black spruce decrease carbon availability for secondary growth without any further investment of carbon into defence, as has been observed in balsam fir (Deslauriers et *al.*, 2015).

Our results indicate that cell traits experience the joint action of enlargement and secondary wall deposition in shaping the intra-annual patterns of tree rings. During the growing season, the amount of carbon allocated to wood formation largely influences the duration of cell differentiation, thus modulating cell diameter and cell wall thickness (Cartenì *et al.*, 2018; Traversari *et al.,* 2018). During earlywood formation, larger cells are formed because reduced carbon availability for stem growth in the spring allows for a longer duration of cell enlargement before the onset of secondary wall deposition (Cartenì *et al.*, 2018). In turn, as indicated by our results, a longer duration of enlargement negatively affects cell wall thickness by increasing the area that must be covered by secondary wall once enlargement is achieved, thereby reducing cell wall thickness (Cuny *et al.*, 2014). During latewood formation, carbon can be transferred massively into secondary wall deposition—over a period lasting up to 40 days—and allows trees to triple their micro-density (Deslauriers *et al.*, 2003; Balducci *et al.*, 2015). At this stage, carbohydrate metabolism is highly related to the carbon requirements of the maturing xylem cells; this indicates a high investment of carbon allocation towards secondary growth (Traversari *et al.*, 2018). The high amount of carbon available for wood growth constrains tracheid enlargement by cell wall stiffening, thereby affecting the elasticity of the cell wall and the capacity of cells to increase in size. The result is smaller cells (Dünser & Kleine-Vehn, 2015).

In agreement with Cato *et al.,* 2006, we observed a negative relationship between the rate of cell division and wood density, that mirrors a negative correlation between radial growth rate and the duration of secondary wall deposition. Cambium and developing xylem are both carbon sinks, and their intra-annual patterns affect sugar availability for secondary wall deposition (Cartenì *et al*., 2018). The residence time of cells in the different developmental zones is then affected by cambium activity (Cuny *et al.,* 2013). Nevertheless, in environments where water is not a limiting factor, cell wall thickening requires more carbon than cell division and cell enlargement (Deslauriers *et al*. 2016), as the deposition of secondary wall is responsible for 90% of biomass accumulation in conifers (Cuny *et al.,* 2015). Hence the modest effect of the rate of cell division on micro-density variation across the tree ring *(*$r < 0.3$, Table S1).

4.5.2 Direct and indirect effects of environmental factors on micro-density

Several studies have found that shorter photoperiods affect carbon partitioning in sink tissues, especially by promoting sucrose allocation to active sinks, such as growing stems. This allocation of sucrose increases both plant productivity and biomass accumulation (Kühn & Grof, 2010; Khadilkar *et al.,* 2016). At shorter photoperiods, a developmental switch in carbon allocation is operated by the expression of sucrose transporter (SUT) genes, which encode plasmalemma proteins. These proteins are sucrose carriers that are directly involved in phloem loading and unloading processes

(Kühn, 2003; Payyavula *et al.*, 2011; Chincinska *et al.*, 2013). In smaller plants, daylight affects carbon partitioning in plants, which under a decreasing photoperiod results in a greater investment of sugars in the stem (Bendevis *et al.*, 2014). The intensified activity of sucrose transporter genes, combined with an increased availability of carbohydrates for secondary wall deposition (Deslauriers *et al.*, 2016; Cartenì *et al.*, 2018), results in an increase in cell wall thickness and micro-density under conditions of shorter days. In turn, high concentrations of sugars enhance lignin production to cause the up-regulation of lignin content with shorter days and thus further increasing micro-density (Rogers *et al.*, 2005; Deslauriers *et al.*, 2016).

Photoperiod had both a direct effect on micro-density and an indirect effect through a positive correlation with the duration of enlargement and cell diameter. Recently, photoperiod has been shown to influence cell wall extensibility (Ivakov *et al.*, 2017). Accordingly, longer days would favour cell wall extensibility by promoting the expression of several expansins that control cell wall loosening via a circadian clock signalling (Ivakov *et al.*, 2017). Therefore, an increase in day length positively influences cell diameter, not only because of an increase in the duration of cell enlargement (Anfodillo *et al.*, 2011; Cuny *et al.*, 2014; Balducci *et al.*, 2016) but also because longer days enhance cell wall loosening. Cell expansion is indeed driven by changes in cell wall properties that allow for vacuole expansion while water uptake is in progress (Cosgrove, 2016). This turgor-driven cell expansion occurs mostly at

night when water transpiration is limited, and it also relies on sugar accumulation (glucose, fructose), which attracts water molecules to inside the vacuole. This sugar accumulation occurs during the day (Sulpice *et al.*, 2014; Steppe *et al.*, 2015).

Temperature during wood formation had a positive and direct influence on cell diameter, cell wall thickness, and micro-density. Warmer temperatures (when falling within the optimal temperature range for the species) enhance photosynthesis and promote carbon assimilation by increasing the rate of carboxylation of Rubisco and electron transport (Way & Sage, 2008; Way & Oren, 2010). This intensified activity has different effects on the cambium depending on the moment of the growing season. Early in the growing season, by inducing an earlier snow melting, warming temperatures cause snow to melt and thereby increase water and nutrient availability for roots, leading to the onset of stem rehydration (Turcotte *et al.*, 2009). The increased supply of sugars linked to these warmer temperatures promotes water conduction by increasing the number and size of earlywood tracheids (Fonti *et al.*, 2013; Castagneri *et al.*, 2017). Later during the growing season, the enhancement of carbon capacity, induced by early warming, can have a carry-over effect on the radial growth of trees because of increased carbon assimilation during latewood formation (Fonti *et al.*, 2013). By favouring carbon assimilation, warm temperatures increase cell wall thickness and wood density during latewood formation (Simard *et al.*, 2013).

We observed that regardless of latitude, mean temperature during the period of wood formation was stable at approximately 14°C, where adjustments in the timing of wood formation allowed for a longer growing season in the southernmost sites, i.e. trees in the southernmost sites began wood formation earlier and ended wood formation later. In black spruce, a mean temperature of 14°C has been identified as the optimal temperature for photosynthesis (Goulden *et al.*, 1997). It is therefore likely that the period of wood formation is centred around 14°C to optimize wood growth processes with photosynthesis.

The positive effect of soil water content on micro-density and cell diameter has different ecological explanations linked to tree physiological needs during cell enlargement but also the modulatory role played by water in regard to sugar allocation and biomass production in black spruce (Deslauriers *et al*. 2016). The positive influence of soil water content on cell diameter can be explained by the demand of water during cell enlargement, which makes cell diameter strongly dependent on water availability (Cosgrove, 1997; Deslauriers *et al.*, 2016; Castagneri *et al.*, 2017). Accordingly, during earlywood formation, Björklund *et al.* (2017) observed increased sensitivity of cell diameter to water availability or precipitation, which makes this factor particularly important earlier in the growing season. As for micro-density, long-term experiments have shown that in cold environments it is positively affected by irrigation (Nilsson, 1997; Bergh *et al.*, 1999). Greater water

availability in the soil also increases N-uptake and, consequently, the dry mass and retention of needles, increasing their photosynthetic efficiency and carbon sequestration, which results in higher wood density (Nilsson, 1997). Experiments coupling irrigation and N-fertilization have demonstrated that the positive effect of water availability during the growing season on mean density is enhanced by soil fertilization because of the limiting nature of N in cold environments (Lim *et al.*, 2015).

4.5.3 High plasticity in wood formation dynamics modulates wood traits as a conservative strategy

We found that the average intra-annual patterns across the tree ring, calculated for 15 years, were independent of latitude. This pattern suggests a conservative strategy for xylem traits across latitudes. At each site, however, we observed large variability in these patterns, which may reflect both genotypic and micro-site variability in terms of mean temperature and soil water content during cell differentiation. We propose that black spruce trees, regardless of latitude, are capable of showing a highly plastic response and can promptly modulate cell differentiation at an intra-annual scale (Balzano *et al.*, 2019) to adapt to variations in photoperiod, temperature, and soil water content.

Under both controlled and natural conditions, a little variability has been observed in the xylem-related traits in black spruce wood. Relative to other species, black spruce adopts a very conservative growth strategy, resulting in an unexpected inertia in wood anatomy vis-à-vis induced or natural environmental change (Belien *et al.*, 2012; Balducci *et al.*, 2016; Sniderhan *et al.*, 2018). Chen *et al.*, (2019) observed a reduced responsiveness by black spruce to variations in environmental factors. In this taxon, adaptive responses reflect a slow-growth strategy, which is poorly suited to responding to short-term environmental change. By counterbalancing the duration and rate of cell differentiation, black spruce trees respond to environmental variations, such as water stress or temperature increase, and adjust their cell anatomy across the tree ring (Balducci *et al.*, 2016). The poor correlations between wood formation dynamics and environmental factors. i.e. soil water content and temperature variations during cell differentiation may thus be a consequence of the compensation effect of wood formation dynamics, which are finely tuned to long periods of climatic signalling. Consistent with this assumption, investigations covering longer periods (1943–2010) at our sites demonstrated a decade-dependent tree growth response of black spruce to temperature and precipitation (Puchi *et al.*, 2019). It is thus likely that only the effect of persistent drought induced by high temperatures and low precipitation would trigger substantial changes in wood formation dynamics, thereby modifying cell anatomy (Puchi *et al.*, 2019). To a certain extent, these responses can be related to the longer-term mechanisms of

evolutionary adaptation, which in this study encompasses part of the inter-tree variation at both intrasite and intersite scales and ensure black spruce resilience in under very different growing conditions.

4.6 Conclusion

We disentangled the effects of environmental factors, dynamics of cell formation, and xylem cell traits on wood density by relying on one of the longest chronologies of weekly xylem formation currently available. Such a framework provides a greater understanding of the growth–environment relationships in species characterized by a wide geographical distribution, where plastic adjustments in wood formation dynamics can override climate responses. These adjustments are not directly detectable in wood trait size variations because of their pronounced dependency on developmental control. Accordingly, black spruce shows a slow-growth strategy, which makes this species moderately sensitive to short-term environmental variations; this quality thereby favours longer-term adaptive responses (Rossi, 2015; Martin *et al.*, 2020).

Cell trait size and, indirectly, micro-density across the tree ring were shaped by the interplay of the cell trait differentiation phases; their combined actions drive the extension of the cell wall and its thickening during cell development. Interestingly, the effects of environmental factors on cell anatomy and micro-density were not

additive, in agreement with Preston *et al.* (2006), who observed that wood density and cell anatomy display distinct patterns of ecological correlations. We demonstrated that the carbon allocated to wood is indirectly but tightly linked to wood formation dynamics, which occurs for both short- and long-term growth signalling and has a great predictive power of wood density variation across the tree ring.

4.7 Tables

Table 4.1 Geographical coordinates, elevation, climatic conditions, and characteristics of *Picea mariana* trees for the study sites. Annual statistics for temperature and precipitation were calculated using 1950–2016 climate data with the ANUSPLIN algorithm to obtain long-term means downscaled to our sites (McKenney *et al*., 2011).

Site	Latitude (N)	Longitude (W)	Altitude (m a.s.l.)	Mean annual temperature (°C)	Total annual precipitation (mm)	DBH (cm)	Tree height (m)
SIM	48°13′	71°15′	338	1.9	909	20.4 ± 2.4	16.1 ± 1.2
BER	48°51′	70°20′	611	0.2	890	21.1 ± 3.7	17.3 ± 1.8
MIS	49°43′	71°56′	342	0.3	758	19.6 ± 2.8	18.3 ± 1.1
DAN	50°41′	72°11′	487	-1.2	736	18.5 ± 2.9	16.6 ± 2.2
MIR	53°47′	72°52′	384	-3.3	627	19.6 ± 3.0	13.1 ± 1.2

DBH, diameter at breast height, mean ± standard deviation for DBH and tree height

Table 4.2 Correlation between axes of the principal component analysis (PC_1 and PC_2) and the environmental factors, the wood formation dynamics, cell anatomy and micro-density measured in *Picea mariana*, used in the PCA with their contribution to the axis definition (%). Only significant correlations ($P < 0.05$) are presented.

PCA	Variable		Correlation	Contribution
PCA_1	Environmental factors	Photoperiod	0.89	18.16
		Mean temperature	−0.06	0.07
		Soil water content	0.05	0.06
	Wood formation dynamics	Duration of enlargement	0.76	13.30
		Duration of secondary wall deposition	−0.74	12.51
	Cell anatomy	Cell diameter	0.91	18.88
		Cell wall thickness	−0.92	19.21
	Micro-density	Micro-density	−0.88	17.81
PCA_2	Environmental factors	Mean temperature	0.90	76.50
		Soil water content	0.39	14.16
	Wood formation dynamics	Duration of enlargement	−0.14	1.90
		Duration of secondary wall deposition	−0.19	3.38
	Cell anatomy	Cell diameter	0.15	2.02
	Micro-density	Micro-density	0.15	2.03

Table 4.3 Parameters defining the structural equation model (SEM) with standardized estimate coefficients (σ), the standardized estimate coefficient error (σ error), *z*-value, and *P*-value for all SEM regressions (micro-density, cell diameter, and cell wall thickness measured in *Picea mariana*).

Regression	**Regressors**	σ	σ **error**	***z*-value**	***P*(>|*z*|)**
Micro-density	Cell diameter	-0.06	0.013	−5.14	<0.001
	Wall thickness	0.61	0.011	56.725	<0.001
	Soil water content	0.09	0.006	13.304	<0.001
	Mean temperature	0.10	0.006	15.384	<0.001
	Photoperiod	-0.26	0.011	−23.383	<0.001
Cell diameter	Duration of enlargement	0.17	0.009	23.514	<0.001
	Duration of cell wall deposition	-0.10	0.009	−14.86	<0.001
	Soil water content	0.20	0.007	29.421	<0.001
	Mean temperature	0.05	0.007	6.814	<0.001
	Photoperiod	0.81	0.007	56.344	<0.001
Wall thickness	Duration of cell wall deposition	0.13	0.009	17.881	<0.001
	Duration of enlargement	-0.11	0.01	−14.453	<0.001
	Cell diameter	-0.51	0.013	−37.21	<0.001
	Soil water content	-0.03	0.007	−4.391	<0.001
	Mean temperature	0.09	0.007	11.802	<0.001
	Photoperiod	-0.32	0.013	−9.382	<0.001

4.8 Figures

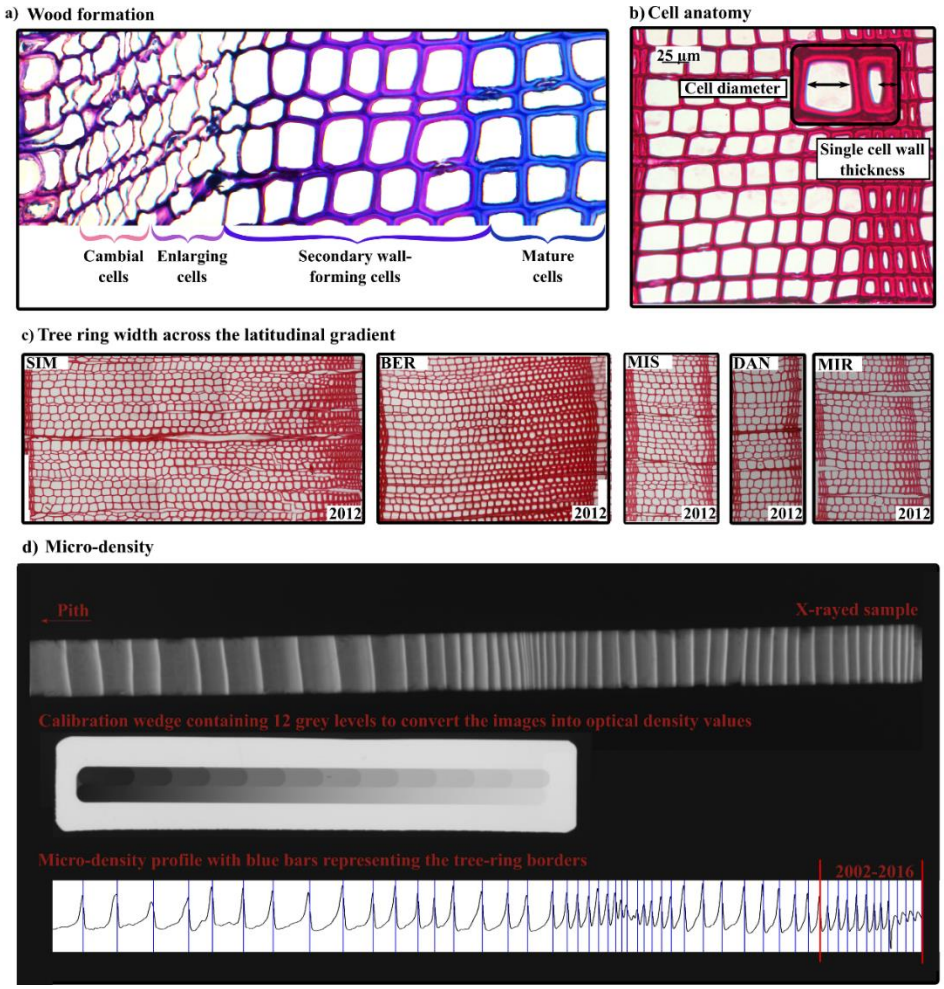

Figure 4.1 Wood formation, cell anatomy and micro-density measurements in tree rings of *Picea mariana* a) Transverse section of a weekly sampled microcore, observed at 400× magnification, for counting the developing cells; b) transverse section of a fully formed tree ring observed at 20× magnification with the measured anatomical parameters; c) variability of tree-ring width across the latitudinal gradient for the 2012 tree ring; d) X-ray of a sample with the calibration wedge and micro-density profile.

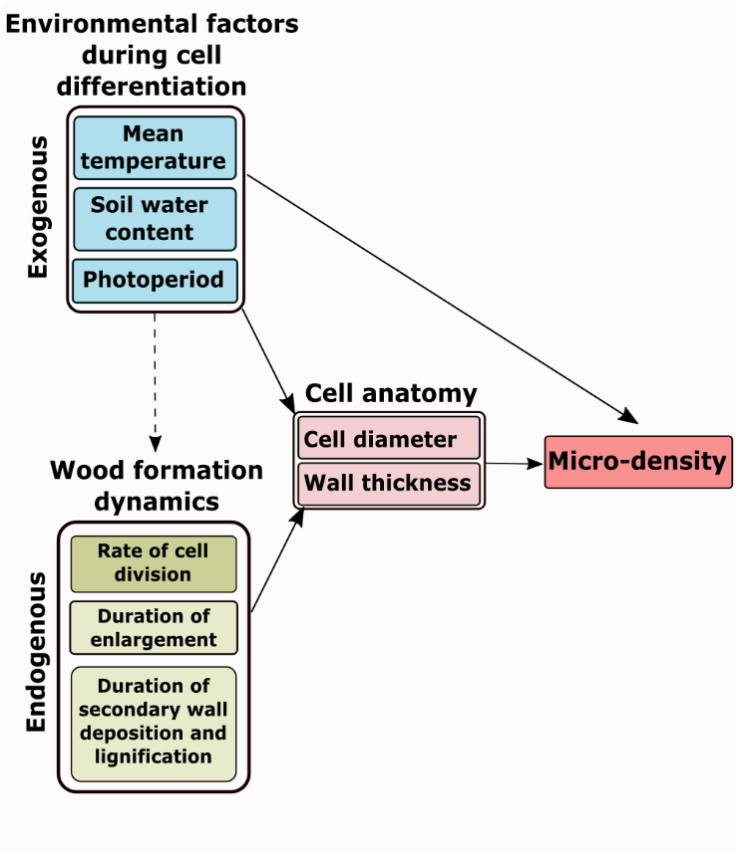

Figure 4.2. Conceptual framework behind the structural equation model (SEM) linking environmental factors with cell differentiation, wood formation dynamics, cell anatomy, and micro-density

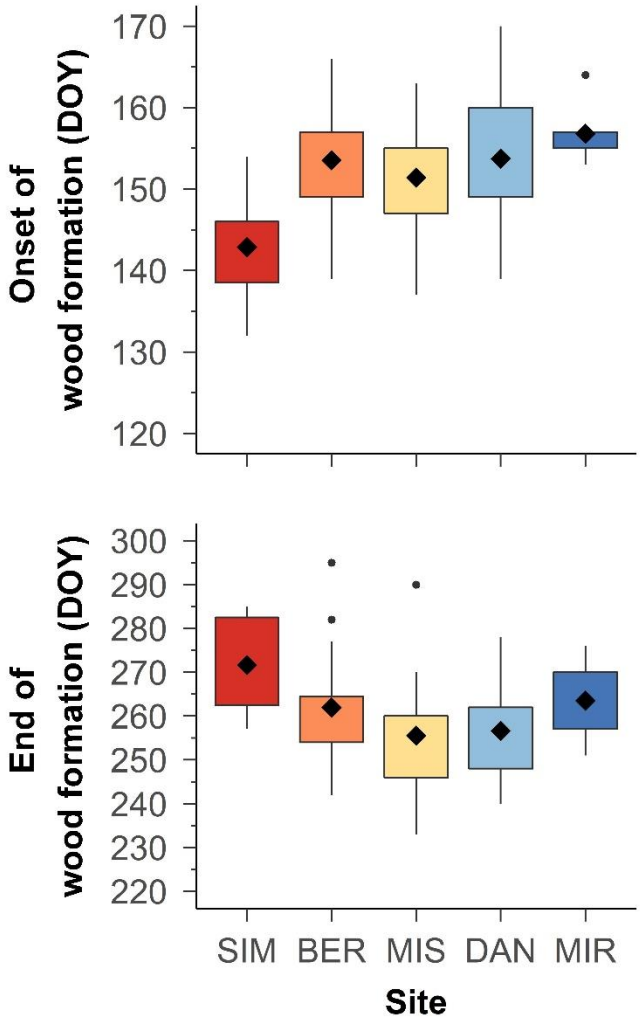

Figure 4.3 Box and whisker diagram representing the date of onset and the end of wood formation (expressed in DOY) for *Picea mariana*. Data were collected between 2002 and 2016 (except for MIR, 2012–2016) along a latitudinal gradient. Sites on the plot are organized from southernmost (left; red) to northernmost (right, blue). Black diamonds represent mean values, lower and upper box limits represent the first and third quartiles, vertical bars represent 1.5× the interquartile range, and black dots represent outliers.

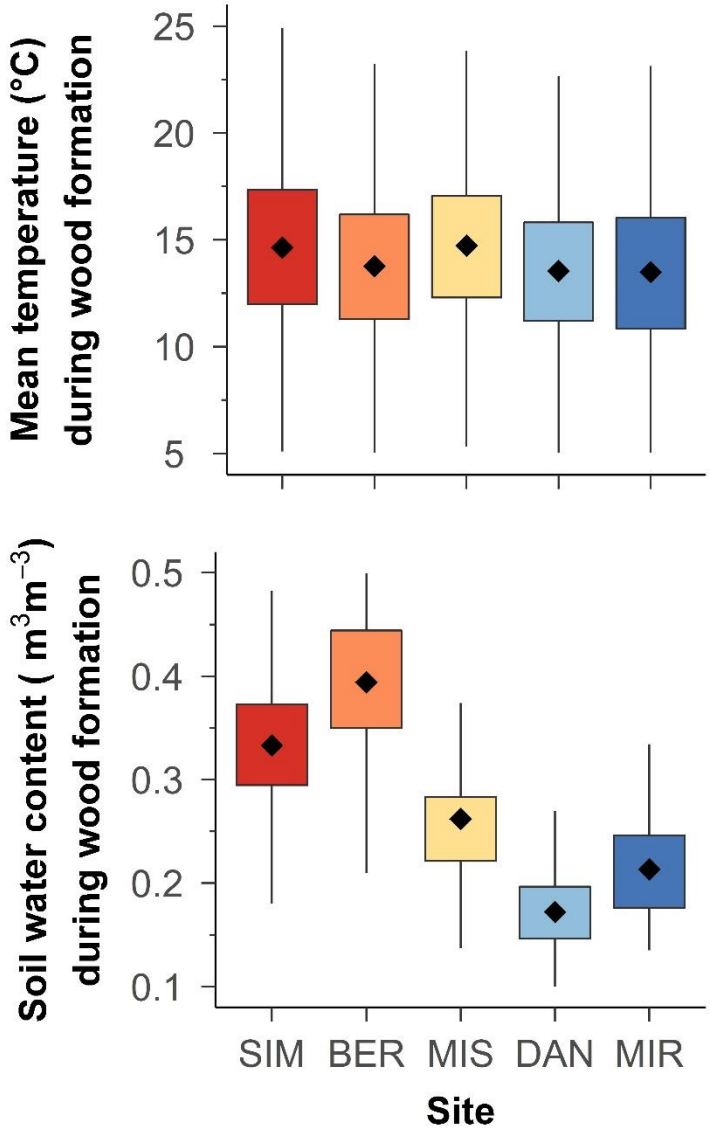

Figure 4.4 Box and whisker diagram representing mean temperature (°C) and soil water content (m3·m-3) during the entire period of wood formation of Picea mariana. Data were collected between 2002 and 2016 (except for MIR, 2012–2016) across a latitudinal gradient. Sites on the plot are organized from southernmost (left; red) to northernmost (right, blue). Black diamonds represent mean values, lower and upper box limits represent the first and third quartiles, vertical bars represent 1.5× the interquartile range, and black dots represent outliers.

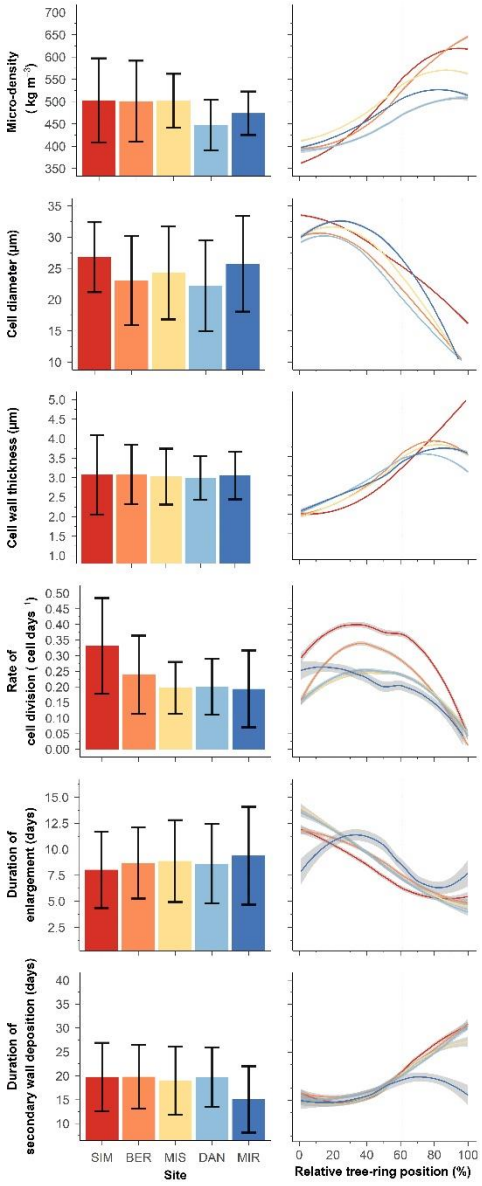

Figure 4.5 **Left side**: Average with standard deviation error bars of micro-density ($kg \cdot m^{-3}$), cell anatomy (diameter and wall thickness of the cell, µm), rate of cell division ($cell \cdot day^{-1}$), duration of the wood formation phases (cell enlargement and secondary cell wall deposition, days) of *Picea mariana* for 2002–2016 (except for MIR, 2012–2016) along a latitudinal gradient. On the **right side**, the average patterns for each site are represented across the tree ring (expressed in %). The main trends were highlighted by means of loess function (span 0.9), with shading representing the 95% confidence interval. Sites on the plot are organized from southernmost (left; red) to northernmost (right, blue).

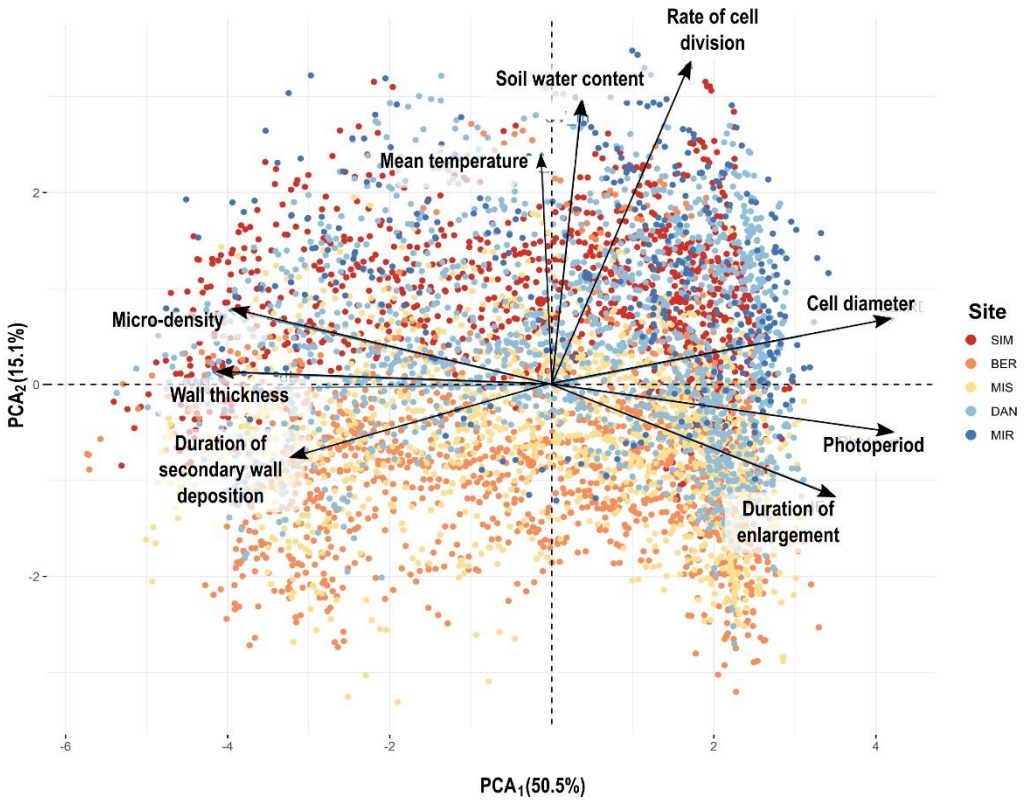

Figure 4.6 Principal component analysis (PCA) representing the variability explained by the first two dimensions and their relative contribution (%). The PCA projects the variables related to environmental factors recorded during wood formation (temperature, photoperiod, and soil water content), wood formation dynamics (rate of cell division, duration cell enlargement, and duration of secondary cell wall deposition), cell anatomy (cell diameter and cell wall thickness), and tree ring's micro-density of *Picea mariana* at the sampling sites along a latitudinal gradient. Warmest colours (red) represent the southernmost sites, whereas coldest colours represent the northernmost sites

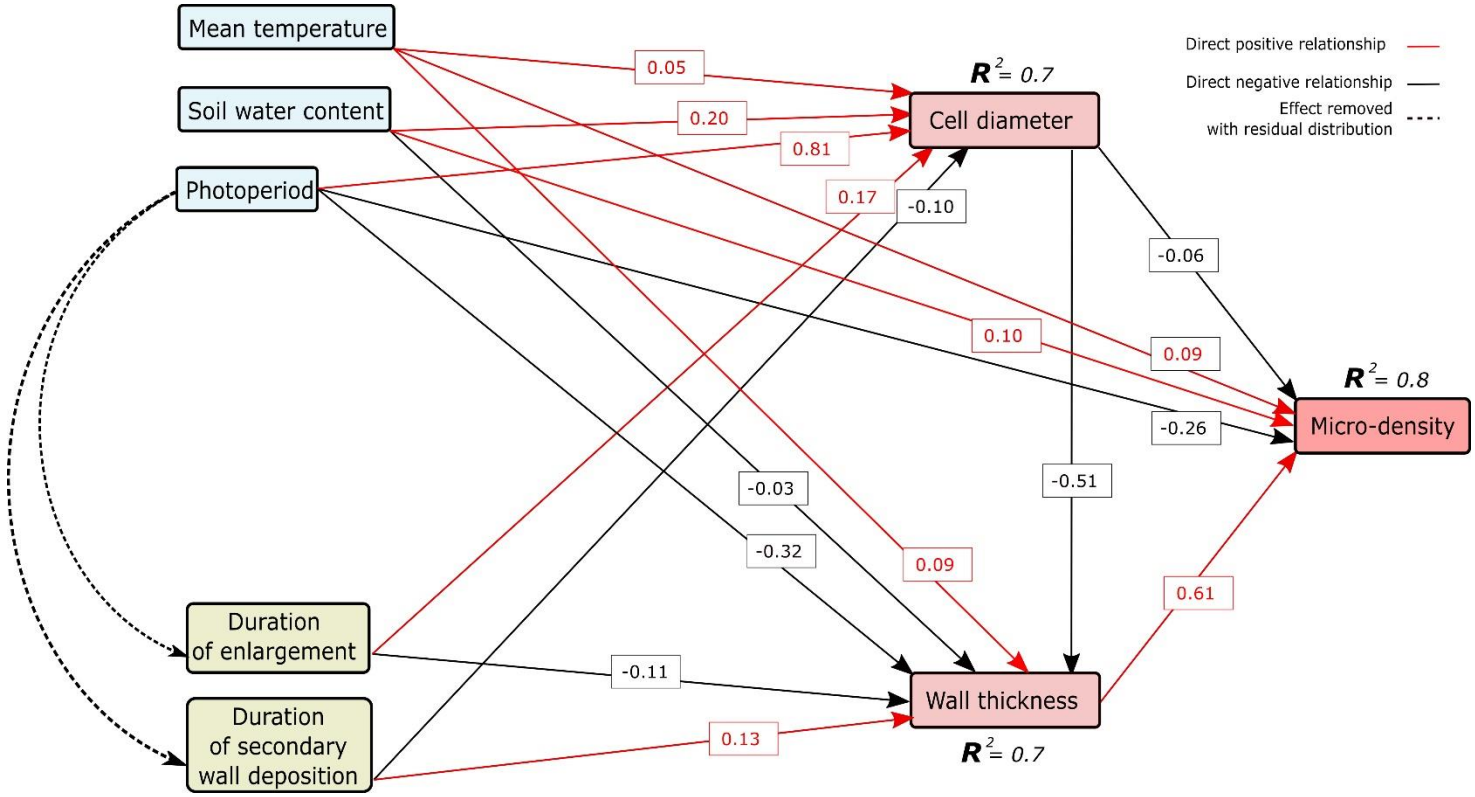

Figure 4.7 Structural equation model (SEM) linking environmental factors during cell differentiation (temperature, photoperiod, and soil water content), wood formation dynamics (duration cell enlargement and duration of secondary cell wall deposition), cell anatomy (cell diameter and cell wall thickness), and tree ring's micro-density of *Picea mariana.* Red and black lines represent positive and negative relationships, respectively. Dashed lines represent the correlations between photoperiod and wood formation dynamics, i.e. duration of enlargement (r = 0.64) and duration of secondary wall deposition (r = −0.62). The effect of photoperiod on wood formation dynamics has been removed by using their residual distributions in the SEM, which were obtained by the regression between the duration of enlargement (or duration of secondary wall deposition) and photoperiod.

4.9 References

Anfodillo T, Deslauriers A, Menardi R, Tedoldi L, Petit G, Rossi S. **2011**. Widening of xylem conduits in a conifer tree depends on the longer time of cell expansion downwards along the stem. *Journal of experimental botany* **63**: 837–845.

Arzac A, Rozas V, Rozenberg P, Olano JM. **2018**. Water availability controls Pinus pinaster xylem growth and density: A multi-proxy approach along its environmental range. *Agricultural and Forest Meteorology* **250**–**251**: 171–180.

Balducci L, Cuny HE, Rathgeber CBK, Deslauriers A, Giovannelli A, Rossi S. **2016**. Compensatory mechanisms mitigate the effect of warming and drought on wood formation. *Plant, Cell and Environment* **39**: 1338–1352.

Balducci L, Deslauriers A, Giovannelli A, Beaulieu M, Delzon S, Rossi S, Rathgeber CBK. **2015**. How do drought and warming influence survival and wood traits of *Picea mariana* saplings. *Journal of experimental botany* **66**: 377–89.

Balducci L, Deslauriers A, Giovannelli A, Rossi S, Rathgeber CBK. **2013**. Effects of temperature and water deficit on cambial activity and woody ring features in *Picea mariana* saplings. *Tree physiology* **33**: 1006–17.

Balzano A, Battipaglia G, De Micco V. **2019**. Wood-Trait analysis to understand climatic factors triggering intra-Annual density-fluctuations in co-occurring Mediterranean trees. *IAWA Journal* **40**: 241–258.

Barnett JR, Jeronimidis G. **2003**. *Wood quality and its biological basis*. Blackwell.

Beaujean, A. A. 2014. Latent variable modeling using R: A step-by-step guide. Routledge, Taylor & Francis Group, New York.

Belien E, Rossi S, Morin H, Deslauriers A. **2012**. Xylogenesis in black spruce subjected to rain exclusion in the field. *Canadian journal of forest research* **42**: 1306–1315.

Bendevis MA, Sun Y, Rosenqvist E, Shabala S, Liu F, Jacobsen SE. **2014**. Photoperiodic effects on short-pulse 14C assimilation and overall carbon and nitrogen allocation patterns in contrasting quinoa cultivars. *Environmental and Experimental Botany* **104**: 9–15.

Bergh J, Linder S, Lundmark T, Elfving B. **1999**. The effect of water and nutrient availability on the productivity of Norway spruce in northern and southern Sweden. *Forest Ecology and Management* **119**: 51–62.

Björklund J, Seftigen K, Schweingruber F, Fonti P, Arx G, Bryukhanova M V, Cuny HE, Carrer M, Castagneri D, Frank DC. **2017**. Cell size and wall dimensions drive distinct variability of earlywood and latewood density in Northern Hemisphere conifers. *New Phytologist* **216**: 728–740.

Boudreau J, Nelson RF, Margolis HA, Beaudoin A, Guindon L, Kimes DS. **2008**. Regional aboveground forest biomass using airborne and spaceborne LiDAR in Québec. *Remote Sensing of Environment* **112**: 3876–3890.

Bradshaw CJA, Warkentin IG. **2015**. Global estimates of boreal forest carbon stocks and flux. *Global and Planetary Change* **128**: 24–30.

Buttò V, Deslauriers A, Rossi S, Rozenberg P, Shishov V, Morin H. **2020**. The role of plant hormones in tree-ring formation. *Trees - Structure and Function* **34**: 315–335.

Buttò V, Rossi S, Deslauriers A, Morin H. **2019**. Is size an issue of time? Relationship between the duration of xylem development and cell traits. *Annals of Botany* **123**: 1257–1265.

Cabon A, Fernández-de-Uña L, Gea-Izquierdo G, Meinzer FC, Woodruff DR, Martínez-Vilalta J, De Cáceres M. **2020**. Water potential control of turgor-driven tracheid enlargement in Scots pine at its xeric distribution edge. *New Phytologist* **225**: 209–221.

Cartenì F, Deslauriers A, Rossi S, Morin H, De Micco V, Mazzoleni S, Giannino F. **2018**. The physiological mechanisms behind the earlywood-to-latewood transition: a process-based modelling approach. *Frontiers in Plant Science* **9**: 1053.

Castagneri D, Fonti P, Von Arx G, Carrer M. **2017**. How does climate influence xylem morphogenesis over the growing season? Insights from long-Term intra-ring anatomy in Picea abies. *Annals of Botany* **119**: 1011–1020.

Cato S, McMillan L, Donaldson L, Richardson T, Echt C, Gardner R. **2006**. Wood formation from the base to the crown in *Pinus radiata*: gradients of tracheid wall thickness, wood density, radial growth rate and gene expression. Plant Mol Biol. *Plant molecular biology* **60**: 565–581.

Chave J, Coomes D, Jansen S, Lewis SL, Swenson NG, Zanne AE. **2009**. Towards a worldwide wood economics spectrum. *Ecology letters* **12**: 351–366.

Chen L, Rossi S, Deslauriers A, Liu J. **2019**. Contrasting strategies of xylem formation between black spruce and balsam fir in Quebec, Canada. *Tree Physiology* **39**: 747–754.

Chincinska I, Gier K, Krügel U, Liesche J, He H, Grimm B, Harren FJM, Cristescu SM, Kühn C. **2013**. Photoperiodic regulation of the sucrose transporter StSUT4 affects the expression of circadian-regulated genes and ethylene production. *Frontiers in Plant Science* **4**: 26.

Cosgrove DJ. **1997**. Relaxation in a high-stress environment: The molecular bases of extensible cell walls and cell enlargement. *Plant Cell* **9**: 1031–1041.

Cosgrove DJ. **2016**. Plant cell wall extensibility: Connecting plant cell growth with cell wall structure, mechanics, and the action of wall-modifying enzymes. *Journal of Experimental Botany* **67**: 463–476.

Cuny HE, Rathgeber CBK. **2016**. Xylogenesis: coniferous trees of temperate forests are listening to the climate tale during the growing season but only remember the last words! *Plant Physiology* **171**: 306–317.

Cuny HE, Rathgeber CBK, Frank D, Fonti P, Fournier M. **2014**. Kinetics of tracheid development explain conifer tree-ring structure. *New Phytologist* **203**: 1231–1241.

Cuny HE, Rathgeber CBK, Frank D, Fonti P, Makinen H, Prislan P, Rossi S, Del Castillo EM, Campelo F, Vavrčík H, *et al.* 2015. Woody biomass production lags stem-girth increase by over one month in coniferous forests. *Nature Plants* **1**: 1–6.

Cuny HE, Rathgeber CBK, Kiessé TS, Hartmann FP, Barbeito I, Fournier M. **2013**. Generalized additive models reveal the intrinsic complexity of wood formation dynamics. *Journal of Experimental Botany* **64**: 1983–94.

Delpierre N, Lireux S, Hartig F, Camarero JJ, Cheaib A, Čufar K, Cuny H, Deslauriers A, Fonti P, Gričar J, *et al.* 2019. Chilling and forcing temperatures interact to predict the onset of wood formation in Northern Hemisphere conifers. *Global change biology* **25**: 1089–1105.

Deslauriers A, Fournier MP, Cartenì F, Mackay J. **2019**. Phenological shifts in conifer species stressed by spruce budworm defoliation. *Tree Physiology* **39**: 590–605.

Deslauriers A, Huang J-G, Balducci L, Beaulieu M, Rossi S. **2016**. The contribution of carbon and water in modulating wood formation in black spruce saplings. *Plant Physiology* **170**(4): 2072–2084.

Deslauriers A, Caron L, Rossi S. **2015**. Carbon allocation during defoliation: Testing a defense-growth trade-off in balsam fir. *Frontiers in Plant Science* **6**: 1–13.

Deslauriers A, Morin H. **2005**. Intra-annual tracheid production in balsam fir stems and the effect of meteorological variables. *Trees* **19**: 402–408.

Deslauriers A, Morin H, Begin Y. **2003**. Cellular phenology of annual ring formation of *Abies balsamea* in the Quebec boreal forest (Canada). *Canadian Journal of Forest Research* **33**: 190–200.

Deslauriers A, Rossi S, Anfodillo T, Saracino A. **2008**. Cambial phenology, wood formation and temperature thresholds in two contrasting years at high altitude in southern Italy. *Tree physiology* **28**: 863–871.

Drew DM, Allen K, Downes GM, Evans R, Battaglia M, Baker P. **2013**. Wood properties in a long-lived conifer reveal strong climate signals where ring-width series do not. *Tree Physiology* **33**: 37–47.

Dünser K, Kleine-Vehn J. **2015**. Differential growth regulation in plants—the acid growth balloon theory. *Current opinion in plant biology* **28**: 55–59.

Ericsson T, Rytter L, Vapaavuori E. **1996**. Physiology of carbon allocation in trees. *Biomass and Bioenergy* **11**(2-3): 115–127.

Fonti P, Bryukhanova M V., Myglan VS, Kirdyanov A V., Naumova O V., Vaganov EA. **2013**. Temperature-induced responses of xylem structure of Larix sibirica (Pinaceae) from the Russian Altay. *American journal of botany* **100**: 1332–1343.

Friend AD, Eckes-Shephard AH, Fonti P, Rademacher TT, Rathgeber CBK, Richardson AD, Turton RH. **2019**. On the need to consider wood formation processes in global vegetation models and a suggested approach. *Annals of Forest Science* **76**: 49.

Gagen M, McCarroll D, Edouard J-L. **2006**. Combining ring width, density and stable carbon isotope proxies to enhance the climate signal in tree-rings: an example from the southern french alps. *Climatic Change* **78**: 363–379.

Gauthier S, Bernier P, Kuuluvainen T, Shvidenko AZ, Schepaschenko DG. **2015**. Boreal forest health and global change. *Science* **349**: 819–822.

Giroud G, Bégin J, Defo M, Ung CH. **2017**. Regional variation in wood density and modulus of elasticity of Quebec's main boreal tree species. *Forest Ecology and Management* **400**: 289–299.

Goulden ML, Daube BC, Fan SM, Sutton DJ, Bazzaz A, Munger JW, Wofsy SC. **1997**. Physiological responses of a black spruce forest to weather. *Journal of Geophysical Research Atmospheres* **102**: 28987–28996.

Guerriero G, Hausman J-F, Cai G. **2014**. No stress! Relax! Mechanisms governing growth and shape in plant cells. *International journal of molecular sciences* **15**: 5094–5114.

Hacke UG, Spicer R, Schreiber SG, Plavcová L. **2017**. An ecophysiological and developmental perspective on variation in vessel diameter. *Plant Cell and Environment* **40**: 831–845.

Hartmann FP, Rathgeber CBK, Fournier M, Moulia B. **2017**. Modelling wood formation and structure: power and limits of a morphogenetic gradient in controlling xylem cell proliferation and growth. *Annals of forest science* **74**: 14.

Hayes DJ, Turner DP, Stinson G, McGuire AD, Wei Y, West TO, Heath LS, Jong B, McConkey BG, Birdsey RA, *et al.* 2012. Reconciling estimates of the contemporary North American carbon balance among terrestrial biosphere models, atmospheric inversions, and a new approach for estimating net ecosystem exchange from inventory-based data. *Global Change Biology* **18**: 1282–1299.

Hooper D, Coughlan J, - MM. **2008**. Structural Equation Modelling: Guidelines for Determining Model Fit. *Electronic Journal of Business Research Methods* **6**: 53-60.

Hopkinson RF, Mckenney DW, Milewska EJ, Hutchinson MF, Papadopol P, Vincent ALA. **2011**. Impact of aligning climatological day on gridding daily maximum-minimum temperature and precipitation over Canada. *Journal of Applied Meteorology and Climatology* **50**: 1654–1665.

Hu LT, Bentler PM. **1999**. Cutoff criteria for fit indexes in covariance structure analysis:

Conventional criteria versus new alternatives. *Structural Equation Modeling* **6**: 1–55.

Hutchinson MF, McKenney DW, Lawrence K, Pedlar JH, Hopkinson RF, Milewska E, Papadopol P. **2009**. Development and testing of Canada-wide interpolated spatial models of daily minimum-maximum temperature and precipitation for 1961-2003. *Journal of Applied Meteorology and Climatology* **48**: 725–741.

Ivakov A, Flis A, Apelt F, Fünfgeld M, Scherer U, Stitt M, Kragler F, Vissenberg K, Persson S, Suslov D. **2017**. Cellulose synthesis and cell expansion are regulated by different mechanisms in growing arabidopsis hypocotyls. *Plant Cell* **29**: 1305–1315.

Khadilkar AS, Yadav UP, Salazar C, Shulaev V, Paez-Valencia J, Pizzio GA, Gaxiola RA, Ayre BG. **2016**. Constitutive and companion cell-specific overexpression of AVP1, encoding a proton-pumping pyrophosphatase, enhances biomass accumulation, phloem loading, and long-distance transport1[OPEN]. *Plant Physiology* **170**: 401–414.

Körner C. **2012**. Growth and development. In *Alpine treelines: functional ecology of the global high elevation tree limits*. Springer, Basel: 85–104

Kühn C. **2003**. A comparison of the sucrose transporter systems of different plant species. *Plant Biology* **5**: 215–232.

Kühn C, Grof CPL. **2010**. Sucrose transporters of higher plants. *Current Opinion in Plant Biology* **13**: 287–297.

Kuptz D, Fleischmann F, Matyssek R, Grams TEE. **2011**. Seasonal patterns of carbon allocation to respiratory pools in 60-yr-old deciduous (Fagus sylvatica) and evergreen (Picea abies) trees assessed via whole-tree stable carbon isotope labeling. *New Phytologist* **191**: 160–172.

Lemay A, Krause C, Achim A. **2017**. Comparison of wood density in roots and stems of black spruce before and after commercial thinning. *Forest Ecology and Management* **40**: 94-102.

Lim H, Oren R, Palmroth S, Tor-ngern P, Mörling T, Näsholm T, Lundmark T, Helmisaari H-S, Leppälammi-Kujansuu J, Linder S. **2015**. Inter-annual variability of precipitation constrains the production response of boreal *Pinus sylvestris* to nitrogen fertilization. *Forest Ecology and Management* **348**: 31–45.

Little E. 1999. Digital representation of "Atlas of United States Trees". US Geological Survey, Reston, VA. http://esp. cr. usgs. gov/data/atlas/little U.S. Geolo.

Majda M, Robert S. **2018**. The role of auxin in cell wall expansion. *International Journal of Molecular Sciences* **19**: 951.

Martin M, Krause C, Fenton NJ, Morin H. **2020**. Unveiling the Diversity of Tree Growth Patterns in Boreal Old-Growth Forests Reveals the Richness of Their Dynamics. *Forests* **11**: 252.

McKenney DW, Hutchinson Michael F, Papadopol P, Lawrence K, Pedlar J, Campbell K, Milewska E, Hopkinson RF, Price D, Owen T. **2011**. Customized spatial climate models for North America. *Bulletin of the American Meteorological Society* **12**: 1611–22.

Millier F, Verger M, Rozenberg P. **2006**. Microdensitométrie sur arbres forestiers. *Les cahiers des techniques de l'INRA,* INRA, Orléans: 87–91.

Nilsson LO. **1997**. Manipulation of conventional forest management practices to increase forest growth - Results from the Skogaby project. *Forest Ecology and Management* **91**: 53–60.

Paixao C, Krause C, Morin H, Achim A. **2019**. Wood quality of black spruce and balsam fir trees defoliated by spruce budworm: A case study in the boreal forest of Quebec, Canada. *Forest Ecology and Management* **437**: 201–210.

Pan Y, Birdsey RA, Fang J, Houghton R, Kauppi PE, Kurz WA, Phillips OL, Shvidenko A, Lewis SL, Canadell JG, *et al.* 2011. A large and persistent carbon sink in the world's forests. *Science,* **333***(*6045): 988–993.

Payyavula RS, Tay KHC, Tsai C-J, Harding SA. **2011**. The sucrose transporter family in Populus: the importance of a tonoplast PtaSUT4 to biomass and carbon partitioning. *The Plant Journal* **65**: 757–770.

Polge H, Nicholls J. **1972**. Quantitative radiography and the densitometric analysis of wood. *Wood Sci* **5**: 51–59.

Preston KA, Cornwell WK, DeNoyer JL. **2006**. Wood density and vessel traits as distinct correlates of ecological strategy in 51 California coast range angiosperms. *New Phytologist* **170**: 807–818.

Puchi PF, Castagneri D, Rossi S, Carrer M. **2019**. Wood anatomical traits in black spruce reveal latent water constraints on the boreal forest. *Global Change Biology* **26**(3):1767–1777.

Rathgeber CBK. **2017**. Conifer tree-ring density inter-annual variability - anatomical, physiological and environmental determinants. *New Phytologist* **216**: 621–625.

Rathgeber CBK, Decoux V, Leban J-M. **2006**. Linking intra-tree-ring wood density variations and tracheid anatomical characteristics in Douglas fir (*Pseudotsuga menziesii* (Mirb.) Franco). *Annals of Forest Science* **63**: 699–706.

Roderick ML, Berry SL. **2002**. Linking wood density with tree growth and environment: a theoretical analysis based on the motion of water. *New Phytologist* **149**: 473–485.

Rogers LA, Dubos C, Cullis IF, Surman C, Poole M, Willment J, Mansfield SD, Campbell MM. **2005**. Light, the circadian clock, and sugar perception in the control of lignin biosynthesis. *Journal of Experimental Botany* **56**: 1651–1663.

Rosseel Y. **2012**. Lavaan: An R package for structural equation modeling and more. Version 0.5–12 (BETA). *Journal of statistical* **48**: 1–36.

Rossi S. **2015**. Local adaptations and climate change: converging sensitivity of bud break in black spruce provenances. *International Journal of Biometeorology* **59**: 827–835.

Rossi S, Anfodillo T, Deslauriers A. **2006a**. Assessment of cambial activity and xylogenesis by microsampling tree species: an example at the alpine timberline. *IAWA Journal* **27**: 383–394.

Rossi S, Cairo E, Krause C, Deslauriers A. **2015**. Growth and basic wood properties of black spruce along an alti-latitudinal gradient in Quebec, Canada. *Annals of Forest Science* **72**: 77–87.

Rossi S, Deslauriers A, Anfodillo T, Morin H, Saracino A, Motta R, Borghetti M. **2006b**. Conifers in cold environments synchronize maximum growth rate of tree-ring formation with day length. *New phytologist* **170**: 301–310.

Rossi S, Deslauriers A, Griçar J, Seo J-WW, Rathgeber CBK, Anfodillo T, Morin H, Levanic T, Oven PP, Jalkanen R. **2008**. Critical temperatures for xylogenesis in conifers of cold climates. *Global Ecology and Biogeography* **17**: 696–707.

Rossi S, Menardi R, Anfodillo T. **2006c**. Trephor: a new tool for sampling microcores from tree stems. *IAWA Journal* **27**: 89–97.

Rozenberg P, Chauvin T, Escobar-Sandoval M, Huard F, Shishov V, Charpentier JP, Sergent AS, Vargas-Hernandez JJ, Martinez-Meier A, Pâques L. **2020**. Climate warming differently affects Larix decidua ring formation at each end of a French Alps elevational gradient. *Annals of Forest Science* **77**(2)**:** 1–20.

Simard S, Giovannelli A, Treydte K, Traversi ML, King GM, Frank D, Fonti P. **2013**. Intra-annual dynamics of non-structural carbohydrates in the cambium of mature conifer trees reflects radial growth demands. *Tree Physiology* **33**: 913–923.

Sniderhan AE, McNickle GG, Baltzer JL. **2018**. Assessing local adaptation vs. plasticity under different resource conditions in seedlings of a dominant boreal tree species. *AoB PLANTS* **10**: 1–13.

Steppe K, Sterck F, Deslauriers A. **2015**. Diel growth dynamics in tree stems: Linking anatomy and ecophysiology. *Trends in Plant Science* **20**: 335–343.

Sulpice R, Flis A, Ivakov AA, Apelt F, Krohn N, Encke B, Abel C, Feil R, Lunn JE, Stitt M. **2014**. Arabidopsis coordinates the diurnal regulation of carbon allocation and growth across a wide range of Photoperiods. *Molecular Plant* **7**: 137–155.

Teets DA. **2003**. Predicting sunrise and sunset times. *The College Mathematics Journal* **34**: 317–321.

Thurner M, Beer C, Santoro M, Carvalhais N, Wutzler T, Schepaschenko D, Shvidenko A, Kompter E, Ahrens B, Levick SR, *et al.* 2014. Carbon stock and density of northern boreal and temperate forests. *Global Ecology and Biogeography* **23**: 297–310.

Traversari S, Emiliani G, Traversi ML, Anichini M, Giovannelli A. **2018**. Pattern of

carbohydrate changes in maturing xylem and phloem during growth to dormancy transition phase in *Picea abies* (L.) Karst. *Dendrobiology* **80**: 12–23.

Turcotte A, Morin H, Krause C, Deslauriers A, Thibeault-Martel M. **2009**. The timing of spring rehydration and its relation with the onset of wood formation in black spruce. *Agricultural and Forest Meteorology* **149**: 1403–1409.

Verbančič J, Lunn JE, Stitt M, Persson S. **2018**. Carbon Supply and the Regulation of Cell Wall Synthesis. *Molecular Plant* **11**: 75–94.

Vieira J, Carvalho A, Campelo F. **2020**. Tree Growth Under Climate Change : Evidence From Xylogenesis Timings and Kinetics Study Site and Experimental Design. *Frontiers in Plant Science* **11**: 1–11.

Way DA, Montgomery RA. **2015**. Photoperiod constraints on tree phenology, performance and migration in a warming world. *Plant, Cell & Environment* **38**: 1725–1736.

Way DA, Oren R. **2010**. Differential responses to changes in growth temperature between trees from different functional groups and biomes: a review and synthesis of data. *Tree Physiology* **30**: 669–688.

Way DA, Sage RF. **2008**. Elevated growth temperatures reduce the carbon gain of black spruce [Picea mariana (Mill.) B.S.P.]. *Global Change Biology* **14**: 624–636.

Wimmer R, Grabner M. **2000**. A comparison of tree-ring features in Picea abies as correlated with climate. *IAWA Journal* **21**: 403–416.

Zarra I, Revilla G, Sampedro J, Valdivia ER. **2019**. Biosynthesis and Regulation of Secondary Cell Wall. In: Cánovas F., Lüttge U., Leuschner C., Risueño MC. (eds) Progress in Botany Vol. 81. Progress in Botany, vol 81. Springer, Cham.

Ziaco E. **2020**. A phenology-based approach to the analysis of conifers intra-annual xylem anatomy in water-limited environments. *Dendrochronologia* **59**: 125662.

Zuur AF, Ieno EN, Elphick CS. **2010**. A protocol for data exploration to avoid common statistical problems. *Methods in Ecology and Evolution* **1**: 3–14

4.10 Acknowledgements

This study was funded by the NSERC Industrial Research Chair on Spruce Growth and the Influence of Spruce Budworm on Landscape Variability in Boreal Forests, the Canada Foundation for Innovation, le Consortium de Recherche sur la Forêt Boréale Commerciale, les Fonds de Recherche sur la Nature et les Technologies du Québec, and la Forêt d'Enseignement et de Recherche Simoncouche. The authors thank F. Millier and the Phenobois technical platform, M. Boulianne, J. Boulouf, B. Dufour, G. Dumont-Frenette, F. Gionest, M.-J. Girard, A. Lemay, C. Lupi, V. Nèron, S. Pedneault, P.-Y. Plourde, G. Savard, M. Thibeault-Martel, and M.-J. Tremblay for technical support. Murray Hay verified the English.

4.11 Authors' contributions

VB, AD, and SR conceived the ideas;
VB, SR, PR, and AD designed the methodology;
VB analyzed the data and wrote the manuscript;
SR, AD, PR, and HM commented on the manuscript;
All authors contributed critically to the drafts and gave final approval for publication.

4.12 Supplementary materials

Fig. S1 Left side: Spatial distribution of the five study sites along a latitudinal gradient. The inset map represents the spatial distribution of black spruce in North America (inset map modified from from (Little, 1999). **Right side**: Walter & Lieth diagrams representing the average climatic conditions at each site. Climate statistics for temperature and precipitation were calculated using 1950–2016 data and the ANUSPLIN algorithm to obtain the long-term mean (Hutchinson et al., 2009; Hopkinson et al., 2011; McKenney et al., 2011).

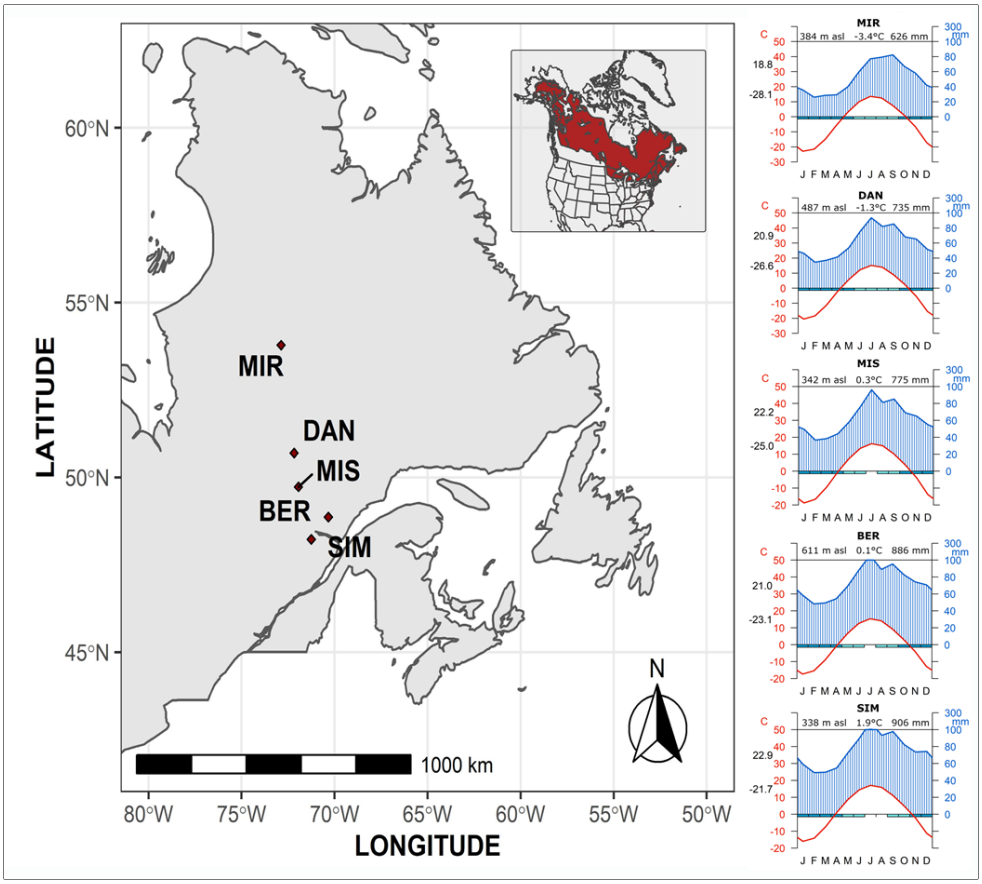

Fig. S2 Average and the interannual variability of the number of cells in *Picea mariana* tree rings measured in the study sites along the latitudinal gradient over the period 2002-2016, except for MIR (2012-2016). Black diamonds represent mean values, lower and upper box limits represent the first and third quartiles, vertical bars represent 1.5× the interquartile range, and black dots represent outliers.

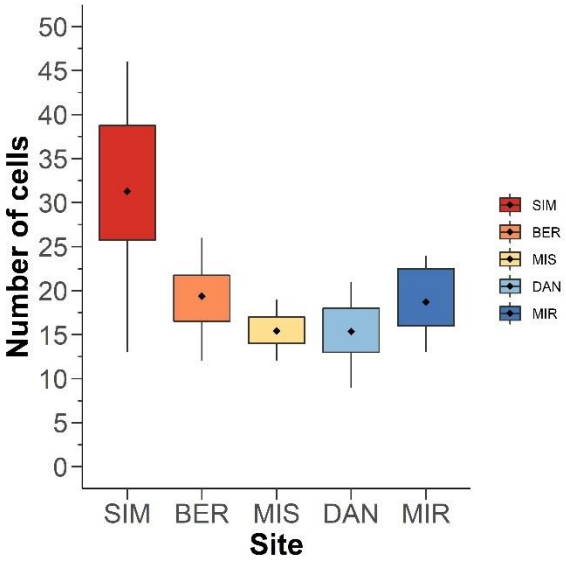

Table S1 Pearson correlation matrix of the endogenous and exogenous factors involved in micro-density variations for *Picea mariana*

	1	2	3	4	5	6	7	8	9
1 Micro-density		-0.74	0.85	-0.32	-0.61	0.55	-0.77	0.05	0.11
2 Cell diameter	-0.74		-0.77	0.55	0.64	-0.57	0.79	0.11	0.1
3 Wall thickness	0.85	-0.77		-0.34	-0.63	0.6	-0.72	0	-0.04
4 Rate of cell division	-0.32	0.55	-0.34		0.12	-0.24	0.37	0.24	0.21
5 Duration of enlargement	-0.61	0.64	-0.63	0.12		-0.44	0.64	-0.06	0.02
6 Duration of secondary wall deposition	0.55	-0.57	0.6	-0.24	-0.44		-0.62	-0.11	0.04
7 Photoperiod	-0.77	0.79	-0.72	0.37	0.64	-0.62		0.06	-0.12
8 Mean temperature	0.05	0.11	0	0.24	-0.06	-0.11	0.06		0.01
9 Soil water content	0.11	0.1	-0.04	0.21	0.02	0.04	-0.12	0.01	

References

Hopkinson RF, Mckenney DW, Milewska EJ, Hutchinson MF, Papadopol P, Vincent ALA. **2011**. Impact of aligning climatological day on gridding daily maximum-minimum temperature and precipitation over Canada. *Journal of Applied Meteorology and Climatology* **50**: 1654–1665.

Hutchinson MF, McKenney DW, Lawrence K, Pedlar JH, Hopkinson RF, Milewska E, Papadopol P. **2009**. Development and testing of Canada-wide interpolated spatial models of daily minimum-maximum temperature and precipitation for 1961-2003. *Journal of Applied Meteorology and Climatology* **48**: 725–741.

Little E. 1999. Digital representation of "Atlas of United States Trees". US Geological Survey, Reston, VA. http://esp. cr. usgs. gov/data/atlas/little U.S. Geolo.

McKenney DW, Hutchinson Michael F, Papadopol P, Lawrence K, Pedlar J, Campbell K, Milewska E, Hopkinson RF, Price D, Owen T. **2011**. Customized spatial climate models for North America. *Bulletin of the American Meteorological Society* **12**: 1611–22.

CHAPITRE IV

COMPARING THE CELL DYNAMICS OF TREE-RING FORMATION OBSERVED IN MICROCORES AND AS PREDICTED BY THE VAGANOV–SHASHKIN MODEL

Published in *Frontiers in Plant Science*

Buttò, V., V. Shishov, I. Tychkov, M. Popkova, M. He, S. Rossi, A. Deslauriers, and H. Morin. "Comparing the cell dynamics of tree-ring formation observed in microcores and as predicted by the Vaganov–Shashkin model." Front. Plant Sci. 11: 1268. doi: 10.3389/fpls (2020).

Comparing the cell dynamics of tree-ring formation observed in microcores and as predicted by the Vaganov–Shashkin model

Valentina Buttò*[1], Vladimir Shishov[2,5], Ivan Tychkov[2], Margarita Popkova[2], Minhui He[3], Sergio Rossi[1, 4,] Annie Deslauriers[1], Hubert Morin[1]

1 Département des Sciences fondamentales, Université du Québec à Chicoutimi, Chicoutimi, QC, Canada

2 Laboratory for integral studies of forest dynamics of Eurasia, Siberian Federal University, Krasnoyarsk, Russia

3 College of Forestry, Northwest Agriculture and Forestry University, Yangling China

4 Key Laboratory of Vegetation Restoration and Management of Degraded Ecosystems, Guangdong Provincial Key Laboratory of Applied Botany, South China Botanical Garden, Chinese Academy of Sciences, Guangzhou, China

5 Environmental and Research Center, South China Botanical Garden, Chinese Academy of Sciences, Guangzhou, China

Running title: Validation of VS model predictions of timing

*Corresponding author: Valentina Buttò (orcid:0000-0003-1595-6745),

Département des Sciences fondamentales, Université du Québec à Chicoutimi,

555, boulevard de l'Université, Chicoutimi (Québec), Canada G7H 2B1

Phone number: +1-418-545-5011 ext. 2330Email: valentina.butto1@uqac.ca

5.1 Abstract

New insights into the intra-annual dynamics of tree-ring formation can improve our understanding of tree-growth response to environmental conditions at high-resolution time scales. Obtaining this information requires, however, a weekly monitoring of wood formation, sampling that is extremely time-intensive and scarcely feasible over vast areas. Estimating the timing of cambial and xylem differentiation by modeling thus represents an interesting alternative for obtaining this important information by other means. Temporal dynamics of cambial divisions can be extracted from the daily tree-ring growth rate computed by the Vaganov–Shashkin (VS) simulation model, assuming that cell production is tightly linked to tree-ring growth. Nonetheless, these predictions have yet to be compared with direct observations of wood development, i.e., via microcoring, over a long time span. We tested the performance of the VS model by comparing the observed and predicted timing of wood formation in black spruce [Picea mariana (Mill.)]. We obtained microcores over 15 years at 5 sites along a latitudinal gradient in Quebec (Canada). The measured variables included cell size and the timing of cell production and differentiation. We calibrated the VS model using daily temperature and precipitation recorded by weather stations located on each site. The predicted and observed timing of cambial and enlarging cells were highly correlated (R2 = 0.8); nonetheless, we detected a systematic overestimation in the predicted timing of cambial cells, with predictions delayed by 1–20 days

compared with observations. The growth rate of cell diameter was correlated with the predicted growth rate assigned to each cambial cell, confirming that cell diameter developmental dynamics have the potential to be inferred by the tree-ring growth curve of the VS model. Model performances decrease substantially in estimating the end of wood formation. The systematic errors suggest that the actual relationships implemented in the model are unable to explain the phenological events in autumn. The mismatch between the observed and predicted timing of wood formation in black spruce within our study area can be reduced by better adapting the VS model to wet sites, a context for which this model has been rarely used.

Keywords: modeling; xylogenesis; cell diameter; timings; cambial cells; black spruce; boreal forest; growth rate

5.1 Introduction

Modeling permits the description of complex biogeochemical processes that occur in nature (Danis et al., 2012), particularly as a suite of factors drive tree-growth response to climate. Tools such as MAIDENiso, TreeRing2000, and the Vaganov–Shashkin (VS) model are mechanistic models for predicting tree growth that account for the endogenous and exogenous factors shaping tree growth and productivity (Vaganov et al., 2006; Danis et al., 2012). Among these models, the VS model requires the smallest number of inputs. Furthermore, these inputs include data that are widely used and easily available, such as tree-ring width chronologies and daily mean precipitation and temperature. The availability of these data has led to an increased use of the VS model, which can now be parameterized using a user-friendly interface, the VS-oscilloscope (Shishov et al., 2016) or new MATLAB version of the model (Anchukaitis et al., 2020). Nonetheless, the intra-annual predictions of the VS model continue to lack validation with long-term field observations that, unlike tree-ring chronologies, are scarce.

The main prediction of the VS model is the daily tree-ring growth rate, which is obtained by integrating three partial growth rates based on day-length (photoperiod), temperature, and soil water content. The variation of these environmental factors over the entire year, including the growing season, affects xylem cell production and development to result finally in different wood increments (Vaganov et al., 2006;

Balducci et al., 2016). The VS model has been applied to simulate long-term climate responses based on the variation of tree-ring width chronologies at a regional scale; study locations include the southeastern United States (Anchukaitis et al., 2006; Evans et al., 2006) and the Tibetan Plateau (He et al., 2017; Yang et al., 2017). Parameterization of the model is necessary to account for the endogenous components of tree-growth response and represents a critical but necessary step of the modeling process, a step that can provide important information about tree growth at the local scale (Evans et al., 2018; Tychkov et al., 2019).

The core of tree-ring growth is cambial activity, and the VS model has been developed to establish not only the start and end of the growing season but also the timing of xylem cell production and the final size of these cells (Popkova et al., 2018). This particular aspect of the VS model has heightened interest in its application with the abundance of literature discussing intra-annual tree-ring dynamics within the cambial zone and xylem; these dynamics are related to both endogenous (developmental patterns and hormones) and exogenous (weather and seasonality) factors (Buttò et al., 2019a). The variation of xylem cell traits, i.e., cell diameter and cell wall thickness, provides important information about the trade-off between hydraulic safety and efficiency, a factor that allows plants to adapt and survive in a changing environment (Hacke et al., 2017). Cell traits depend on the temporal dynamics (duration, rate) of their differentiation phases, and environmental factors, i.e., temperature and precipitation, all of which have an influence that varies

over the growing season (Fonti et al., 2010; Cuny et al., 2019). By disentangling the effects of environmental factors on tree-ring development at a daily scale, the VS model may have the potential to simulate xylem cell differentiation, even though the existing version of the model focuses mainly on cambial cell production.

The dynamics of cell development—computed via the tree-ring growth rate curves of the VS model—are emergent properties that must be validated via observations of xylem formation. The interpretation of these emergent properties of the models should benefit from the observations (Cook and Pederson, 2011); however, unlike the traditional inter-annual tree-ring widths, long intra-annual chronologies of secondary growth are rare and data sets that are limited to a couple of years of observation do not ensure a complete picture of tree-growth response to environmental factors as these responses are often nonlinear (Rossi, 2015). Apart from the study of Popkova et al. (2018), which was based on three years of observation of wood formation, to our knowledge no study has compared the timing of cell development simulated by a VS model with data obtained directly through repeated observations of xylogenesis using microcores.

To validate the VS model predictions with observations, we used our existing 15-year, weekly scaled chronologies of wood formation from across the boreal forest of Quebec, Canada. We aimed to compare the predicted and observed timing of wood growth at both a tree-ring and xylem-cell resolution by using microcores collected

from black spruce (*Picea mariana* Mill.). Black spruce is the dominant species in the Canadian boreal forest and it grows within a great diversity of stand structures, from Alaska to Newfoundland. In Quebec, the distribution of this species extends to 58°N and forms extensive, closed forests in northeastern North America, including some of the wettest and coldest boreal forest stands. The ubiquity of black spruce leads to a very diversified tree-growth response to climate, reflecting the role of various local environmental drivers (Walker and Johnstone, 2014; Nicault et al., 2015).

For model calibration at the tree-ring scale, we relied on the existing literature and field information to assess the performance of the VS model for predicting the variability of factors and parameters that affect black spruce growth. Then, we used observations of xylogenesis to validate the timing of wood formation at the tracheid scale, i.e., cell scale, for which variability is well represented by our long time series of observations.

5.2 Methods

5.2.1 Study sites and tree selection

Samples were collected from five sites in the coniferous boreal forest of Quebec (Canada) along a latitudinal gradient stretching between 48°N and 53°N (Table 1). The sites Simoncouche (SIM) and Bernatchez (BER) are located in the balsam fir [Abies balsamea (L.) Mill.)]–white birch (Betula papyrifera Marsh.) bioclimatic

domain, while Mistassibi (MIS) and Camp Daniel (DAN) lie in the black spruce–moss bioclimatic domain. Mirage (MIR), the northernmost site, lies in the black spruce–lichen domain and is characterized by a lower tree density and growth than the more southern sites. Mean annual temperature ranges between -3.4 and 1.9 °C, with the southernmost and northernmost sites being the warmest and the coldest, respectively (Table 1). Precipitation ranges from 626 to 906 mm along the latitudinal gradient with drier conditions toward the north (Table 1). At each site, we selected ten dominant or co-dominant trees, avoiding individuals having polycormic stems, evident parasite damage, reaction wood, or partially dead crowns (Table 1).

5.2.2 Climate measurements

Precipitation, temperature, and soil water content at 30 cm soil depth were collected by automatic weather stations equipped with CR10X data loggers (Campbell Scientific Corporation, Canada); these stations were installed in a forest gap within each site. We averaged hourly measurements to obtain daily time series. We filled any minor data gaps caused by short-term technical problems using the ANUSPLIN model (Hutchinson et al., 2009; Hopkinson et al., 2011; McKenney et al., 2011).

5.2.3 Xylem formation dynamics

Microcores were collected weekly or fortnightly between April and October (2002–2016) from 10 individuals per site. Sampling was performed using a surgical bone

needle (2002–2007) or Trephor (2007–2016). Sampling at MIR took place from 2012 to 2016. Microcores were dehydrated through successive series of immersions in ethanol and D-limonene. The microcores were embedded in paraffin, cut into 8 µm transversal sections, and stained with cresyl violet acetate (0.16% in water). Xylem cell development was detected by counting the number of cells undergoing each stage of cell differentiation. We counted cambial and xylem cells along three radial lines and identified the differentiation stages of (I) enlargement, (II) cell wall thickening and lignification and (III) mature tracheids. During wood formation, cambial derivatives start dividing and differentiating in xylem and phloem cells by increasing in size. The maturation of the xylem cells is achieved once secondary wall deposition and lignification are completed (Plomion et al., 2001). Cells undergoing different differentiation stages are identified by their different shape, size, color and glistening under polarized light. Cambial cells are irregularly shaped and smaller than xylem cells (Skene, 1969). Due to the different reactions of the components of cell walls to cresyl violet acetate, enlarging cells show pinkish coloration while cells undergoing secondary wall deposition are stained in violet, turning blue when mature (Deslauriers et al., 2003). Mature cells glisten under polarized light.

We estimated the daily sequence of dividing, differentiating, and maturating cells by fitting generalized additive models (GAM) with splines to the number of cells counted for each sampling day, thereby assessing cell production and the timing of division and differentiation of each tree-ring cell at a daily scale (Cuny et al., 2013).

Timing represented the day of the year (DOY) when each cell entered into a new developmental stage (Buttò et al., 2019b). Accordingly, we estimated the DOY in which each cambial cell stopped dividing and differentiated into an enlarging xylem cell i.e. timing of enlargement, and the DOY in which each cell stopped enlarging and started cell wall deposition i.e. timing of secondary wall deposition and lignification. The duration of enlargement was computed as the difference between the timing of secondary wall deposition and the timing of enlargement for each cell. The period considered as wood formation spanned from the DOY when the number of cambial cells increased in spring to the DOY when the last formed tracheids in the tree-ring was fully mature.

5.2.4 Wood anatomy

In summer 2017, we collected additional microcores from 10 individuals per site (Rossi et al., 2006). We prepared these microcores using the abovementioned procedure, stained them in safranin (1 % in water), and permanently fixed the samples on slides using Permount™. We obtained pictures of the transversal sections using a camera fixed on an optical microscope at a magnification of 20×. Radial lumen diameter and cell wall thickness (single wall) were measured for all the study years (15 for all sites except for MIR, for which we had 5 years of observation) using WinCELL (Regent Instruments, Canada). We calculated the tracheidograms of cell diameter, relying on their relative position across the tree ring, and fit our results with

GAMs to obtain values representative of each site and year, accounting for cell production as assessed by xylogenesis monitoring (Buttò et al., 2019b). We assessed the growth rates of cells as a ratio between cell diameter and the duration of enlargement; the value was scaled between 0 and 1 to be compared with the nondimensional tree-ring growth rate computed by the VS model (Table 2).

5.2.5 Tree-ring time-series analysis

We measured tree-ring width using WinCELL (Regent Instruments Inc., Canada) on histological samples obtained from ten microcores collected at all five sample sites. To compare trees with different growth rates, we detrended the chronologies, removing the effects of tree age, genetic growth potential, microsite characteristics, and stand history (Cook et al., 1990). We applied 67% cubic splines with a 1/2 cut-off time-series length to detrend and produce standardized chronologies for the 2002–2016 period using the *detrend* and *chron* functions of the dplR package in R (Bunn, 2008).

5.2.6 VS Model calibration and validation

We used standardized tree-ring width series to calibrate the VS model for 2002–2016 using the VS-oscilloscope (Shishov et al., 2016). We performed parameterization to avoid any contradictions with field observations and available information for the sites (Tychkov et al., 2019). Accordingly, the calibration of the environmental

parameters in the VS oscilloscope, was performed considering the measures of our weather stations during the different moments of the growing season, that we identified by means of the xylogenesisis monitoring. Site-specific parameters were calibrated considering site features, while for parameters linked to black spruce ecology, like root deepness, we relied on literature references to check if the values we established were realistic. Simulations of daily soil water content were improved by activating the soil melting block in the VS-oscilloscope, a parameter that was designed originally to include permafrost melting (Shishov et al., 2016). As we were dealing with wet sites, we used this block to consider the marked amount of water released by snowmelt at the start of the growing season. Nonetheless, the current version of VS model does not estimate soil thawing and soil moisture for the dormancy, because these values are assumed to be constant.

For each site, we evaluated the effect of the environmental factors on tree-ring growth via graphical interpretation of the partial growth rates patterns provided by the VS model simulations (Vaganov et al., 2006). The graphical representation of the daily average partial growth rates simulated by the VS model allows to determinate the most limiting factor to growth at daily scale, which corresponds to factors linked to the lowest growth rate (Shishov et al., 2016). Indeed, tree-ring growth rate is a function of three partial growth rates that depend on daily temperature, soil water content, and photoperiod; these factors are integrated into the tree-ring growth rate and represent an important result of the model simulations (Table 2). The start of the

growing season as predicted by the model depends on the crossing of a critical threshold for all three partial growth rates; this occurs when each environmental factor activates or permits tree-ring growth (Vaganov et al., 2006). In addition to the minimum temperature for growth to start (T_{min}), the sum of temperature for growth initiation (T_{beg}) can be parameterized, in order to consider the forcing needed for cambial resumption. In the current version of VS-oscilloscope, the end of growth occurs when the integral growth rate of the tree ring falls below a critical threshold (critical growth rate Vcr) (Tychkov et al., 2019). We obtained the general pattern of the partial growth rates using the default arguments of the function geom_spline from the R's package "ggformula" (Kaplan and Pruim, 2020).

We computed the cambial cell growth rate, i.e., the average growth rate corresponding to cambial cells produced each year, and then determined their timing of division and enlargement following Popkova et al. (2018) (Table 2). The protocol proposed by Popkova et al. (2018) extrapolates the timing of cell division and enlargement by the tree-ring growth rate, assuming that the production of a new cambial cell occurs only once the previous cells have left the cambial zone. Cell production would indeed occur without overlapping. The observed number of cells produced each year is necessary to calculate temporal dynamics of cell production, which we obtained through our observations of the microcores.

We assessed the robustness of the VS model simulations using the actual and predicted tree-ring width indices; we relied on the Pearson correlation (R) and root mean square error (RMSE). We retained only models showing a significant R ($p < 0.05$), producing the smallest RMSE to minimize the variance of simulated indices and to select the simulation with the smallest average prediction error (James et al., 2013). The model validation involved comparing the simulations (named 'predicted data') with our results from the microcores (named 'observed data'). Pearson correlations and linear regressions served to compare the predicted and observed data. We transformed the data when necessary to meet the assumption of normality, and we fit LOESS functions (span = 0.7) to compare the general patterns visually.

5.3 Results

5.3.1 Climate along the latitudinal gradient

For the 2002–2016, our weather stations recorded warmer monthly mean annual temperatures than the long-term average (Table 1, Table 3). For this same period, mean annual precipitation was higher in the north (715 mm, MIR) and lower in the south (622 mm, SIM), with a greater northward inter-annual and daily intra-annual variability during wood formation (Table 3). However, mean annual and mean daily soil water content decreased from south to north, spanning from 0.17 V/Vs at MIR to 0.36 V/Vs at SIM over the year (Table 3). Daily soil water content during wood formation ranged from 0.17 to 0.42 V/Vs at DAN and BER, respectively.

5.3.2 Duration and rate of xylem growth

For all sites, correlations between the observed and predicted tree-ring width indices were positive and highly significant (SIM and MIS: $P < 0.05$, $N = 15$; BER, DAN: $P < 0.01$, $N = 15$; MIR: $P < 0.01$, $N = 5$) and *R*-values ranged from 0.54 to 0.90 (Supplementary Figure S1). RMSE ranged between 0.06 (DAN) and 0.1 (MIR), staying below the RMSE threshold of 0.3 and attesting to the good fit between the indices and the simulated results (Supplementary Figure S1). Fixed parameters of temperature for tree growth ranged from 4 to 29 °C, showing a 1–5 °C difference depending on the site (Supplementary Table S1). Minimum and maximum soil moisture levels were similar along the entire latitudinal gradient, although MIR had the lowest maximum soil moisture (Supplementary Table S1).

Partial growth rates showed marked inter-annual variability, in particular for temperature growth rate (Figure 1). In general, the temperature growth rate peaked at the end of August (DOY 240), while the photoperiod growth rate peaked around the summer solstice (DOY 170) (Figure 1). The maximum temperature growth rate was highest at SIM, where it reached 0.8 relative units, and decreased to 0.62 at the northernmost site, MIR. The water growth rate reached 1, the maximum value, at SIM, MIS, and DAN, around the middle of July (DOY 200) for SIM and MIS and 20 days later at DAN. At MIR, the water growth rate peaked around DOY 240, although it never attained the maximal value (Figure 1).

From the partial growth rate patterns (Figure 1), wood formation started when temperatures were suitable for the resumption of cambial activity, which according to predictions, occurred between the end of May and the onset of June. Cambial activation was earliest at the southernmost site (SIM, DOY 143) and latest in northernmost site (MIR, DOY 157) (Figure 2, Table 4). The predicted start of wood formation occurred 4–13 days after the observed start (Figure 2, Table 4). The linear relationships between the predicted and observed start of the wood formation produced R^2 values that ranged from 0.4 (MIR) to 0.5 (DAN) and showed a systematic overestimation for the start of wood formation (Figure 2). The end of wood formation—occurring when the photoperiod was the most limiting factor—was predicted latest for the southernmost site (SIM, on average DOY 267) and earliest for the northernmost site (MIR, on average DOY 255, Table 4). The predicted end of wood formation was generally overestimated with wood formation lasting 9–19 days longer than observed (Table 4). The observed end of wood formation showed a higher inter-annual variation of up to 2 weeks, whereas the predicted end of the growing season varied on average 6 days over the years (Table 4). The simulated and observed ends of wood formation showed a weak relationship, having R^2 values of only 0.02 (DAN) to 0.3 (MIS) (Figure 2).

5.3.3 Model parameters and environmental properties

Pearson correlations between the predicted and observed daily soil water content ranged between 1 and -1 (Supplementary Table S2). During dormancy, an average 16% of the simulated years produced a strong correlation ($R > 0.4$) between the predicted

and observed daily soil water content (Supplementary Table S2). MIS showed the best performances, where 33% of the years showed a strong and positive correlation between the predictions and observations. We observed the lowest correlations at SIM, where the predicted and observed soil water content correlated strongly in only 7% of the years (Supplementary Table S2). The model simulations for winter resulted in a constant soil water content that was either an underestimate or overestimate depending on the year and site (Figure 3).

The observed soil water content showed a large intra-annual variation, in particular at the more southern sites (Figure 3). At SIM and BER, soil water content varied in winter between 0.2 and 0.4 V/Vs, culminating at the end of April (DOY 121, Figure 3). From the beginning of May, increased variability in soil water content mirrored a decrease in the observed soil water content, which dropped from 0.5 V/Vs at SIM and 0.6 V/Vs at BER to 0.3 V/Vs at both sites during the first week of October (Figure 3). During the second half of October, soil water content for these sites began to increase slightly and produced a smaller peak in mid-November. The soil water content at MIS and DAN varied little, peaking on DOY 121, although at a much lower intensity than at other sites; MIS and DAN soil water content varied between 0.2 and 0.3 V/Vs and 0.1 V and 0.2 V/Vs, respectively (Figure 3). In contrast, the predicted soil water content at all sites remained constant until DOY 162, generally underestimated at the southern sites (SIM, BER, and MIS), and overestimated at DAN (Figure 3).

During wood formation, we noted a strong correlation between the observed and predicted soil water content, with 32% of years having a correlation $R > 0.4$, whereas MIS only showed 7% of the years above this strong correlation threshold (Supplementary Table S2). We observed the best performances at MIR and BER where correlations between the predicted and observed summer soil water content were 60%, and 80%, respectively (Supplementary Table S2). In most years, the predicted soil water content was overestimated at DAN and underestimated at SIM and BER (Figure 3). At MIS and MIR, the predicted vs. observed data points fell on the 1:1 intercept, although we also observed a marked variability (Figure 3).

5.3.4 Variation in the timing of wood formation along the latitudinal gradient

For all sampled years, the predicted and observed timing of cell division and cell enlargement were highly correlated ($R > 0.9$, Supplementary Table S2). On average, the general pattern of the predicted timing of cell division showed a constant trend for cell positions 19 to 2 for DAN and MIR, respectively (Figure 4). Nevertheless, the predicted and observed timing for cambial cells demonstrated a strong linear relationship and R^2 values between 0.8 and 0.9 (Figure 4).

We obtained similar strong correlations and relationships for the predicted and observed timings of cell enlargement (Supplementary Table S2, Figure 5); at the beginning of the growing season, however, the differences between the observed and

predicted timings of cell enlargement were initially quite small—from 1 to 2 days depending on the site—and increased consistently with cell position, attaining a difference of 40 DOY (Figure 5).

The relationship between predicted cambial cell growth rate and observed cell growth rate for all five sites showed R^2 values of 0.4 at MIR, DAN, and SIM to 0.3 at MIS (Figure 6). The predicted cambial cell and observed cell growth rates were highly correlated for 89% of the years (Supplementary Table S2). Contrary to what we observed at the other sites, the correlation values at MIR varied considerably and were occasionally strongly negative (2015) (Supplementary Table S2). On average, the cambial cell growth rate was highest for the first cells of the tree ring, being 0.5 at all sites—except at SIM where it was 0.6—and decreased to 0.1 for the final cells (Figure 6). The difference between the predicted cambial cell growth rate and the observed cell growth rates ranged between 0.3 (BER) and 0.4 (DAN), having a systematic overestimation of the predicted values. The overestimation of the cell growth rates occurred for the first cells at all the sites in particular and became smaller when cell growth slowed (Figure 6). Inter-annual variations of the model predictions were similar to those of our observations (Figure 6). Accordingly, a greater variation of the intra-annual growth rate predicted in MIR matched with a greater variation in observed values (Figure 6). Regardless, the greater variability in growth rates in MIR could also be linked to the reduced number of available observations for this last site.

5.4 Discussion

Understanding the effect of the environmental drivers on black spruce growth is crucial for predicting how environmental change will affect wood formation for this economically and ecologically important species. In Canada, correlations between tree-ring growth and the temperature and precipitation follow two different gradients, unraveling complex patterns in black spruce growth responses to these environmental factors (Nicault et al., 2015). Correlation with temperature is strongest in the North, whereas tree growth is most correlated with precipitation in the Western Canada (Huang et al., 2010; Walker and Johnstone, 2014). Correlations of tree growth with temperature and precipitation have also been confirmed by dendro-anatomical analyses at the cellular scale and have demonstrated that environmental factors affect xylem conductivity and long-term patterns of intra-annual cell traits (Puchi et al., 2019). According to the existing literature, the correlation between temperature and tree-ring growth is positive when temperature represents the most limiting factor and is negative in response to warming during the previous growing season and the current spring—probably reflecting drought stress (Huang et al., 2010; Walker and Johnstone, 2014; Nicault et al., 2015; Puchi et al., 2019). Correlation with precipitation, when significant, is always positive (Walker and Johnstone, 2014; Girardin et al., 2016; Puchi et al., 2019).

The variation in the local responses to environmental factors might indicate a long-term effect of the environmental factors, which is consistent with the conservative black spruce growth strategy (Chen et al., 2019). In this sense, VS model simulations improvements targeted on black spruce and VS model application on a larger territory could disentangle the common drivers of black spruce adaptation to environmental factors and their effect on tree-ring growth and wood formation at local scale. According to Vaganov et al. (2006), the algorithms underlying the VS model are based on the assumptions that intra-seasonal dynamics are the result of current environments, while the variability in cell production is determined by long-term conditions experienced by the trees, which are integrated to model's simulations by parameterization. The effect of previous years conditions on growth is thus implicit, but the model has never been formulated to split the carryover effect of the environmental factors from the effect of the current environmental conditions.

The partial growth rates for the three main environmental factors predicted by the VS model revealed that different limiting factors shape tree-ring production in black spruce. At the beginning of the growing season, which is predicted by VS model for the end of May, temperature is the most limiting factor at all the sites. In cold environments, temperature is the major limiting factor of tree growth. Mean air temperature thresholds during xylogenesis range between 6 and 8 °C (Rossi et al., 2007). Accordingly, the average temperature of the lower range of optimal temperatures for our sites (T_{opt1}, T_{min}), as estimated by the parameters, was between 6

and 7.6 °C (Supplementary Table S1). The predicted end of the growing season occurred around the middle of September when photoperiod became the most limiting factor. In boreal and temperate forests, short days induce cambium dormancy by triggering the physiological mechanisms that lead to growth cessation (Buttò et al., 2019a). At high latitudes, the shortening of day length also allows trees to anticipate lower temperatures and induces cold acclimation responses (Wingler, 2015).

The growth rate determined by water, i.e., water growth rate, was never a limiting factor along the gradient—except at BER where the predicted soil water content was heavily underestimated. This result confirms both field and greenhouse observations that the cell production and cell trait sizes of black spruce in eastern Canada do not change significantly with changes in soil moisture (Belien et al., 2012; Balducci et al., 2016). In contrast, Girardin et al. (2016) observed that stands growing in western Canadian ecoregions are very responsive to variations in soil water availability; this affects tree productivity by reducing the capacity of black spruce to fix carbon (Girardin et al., 2016). Thus, the lack of response of black spruce growth to variations in soil moisture must be ascribed to site conditions, which were well represented by the water growth rate of the VS model.

5.4.1 Site conditions

The best model performances in terms of prediction of tree-ring width, soil water content, as well as the onset and end of the growing season were obtained at the

northernmost site (MIR), one of the driest sites along the gradient. These results confirm that the VS model parameter specification is based mainly on sites characterized by very cold conditions, such as in Siberia or on the Tibetan Plateau (Vaganov et al., 2011; He et al., 2017) and semi-arid or arid conditions, such as those in the southwestern US or northern Africa (Evans et al., 2006; Touchan et al., 2012). Therefore, the VS model ensures better simulations in dry environments, where it has been successfully applied to the study of the long-term response of tree growth to climate (Anchukaitis et al., 2006; Touchan et al., 2012; Zhang et al., 2016; Yang et al., 2017). However, our application of the VS model also provides useful guidance for improving model parameterization and its performance for wetter sites by involving the boreal forest characteristics of soil water balance and soil properties. According to the assumptions of the VS model, soil water content—deemed as the water available for tree growth—depends on precipitation, snowmelt, evaporation, and runoff (Vaganov et al., 2011). In the Canadian boreal forest, however, soil water balance and, in general, water and nutrient distribution within the soil horizons, are correlated strongly with organic layer composition and thickness—boreal soils can reach a depth of 150 cm (Simard et al., 2007; Laamrani et al., 2014). The forest floor of black spruce stands is composed generally of mosses and lichens, which modify the soil thermal conductivity and water content (O'Donnell et al., 2009). Due to its thickness and species-specific composition, the forest floor promotes water retention in the surface soil, thereby acting as a thermal buffer between the atmosphere and soil to decrease thermal conductivity (Sharratt, 1997; Turetsky et al., 2010).

Accumulation on the forest floor entails a drop in soil temperature, and as such the decomposition rate of the organic matter slows; these conditions result in decreased tree growth (Fenton et al., 2005; Lavoie et al., 2005).

All soils at our study sites are podzols, although they differ in terms of depth to bedrock, soil thickness, and species composition on the forest floor. These peculiarities likely explain the mismatch between precipitation and soil water content that we observed along the gradient between 2002 and 2016. Despite receiving less precipitation, the southernmost sites of BER and SIM remained the wettest of the gradient. SIM is characterized by a thin organic layer (10–20 cm thick) and a very shallow bedrock (Rossi et al., 2016). As mentioned previously, the soil organic layer can negatively affect tree growth in boreal forest stands. However, the thickness of the organic layer at SIM was too thin to affect tree productivity (Lavoie et al., 2007); thus, the site at SIM is particularly favorable to black spruce growth. The other sites had deeper soils, 20–40 cm in depth, and differed in their forest floor characteristics (Rossi et al., 2016). The presence of mosses and a deeper soil at MIS and DAN foster a greater soil retention in the upper layer of the soil. In contrast, MIR has a forest floor dominated by lichens and contains a very thin soil depth; these properties favor the establishment of a thinner and drier forest floor (Waldron et al., 2013).

In this study, predictions of soil water content have improved via the activation of the "soil melting block" in the VS model, a specific module of the model that considers

the contribution of snowmelt to soil moisture at the beginning of the growing season (Shishov et al., 2016). Rossi et al. (2011) had previously highlighted the importance of snowmelt at our sites by observing the effects of snowmelt on the duration of xylogenesis and cell production. The presence of accumulated snow prevents soil warming in the spring, and these colder temperatures inhibit root reactivation, delaying spring rehydration and, in turn, cambial reactivation (Turcotte et al., 2009). A later snowmelt corresponds to delays in soil warming, cambium activation, and cell production (Vaganov et al., 1999). Thus, the date of snowmelt influences the timing of wood formation and may explain some of the difference between the observed and the predicted onset of the growing season.

5.4.2 Timing of cell division and differentiation

Compared to the observed data, the predicted timings of cell division and enlargement were delayed from a few days to two weeks. This overestimation was more constant for the timings of cell division, and gradually higher across the tree ring for the timings of cell enlargement. For this, we advance the hypothesis that the upward shift of the predicted timings of cell division relative to observations can be improved by a more precise prediction of the start of the growing season. The increased mismatch between the predicted and observed timing of enlargement can be reduced further by including some information. Popkova et al. (2018) illustrate that the time that dividing cells spend in the cambial zone can be determined by splitting the predicted growing season into a number of periods equal to cell production. To

leave the cambium, each cell must attain an average growth rate computed by the ratio between the cumulative sum of the daily growth rate obtained by VS model and cell production. However, to obtain a more reliable reconstruction of the temporal dynamics of cell division, a new assumption can be added to the model, one that considers the natural variation of cell production rates over the growing season. Furthermore, an accurate estimate of the number and order of cells entering the xylem should account for the number of cells that will never differentiate, i.e., the number of dormant cambial cells that constitute the mother cells and the cambial cells that undergo phloem differentiation (Plomion et al., 2001).

Cell production rates, depending by cambial activity, interact with the residence time of each cell within the differentiation zones. Variations in these cell production rates stem from the complex seasonal patterns that occur during tree-ring formation (Cuny et al., 2013; Balducci et al., 2016). An improved performance of the VS model timing procedure can be achieved by considering the specific pattern of the cell production seasonal rate. Cell production rate is characterized by a bell-shaped curve, with the peak and following decrease being in response to intra-seasonal dynamics and internal factors (Deslauriers and Morin, 2005). The peak in the cambial growth rate i.e. the number of cells produced per time units, matches a peak of auxin, the main hormone promoting cell division, and occurs during earlywood formation (Buttò et al., 2019a). At the same time, soil water content and temperature affect cambial growth rate and cell production, the first prevailing in dry environments and the

second in boreal climates (Deslauriers et al., 2008; Ziaco et al., 2018; Ren et al., 2019).

5.4.3 VS tree-ring growth rate and cell differentiation

We compared cell growth rates with the cambial cell growth rates predicted by the protocol of Popkova et al. (2018). In particular, we tested the possibility of inferring the cell growth rate from the tree-ring growth curve obtained by the VS model by adjusting the procedure of Popkova et al. (2018) by focusing on the differentiation zones rather than the cambial zone. Once cell production is known, Popkova et al. (2018) infer the cambial cell growth rate using the curve of tree-ring growth rate and perform the most suitable regression between cambial cell growth rates and the measured cell diameters from actual tracheidograms. With the coefficients from the abovementioned regression, Popkova et al. (2018) then obtain those parameters useful for producing synthetic tracheidograms. However, cell diameter can be computed without using observations by integrating the relationship between cell traits and their temporal dynamics of differentiation (Cuny et al., 2014; Buttò et al., 2019b). The timings of enlargement computed by the protocol proposed by Popkova et al. (2018), identify the start of cell differentiation i.e. the timings of cell enlargement, which is the day in which a cell starts increasing in size (table 2). Xylem cell differentiation temporal dynamics assessment requires the computation of the timings of secondary wall deposition and cell maturation to estimate the duration of cell enlargement and the duration of secondary wall deposition. The duration of these

differentiation phases depends on exogenous factors i.e. photoperiod, soil water content and temperature, which are already included in the model, and on endogenous factors i.e. hormonal signaling, sugars concentration (Rathgeber, 2017; Cartenì et al., 2018; Buttò et al., 2019a). Then, a new framework that considers the nonlinear relationship between the duration of cell enlargement and cell diameter can be implemented, which also includes the effect of the secondary wall on the process of cell expansion (Buttò et al., 2019b). During cell differentiation, secondary wall deposition influences cell diameter by altering the plastic properties of cell walls. Cell wall thickening, which occurs during cell trait differentiation, constrains cell expansion, especially during latewood formation when cell deposition lasts longer than during earlywood formation (Cartenì et al., 2018). These new findings that assess the quantitative relationships between cell traits, developmental temporal dynamics, and environmental factors should be implemented into the next versions of the VS model to improve simulations (Ziaco, 2020).

5.4.4 The end of the growing season

The end of growth was one of the most critical portions for our comparisons, and in a wider sense, for studies of both xylem and bud phenology (Gallinat et al., 2015). At our sites, the end of wood formation occurred latest at the southernmost sites and showed a clear latitudinal pattern. Among the climatic factors, photoperiod and temperature are the main known drivers of the end of the wood formation, and the end of growth occurred earliest at the northernmost sites (Rossi et al., 2014; Cuny et

al., 2019). However, other factors may also affect the end of the growing season, including cell production and sugar availability, the latter being crucial for cell wall deposition. Cell wall thickening at the end of the growing season lasts 30–40 days after the last cell is differentiated and drives the timing of latewood formation (Deslauriers et al., 2016; Cartenì et al., 2018). Cell production, which is the result of cambial activity, also influences the kinetics of wood formation, since competition for resources increases with the number of cells, and sugar availability shapes cell traits by modifying their differentiation phases (Cartenì et al., 2018). The end of the growing season can be parameterized during VS model calibration thought the critical growth rate, a coefficient representing the threshold under which the integral growth rate of the VS model does not allow wood formation anymore. Being based on the integration of the three partial growth rates linked to the environmental factors, the critical growth rate may not be sufficient for establishing a realistic end of the growing season, a moment that is not highly dependent on weather conditions, unlike at the start of the growing season (Rossi et al., 2012).

5.5 Conclusions

In this study, we compared the predictions of intra-annual tree-ring formation dynamics estimated by the Vaganov-Shashkin (VS) model with field observations based on a 15 years-long monitoring of xylogenesis across a latitudinal gradient. Our

results show that the model successfully describes the influence of climate variables on black spruce tree-ring growth. However, algorithms can still be improved to ensure a more reliable estimate of the timing of wood formation. Considering that the model has been tested for the first time on the Canadian boreal forest, it is difficult to relate the mismatch between predictions and observations to issues linked to the use of the model on wet environments or to the underlying algorithms computing the development timings. VS-model parameterization is indeed based on semi-dry, dry or permafrost environments, which better support the assumptions of a constant soil water content during dormancy and of a closer relationship between tree growth and water availability at growth resumption. In our case, we tested the model on wet sites, and observed a low representativeness of the soil water content in spring, leading to cumulative errors in soil water estimation during the growing season. A recalibration of the model on other wet sites could provide more robust elements to improve the performance in terms of predicted water content and partial growth rate. Moreover, the algorithms computing the timings of cell production should consider that the cambial growth rate varies during the growing season with consequent effects on the residence time of each cell within the cambial zone. The development of a new procedure must involve phenology and dynamics of each cell during development, based on the underlying biological processes. As a consequence of cell differentiation dynamics, the computation of the cell traits, i.e. diameter and cell wall thickness, should be included in form of new module of the VS model based on larger datasets,

encompassing species from different environments to obtain more extensive and exhaustive growth simulations.

5.6 Tables

Table 5.1 Location, climatic conditions, and tree characteristics at the five study sites, ordered in terms of latitude. DBH: diameter at breast height. Annual statistics for temperature and precipitation were calculated from 1950–2016 data using the ANUSPLIN algorithm (McKenney et al., 2011).

Site	Latitude (N)	Longitude (W)	Altitude (m asl)	Annual temperature (°C)	Annual precipitation (mm)	DBH (cm)	Height (m)
SIM	48°13′	71°15′	338	1.9	906	20.4 ± 2.4	16.1 ± 1.2
BER	48°51′	70°20′	611	0.1	886	21.1 ± 3.7	17.3 ± 1.8
MIS	49°43′	71°56′	342	0.3	755	19.6 ± 2.8	18.3 ± 1.1
DAN	50°41′	72°11′	487	-1.3	735	18.5 ± 2.9	16.6 ± 2.2
MIR	53°47′	72°52′	384	-3.4	626	19.6 ± 3.0	13.1 ± 1.2

Table 5.2 Glossary of all terms linked to tree growth and cell temporal dynamics.

ID	Description	Units
Timing of cell division	Day of the year in which a cell starts dividing	DOY (Julian days)
Timing of cell enlargement	Day of the year in which a cell starts enlarging	DOY (Julian days)
Cell growth rate	Growth rate of cell diameter	µm per day
Partial growth rate (photoperiod, water, temperature growth rates)	Growth rate linked to environmental factors; their integration produces the tree-ring growth rate	Nondimensional (min 0, max 1)
Tree-ring growth rate	The main output of the VS model and represents the daily tree-ring growth rate	Nondimensional (min 0, max 1)
Cambial cell growth rate	Growth rate corresponding to the production of a new cambial cell	Nondimensional (min 0,max 1)

Table 5.3 Average weather conditions and soil water content (with standard deviation) for 2002–2016 as recorded by the weather stations established at the study sites; data for MIR covers 2012–2016. Wood formation occurred from May to September, although specific dates varied between sites and years (see Table 4 for details). SWC = soil water content.

	During the year			**During wood formation**		
Site	**Mean temperature (°C)**	**Mean precipitation (mm)**	**SWC (V/Vs)**	**Mean daily temperature (°C)**	**Mean daily precipitation (mm)**	**Daily SWC (V/Vs)**
SIM	2.1 ± 0.8	622 ± 106	0.33 ± 0.04	14.5 ± 4.4	2.45 ± 5.2	0.33 ± 0.05
BER	0.4± 0.9	704 ± 105	0.36 ± 0.07	13.5± 4.0	2.93 ± 5.8	0.42 ± 0.08
MIS	1.0± 0.9	794 ± 145	0.25 ± 0.06	14.6 ± 3.9	3.33 ± 6.5	0.26 ± 0.07
DAN	−1.0± 1.0	708 ± 221	0.18 ± 0.03	13.4± 3.8	3.36 ± 6.5	0.17 ± 0.04
MIR	-2.6 ± 0.7	715 ± 126	0.17 ± 0.02	13.1 ± 4.0	3.79 ± 6.0	0.21 ± 0.05

Table 5.4 Start and end of wood formation (DOY) including inter-annual variation as determined by observations of xylogenesis and that simulated by the VS model.

	Start		**End**	
Site	**Observed**	**Predicted**	**Observed**	**Predicted**
SIM	143 ± 6.1	147 ± 9.7	267 ± 12.2	283 ± 6.7
BER	154 ± 6.6	157 ± 8.6	262 ± 13.6	275 ± 5.7
MIS	151 ± 6.4	158 ± 9.6	256 ± 13.6	275 ± 6.8
DAN	153 ± 7.6	162 ± 10.1	257 ± 10.7	267 ± 5.8
MIR	157 ± 3.9	170 ± 8.6	255 ± 19.7	264 ± 4.8

5.7 Figures

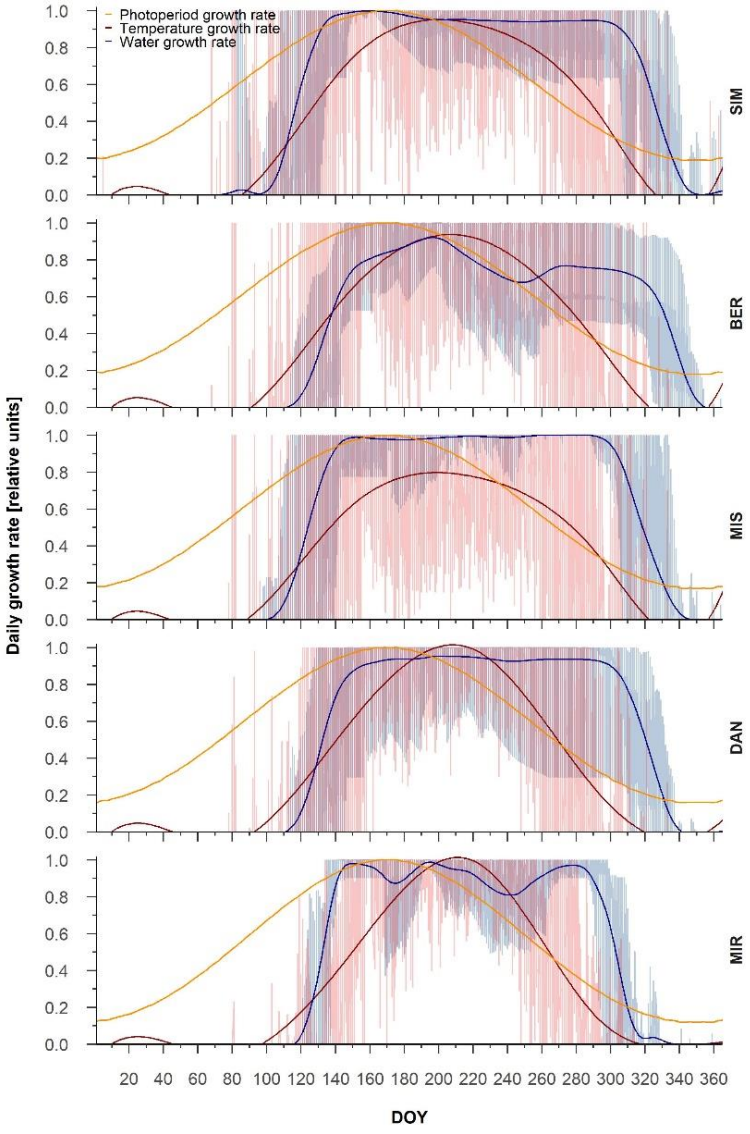

Figure 5.1 Intra-annual partial tree-ring growth rates linked to photoperiod (yellow), temperature (red), and water (blue). General trends for the three partial growth rates are represented by splines. The lowest partial growth rate represents the most limiting factor for each DOY

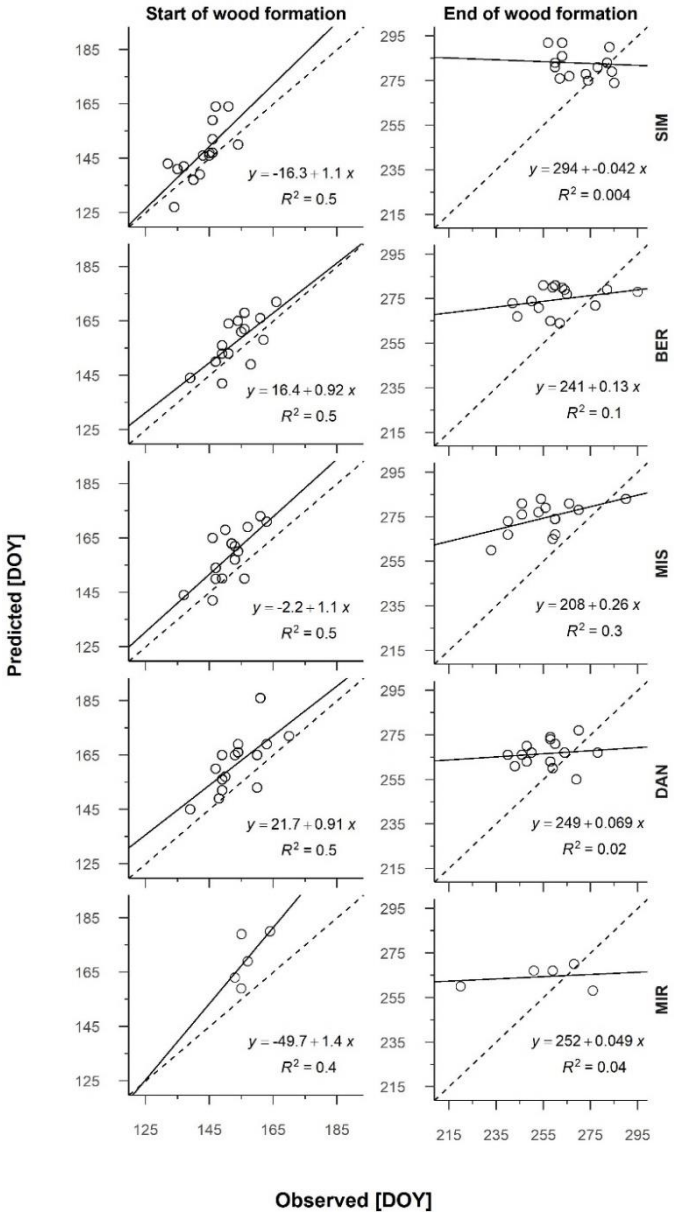

Figure 5.2 Linear regression of the predicted and observed start and end of wood formation for all sites and years (2002–2016; 2012–2016 for MIR). Each graph has a dashed 1:1 line. Sites are organized along the latitudinal gradient with the southernmost site (SIM) as the top row.

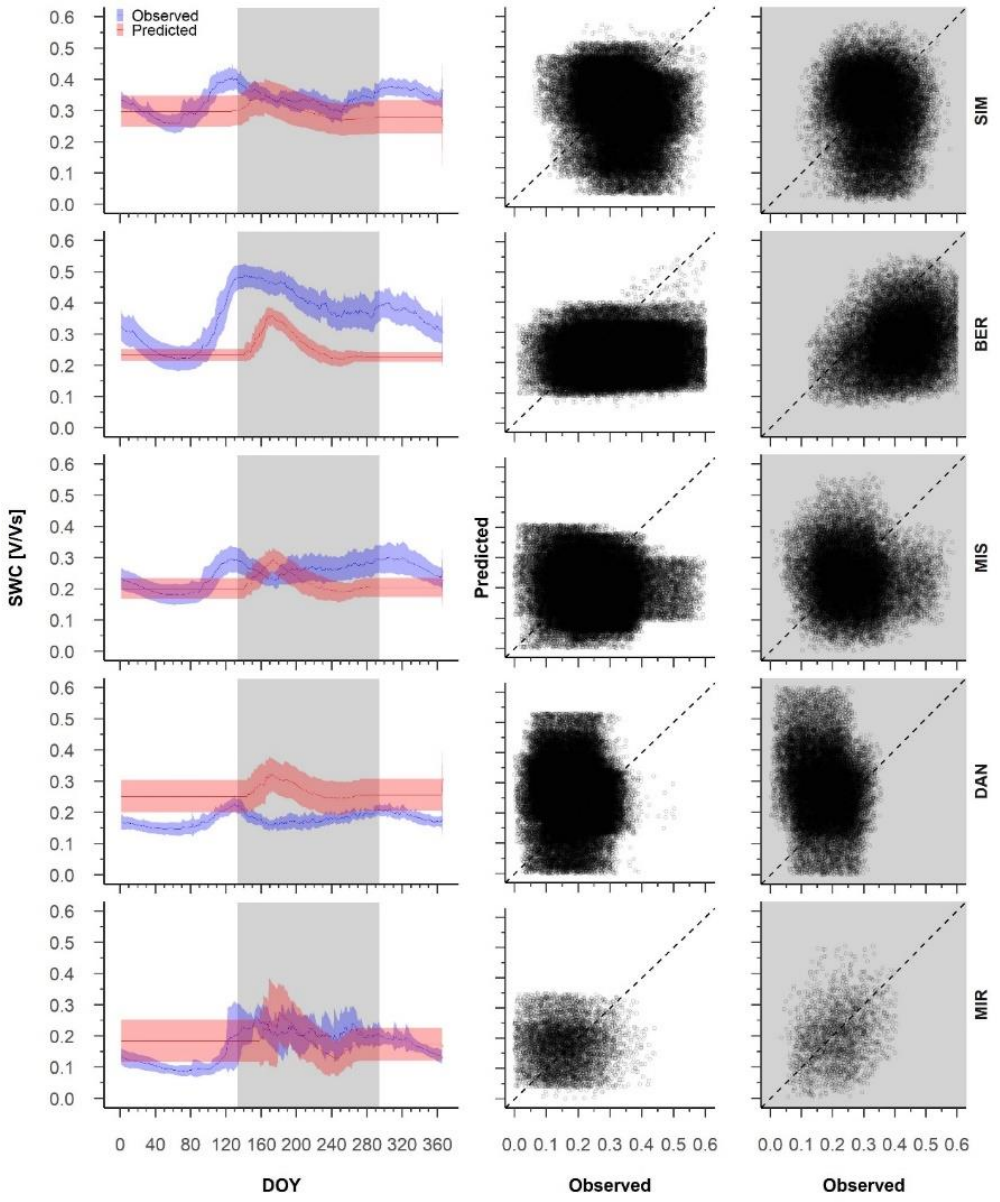

Figure 5.3 From the left to the right, average pattern of predicted (red) and observed (blue) soil water content with 95% confidence intervals (left), observed and predicted variations of soil water content during dormancy (middle) and during growing period (right). The white background on the graphs represents the dormancy period, whereas the shaded background represents the period of wood formation; Predicted versus observed soil water content for the dormant and wood formation periods. Sites are organized according to latitude (the southernmost site (SIM) as the top row of graphs, the northernmost (MIR) is on the bottom row)

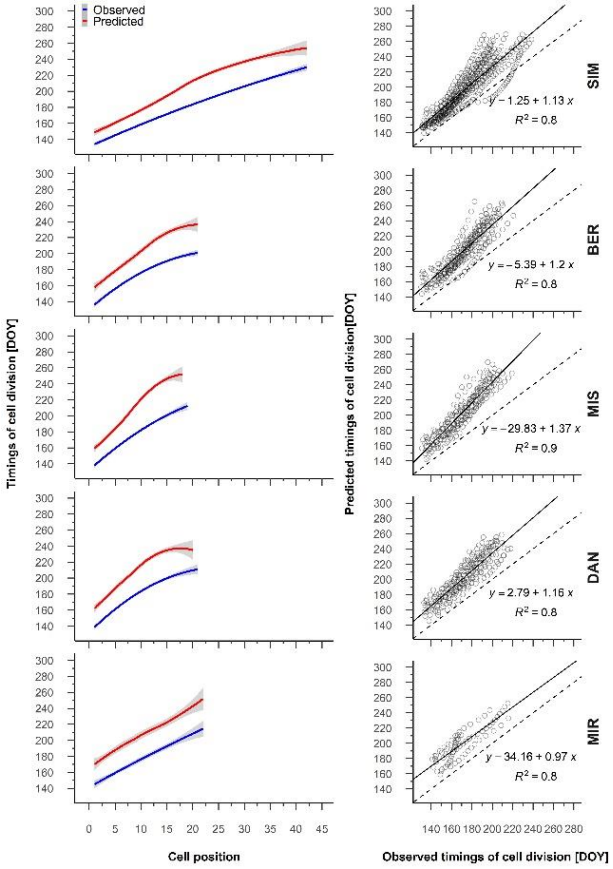

Figure 5.4 From the left to the right, average patterns for observed (blue) and predicted (red) timing of cell division in relation to cell position, gray shading represents the 95% confidence interval (left); regression between the predicted and observed timing of cell division (right). Sites are organized according to latitude (the southernmost site (SIM) as the top row of graphs, the northernmost (MIR) is on the bottom row).

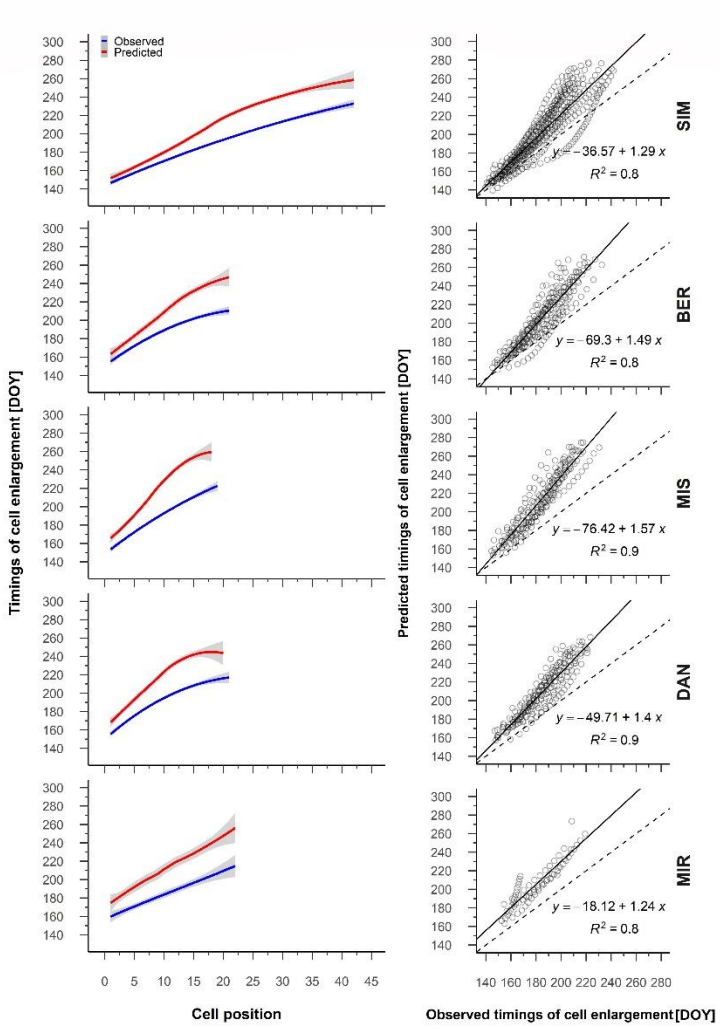

Figure 5.5 From the left to the right, average patterns for observed (blue) and predicted (red) timing of cell enlargement in relation to cell position, gray shading represents the 95% confidence interval (left); regression between the predicted and observed timing of cell enlargement (right). Sites are organized according to latitude (the southernmost site (SIM) as the top row of graphs, the northernmost (MIR) is on the bottom row).

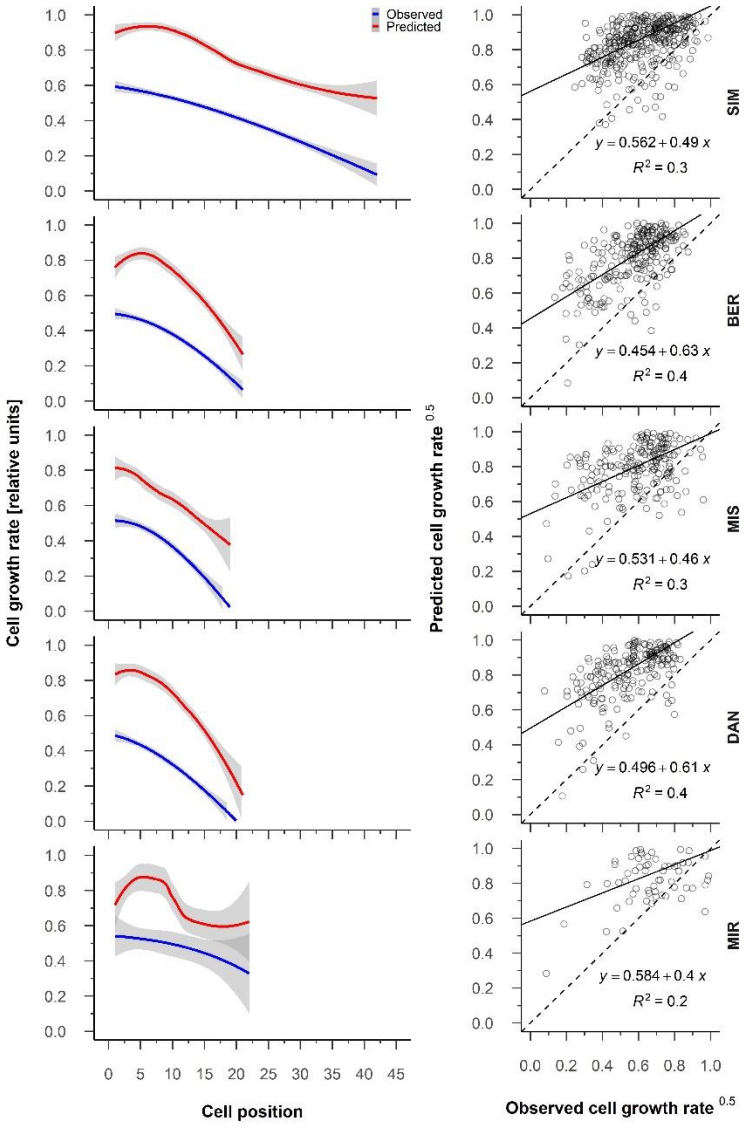

Figure 5.6 From the left to the right, average patterns for observed (blue) and predicted (red) cell growth rates in relation to cell position, gray shading represents the 95% confidence interval (left); regression between the predicted and observed cell growth rate (right). Sites are organized according to latitude (the southernmost site (SIM) as the top row of graphs, the northernmost (MIR) is on the bottom row).

5.8 Supplementary materials

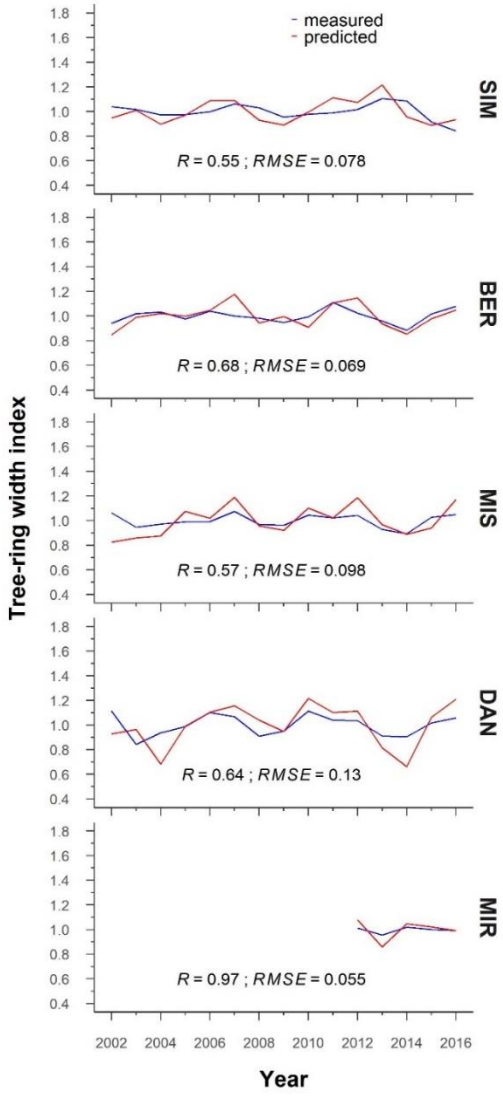

Supplementary figure 5.1 Standardized tree-ring width chronologies for the five study sites along the latitudinal gradient. Sites are organized according to latitude (the southernmost site (SIM) as the top row of graphs, the northernmost (MIR) is on the bottom row). *R* and RMSE are the Pearson correlation and the root mean squared error for each pair of curves, respectively.

Supplementary table 5.1 Estimated VS model parameters for the five chronologies of the five sites along the latitudinal gradient.

Parameter	Description (units)	SIM	BER	MIS	DAN	MIR
$\mathbf{T_{min}}$	Minimum temperature for tree growth (°C)	4	4	5	4	4
$\mathbf{T_{opt1}}$	Lower end of the optimal temperature range (°C)	8	7	8	9	11
$\mathbf{T_{opt2}}$	Upper end of the optimal temperature range (°C)	17	15	13	15	17
$\mathbf{T_{max}}$	Maximum temperature for tree growth	27	24	25	29	26
$\mathbf{W_{min}}$	Minimum soil moisture for tree growth (V/Vs)	0.0025	0.135	0.0125	0.0225	0.005
$\mathbf{W_{opt1}}$	Lower end of the range of the optimal soil moisture (V/Vs)	0.175	0.25	0.125	0.15	0.15
$\mathbf{W_{opt2}}$	Upper end of the optimal soil moisture range (V/Vs)	0.459	0.3	0.375	0.45	0.325
$\mathbf{W_{max}}$	Growth is stopped at this soil moisture (V/Vs)	0.525	0.675	0.6	0.6	0.45
$\mathbf{W_0}$	Initial soil moisture (V/Vs)	0.4	0.3	0.14	0.2	0.25
$\mathbf{T_{beg}}$	Sum of temperature at the start growth (°C)	115	105	125	120	130
lr	Depth of the root system (mm)	150	200	150	200	200

P_{max}	Maximum daily precipitation for a saturated soil (mm/day)	24	46	22	24	35
C_1	Fraction of precipitation penetrating the soil (not captured by the canopy)	0.06	0.17	0.14	0.15	0.17
C_2	First coefficient for calculating transpiration (mm/day)	0.0725	0.14	0.0925	0.12	0.125
C_3	Second coefficient for calculating transpiration (mm/day)	0.09	0.12	0.13	0.115	0.145
λ	Coefficient for water drainage from the soil (rel. unit)	0.001	0.006	0.008	0.005	0.008
T_{sm}	Snowmelt sum of temperatures	30	30	30	30	30
Sm_1	First coefficient for snowmelt	12	9	8	10	13
Sm_2	Second coefficient for snowmelt	0.0125	0.155	0.0065	0.012	0.0045
V_{cr}	Critical growth rate	0.15	0.12	0.03	0.16	0.07

Supplementary table 5.2 Intra-annual correlation between the predicted and observed variables for soil water content during dormancy and wood formation and the timing of both cell division and enlargement. Growth rate correlation was performed between the predicted cambial cell growth rate and the observed cell growth rate

Site	r correlation	2002	2003	2004	2005	2006	2007	2008	2009	2010	2011	2012	2013	2014	2015	2016
SIM	**Soil water content during dormancy**	0.27	-0.37	0	0.61	-0.13	-0.49	-0.9	0.33	0.02	-0.24	-0.08	0.42	-0.35	-0.43	0.46
BER		-0.2	0.43	0.12	-0.2	0.47	-0.33	-0.05	0.68	-0.3	0.31	0.3	0.11	-0.23	-0.02	0.45
MIS		0.01	0.28	-0.87	-0.82	0.64	-0.66	0.86	-0.52	0.51	0.26	0.62	-0.53	-0.59	-0.76	0.55
DAN		0.48	0.52	0.68	-0.24	-0.16	-0.24	-0.88	-0.04	-0.14	-0.12	-0.19	-0.11	0.38	0.3	0.16
MIR												-0.46	0.06	-0.6	0.7	-0.59
SIM	**Soil water content during wood formation**	0.73	0.63	0.14	0.66	0.58	-0.11	-0.08	0.16	0.58	-0.24	0.56	0.38	0.69	0.51	0.71
BER		0.55	-0.04	0.73	0.89	0.82	0.26	0.88	0.42	0.93	0.92	0.86	0.55	0.93	0.58	0.86
MIS		-0.04	-0.64	0.51	-0.49	0.43	0.41	0.01	-0.73	0.17	-0.39	-0.08	-0.45	0.35	-0.58	0.45
DAN		-0.08	-0.21	-0.26	0.14	-0.25	0.35	0.02	-0.01	-0.24	-0.21	-0.1	-0.57	0.2	0.07	0.38
MIR												0.64	-0.11	0.31	0.64	0.32
SIM		0.96	0.99	0.99	0.99	0.99	1	0.98	0.96	1	0.97	0.99	1	0.99	0.97	0.95

BER	**Timing of cell division**	0.97	0.99	0.98	0.96	0.99	0.99	0.93	0.99	0.98	0.96	0.94	0.99	0.99	0.98	0.93
MIS		0.96	0.99	0.99	0.98	0.99	0.99	0.99	0.99	0.99	1	0.99	1	0.99	1	0.99

5.9 References

Anchukaitis, K. J., Evans, M. N., Hughes, M. K., and Vaganov, E. A. (2020). An interpreted language implementation of the Vaganov–Shashkin tree-ring proxy system model. Dendrochronologia 60. doi:10.1016/j.dendro.2020.125677.

Anchukaitis, K. J., Evans, M. N., Kaplan, A., Vaganov, E. A., Hughes, M. K., Grissino-Mayer, H. D., et al. (2006). Forward modeling of regional scale tree-ring patterns in the southeastern United States and the recent influence of summer drought. Geophys. Res. Lett. 33, 2–5. doi:10.1029/2005GL025050.

Balducci, L., Cuny, H. E., Rathgeber, C. B. K., Deslauriers, A., Giovannelli, A., and Rossi, S. (2016). Compensatory mechanisms mitigate the effect of warming and drought on wood formation. Plant, Cell Environ. 39, 1338–1352. doi:10.1111/pce.12689.

Belien, E., Rossi, S., Morin, H., and Deslauriers, A. (2012). Xylogenesis in black spruce subjected to rain exclusion in the field. Can. J. For. Res. 42, 1306–1315.

Bunn, A. G. (2008). A dendrochronology program library in R (dplR). Dendrochronologia 26, 115–124. doi:10.1016/j.dendro.2008.01.002.

Buttò, V., Deslauriers, A., Rossi, S., Rozenberg, P., Shishov, V., and Morin, H. (2019a). The role of plant hormones in tree-ring formation. Trees - Struct. Funct. 34, 315–335. doi:10.1007/s00468-019-01940-4.

Buttò, V., Rossi, S., Deslauriers, A., and Morin, H. (2019b). Is size an issue of time? Relationship between the duration of xylem development and cell traits. Ann. Bot. 123, 1257–1265. doi:10.1093/aob/mcz032.

Cartenì, F., Deslauriers, A., Rossi, S., Morin, H., De Micco, V., Mazzoleni, S., et al. (2018). The physiological mechanisms behind the earlywood-to-latewood transition: a process-based modelling approach. Front. Plant Sci. 9, 1053.

Chen, L., Rossi, S., Deslauriers, A., and Liu, J. (2019). Contrasting strategies of xylem formation between black spruce and balsam fir in Quebec, Canada. Tree Physiol. 39, 747–754. doi:10.1093/treephys/tpy151.

Cook, E. R., and Pederson, N. (2011). “Uncertainty, Emergence, and Statistics in Dendrochronology,” in, 77–112. doi:10.1007/978-1-4020-5725-0_4.

Cook, E. R., Shiyatov, S. G., Mazepa, V. S., Ecology, A., and Branch, U. (1990). Methods of Dendrochronology: Tree-ring standardization and growth-trend estimation. Methods dendrochronology Appl. Environ. Sci., 104–123.

Cuny, H. E., Fonti, P., Rathgeber, C. B. K., Arx, G., Peters, R. L., and Frank, D. C. (2019). Couplings in cell differentiation kinetics mitigate air temperature influence on conifer wood anatomy. Plant. Cell Environ. 42, 1222–1232. doi:10.1111/pce.13464.

Cuny, H. E., Rathgeber, C. B. K. B. K., Frank, D., Fonti, P., and Fournier, M. (2014). Kinetics of tracheid development explain conifer tree-ring structure. New Phytol. 203, 1231–1241. doi:10.1111/nph.12871.

Cuny, H. E., Rathgeber, C. B. K. K., Kiessé, T. S., Hartmann, F. P., Barbeito, I., and Fournier, M. (2013). Generalized additive models reveal the intrinsic complexity of wood formation dynamics. J. Exp. Bot. 64, 1983–94. doi:10.1093/jxb/ert057.

Danis, P.-A., Hatté, C., Misson, L., and Guiot, J. (2012). MAIDENiso: a multiproxy biophysical model of tree-ring width and oxygen and carbon isotopes. Can. J. For. Res. 42, 1697–1713. doi:10.1139/X2012-089.

Deslauriers, A., Huang, J.-G., Balducci, L., Beaulieu, M., and Rossi, S. (2016). The contribution of carbon and water in modulating wood formation in black spruce saplings. Plant Physiol., pp--01525.

Deslauriers, A., and Morin, H. (2005). Intra-annual tracheid production in balsam fir stems and the effect of meteorological variables. Trees 19, 402–408. doi:10.1007/s00468-004-0398-8.

Deslauriers, A., Morin, H., and Begin, Y. (2003). Cellular phenology of annual ring formation of Abies balsamea in the Quebec boreal forest (Canada). Can. J. For. Res. 33, 190–200. doi:10.1139/x02-178.

Deslauriers, A., Rossi, S., Anfodillo, T., and Saracino, A. (2008). Cambial phenology, wood formation and temperature thresholds in two contrasting years at high altitude in southern Italy. Tree Physiol. 28, 863–871.

Evans, M. E. K., Gugger, P. F., Lynch, A. M., Guiterman, C. H., Fowler, J. C., Klesse, S., et al. (2018). Dendroecology meets genomics in the common garden: new insights into climate adaptation. New Phytol. 218, 401–403. doi:10.1111/NPH.15094.

Evans, M. N., Reichert, B. K., Kaplan, A., Anchukaitis, K. J., Vaganov, E. A., Hughes, M. K., et al. (2006). A forward modeling approach to paleoclimatic interpretation of tree-ring data. J. Geophys. Res. Biogeosciences 111, G03008. doi:10.1029/2006JG000166.

Fenton, N., Lecomte, N., Légaré, S., and Bergeron, Y. (2005). Paludification in black spruce (Picea mariana) forests of eastern Canada: Potential factors and management implications. For. Ecol. Manage. 213, 151–159. doi:10.1016/j.foreco.2005.03.017.

Fonti, P., Von Arx, G., García-González, I., Eilmann, B., Sass-Klaassen, U., Gärtner, H., et al. (2010). Studying global change through investigation of the plastic responses of xylem anatomy in tree rings. New Phytol. 185, 42–53. doi:10.1111/j.1469-8137.2009.03030.x.

Gallinat, A. S., Primack, R. B., and Wagner, D. L. (2015). Autumn, the neglected season in climate change research. Trends Ecol. Evol. 30, 169–176. doi:10.1016/j.tree.2015.01.004.

Girardin, M. P., Hogg, E. H., Bernier, P. Y., Kurz, W. A., Guo, X. J., and Cyr, G. (2016). Negative impacts of high temperatures on growth of black spruce forests intensify with the anticipated climate warming. Glob. Chang. Biol. 22, 627–643. doi:10.1111/gcb.13072.

Hacke, U. G., Spicer, R., Schreiber, S. G., and Plavcová, L. (2017). An ecophysiological and developmental perspective on variation in vessel diameter. Plant Cell Environ. 40, 831–845. doi:10.1111/pce.12777.

He, M., Shishov, V., Kaparova, N., Yang, B., Bräuning, A., and Grießinger, J. (2017). Process-based modeling of tree-ring formation and its relationships with

climate on the Tibetan Plateau. Dendrochronologia 42, 31–41. doi:10.1016/j.dendro.2017.01.002.

Hopkinson, R. F., Mckenney, D. W., Milewska, E. J., Hutchinson, M. F., Papadopol, P., and Vincent, A. L. A. (2011). Impact of aligning climatological day on gridding daily maximum-minimum temperature and precipitation over Canada. J. Appl. Meteorol. Climatol. 50, 1654–1665. doi:10.1175/2011JAMC2684.1.

Huang, J. A., Tardif, J. C., Bergeron, Y., Denneler, B., Berninger, F., and Girardin, M. P. (2010). Radial growth response of four dominant boreal tree species to climate along a latitudinal gradient in the eastern Canadian boreal forest. Glob. Chang. Biol. 16, 711–731. doi:10.1111/j.1365-2486.2009.01990.x.

Hutchinson, M. F., Mckenney, D. W., Lawrence, K., Pedlar, J. H., Hopkinson, R. F., and Canada, E. (2009). Development and Testing of Canada-Wide Interpolated Spatial Models of Daily Minimum-Maximum Temperature and Precipitation for 1961-2003 EWA MILEWSKA. journals.ametsoc.org 48, 725–741. doi:10.1175/2008JAMC1979.1.

James, G., Witten, D., Hastie, T., and Tibshirani, R. (2013). An introduction to statistical learning. Available at: https://link.springer.com/content/pdf/10.1007/978-1-4614-7138-7.pdf [Accessed June 11, 2020].

Kaplan, D., and Pruim, R. (2020). ggformula: Formula Interface to the Grammar of Graphics. Available at: https://github.com/ProjectMOSAIC/ggformula/issues [Accessed June 11, 2020].

Laamrani, A., Valeria, O., Bergeron, Y., Fenton, N., Cheng, L. Z., and Anyomi, K. (2014). Effects of topography and thickness of organic layer on productivity of black spruce boreal forests of the canadian clay belt region. For. Ecol. Manage. 330, 144–157. doi:10.1016/j.foreco.2014.07.013.

Lavoie, M., Harper, K., Paré, D., and Bergeron, Y. (2007). Spatial pattern in the organic layer and tree growth: A case study from regenerating Picea mariana stands prone to paludification. J. Veg. Sci. 18, 213–222. doi:10.1111/j.1654-1103.2007.tb02532.x.

Lavoie, M., Paré, D., Fenton, N., Groot, A., and Taylor, K. (2005). Paludification and management of forested peatlands in Canada: A literature review. Environ. Rev. 13, 21–50. doi:10.1139/a05-006.

McKenney, D. W., Hutchinson, M. F., Papadopol, P., Lawrence, K., Pedlar, J., Campbell, K., et al. (2011). Customized spatial climate models for Canada. Bull. Am. Meteorol. Soc. 92, 1611–1622. Available at: http://www.cfs.nrcan.gc.ca/pubwarehouse/pdfs/27373.pdf [Accessed June 14, 2019].

Nicault, A., Boucher, E., Tapsoba, D., Arseneault, D., Berninger, F., Bégin, C., et al. (2015). Spatial analysis of black spruce (Picea mariana (Mill.) B.S.P.) radial growth response to climate in northern Québec – Labrador Peninsula, Canada. Can. J. For. Res. 45, 343–352. doi:10.1139/cjfr-2014-0080.

O'Donnell, J. A., Romanovsky, V. E., Harden, J. W., and McGuire, A. D. (2009). The effect of moisture content on the thermal conductivity of moss and organic soil horizons from black spruce ecosystems in interior alaska. Soil Sci. 174, 646–651. doi:10.1097/SS.0b013e3181c4a7f8.

Plomion, C., Leprovost, G., and Stokes, A. (2001). Wood Formation in Trees Wood Formation in Trees. Plant Physiol. 127, 1513–1523. doi:10.1104/pp.010816.1.

Popkova, M. I., Vaganov, E. A., Shishov, V. V., Babushkina, E. A., Rossi, S., Fonti, M. V., et al. (2018). Modeled tracheidograms disclose drought influence on Pinus sylvestris tree-rings structure from Siberian forest-steppe. Front. Plant Sci. 9. doi:10.3389/fpls.2018.01144.

Puchi, P. F., Castagneri, D., Rossi, S., and Carrer, M. (2019). Wood anatomical traits in black spruce reveal latent water constraints on the boreal forest. Glob. Chang. Biol., gcb.14906. doi:10.1111/gcb.14906.

Rathgeber, C. B. K. (2017). Conifer tree-ring density inter-annual variability - anatomical, physiological and environmental determinants. New Phytol. 216, 621–625. doi:10.1111/nph.14763.

Ren, P., Ziaco, E., Rossi, S., Biondi, F., Prislan, P., and Liang, E. (2019). Growth rate rather than growing season length determines wood biomass in dry environments. Agric. For. Meteorol. 271, 46–53. doi:10.1016/j.agrformet.2019.02.031.

Rossi, S. (2015). Local adaptations and climate change: converging sensitivity of bud break in black spruce provenances. Int. J. Biometeorol. 59, 827–835. doi:10.1007/s00484-014-0900-y.

Rossi, S., Couture, É., Plante, X., and Morin, H. (2016). Fine roots and ectomycorrhizal colonization in black spruce subjected to reductions in soil moisture. Botany 94, 23–30. doi:10.1139/cjb-2015-0093.

Rossi, S., Deslauriers, A., Anfodillo, T., and Carraro, V. (2007). Evidence of threshold temperatures for xylogenesis in conifers at high altitudes. Oecologia 152, 1–12. doi:10.1007/s00442-006-0625-7.

Rossi, S., Girard, M.-J. J., and Morin, H. (2014). Lengthening of the duration of xylogenesis engenders disproportionate increases in xylem production. Glob. Chang. Biol. 20, 2261–2271. doi:10.1111/gcb.12470.

Rossi, S., Menardi, R., and Anfodillo, T. (2006). Trephor: a new tool for sampling microcores from tree stems. IAWA J. 27, 89–97. doi:10.1163/22941932-90000139.

Rossi, S., Morin, H., and Deslauriers, A. (2012). Causes and correlations in cambium phenology: Towards an integrated framework of xylogenesis. J. Exp. Bot. 63, 2117–2126. doi:10.1093/jxb/err423.

Sharratt, B. S. (1997). Thermal conductivity and water retention of a black spruce forest floor. Soil Sci. 162, 576–582. doi:10.1097/00010694-199708000-00006.

Shishov, V. V., Tychkov, I. I., Popkova, M. I., Ilyin, V. A., Bryukhanova, M. V., and Kirdyanov, A. V. (2016). VS-oscilloscope: A new tool to parameterize tree radial growth based on climate conditions. Dendrochronologia 39, 42–50. doi:10.1016/j.dendro.2015.10.001.

Simard, M., Lecomte, N., Bergeron, Y., Bernier, P. Y., and Paré, D. (2007). Forest productivity decline caused by successional paludification of boreal soils. Ecol. Appl. 17, 1619–1637. doi:10.1890/06-1795.1.

Skene, D. S. (1969). The Period of Time Taken by Cambial Derivatives to Grow and Differentiate into Tracheids in Pinus radiata: D. Don. Ann. Bot. 33, 253–262.

Touchan, R., Shishov, V. V., Meko, D. M., Nouiri, I., and Grachev, A. (2012). Process based model sheds light on climate sensitivity of Mediterranean tree-ring width. Biogeosciences 9, 965–972. doi:10.5194/bg-9-965-2012.

Turcotte, A., Morin, H., Krause, C., Deslauriers, A., and Thibeault-Martel, M. (2009). The timing of spring rehydration and its relation with the onset of wood formation in black spruce. Agric. For. Meteorol. 149, 1403–1409. doi:10.1016/j.agrformet.2009.03.010.

Turetsky, M. R., Mack, M. C., Hollingsworth, T. N., and Harden, J. W. (2010). The role of mosses in ecosystem succession and function in Alaska's boreal forest. Can. J. For. Res. 40, 1237–1264. doi:10.1139/X10-072.

Tychkov, I. I., Sviderskaya, I. V., Babushkina, E. A., Popkova, M. I., Vaganov, E. A., and Shishov, V. V. (2019). How can the parameterization of a process-based model help us understand real tree-ring growth? Trees - Struct. Funct. 33, 345–357. doi:10.1007/s00468-018-1780-2.

Vaganov, E. A. (Evgeniĭ A., Hughes, M. K., Shashkin, A. V. (Aleksandr V., and Hughes, M. K. (2006). Growth Dynamics of Conifer Tree Rings: Images of Past and Future Environments. Ecological. , ed. Springer-Verlag Berlin: Springer doi:10.1086/586955.

Vaganov, E. A. E. A. E. A. E., Anchukaitis, K. J. K. J. K. J., Evans, M. N., Evans, M. N., Evans, M. N., Evans, M. N., et al. (2011). "How Well Understood Are the Processes that Create Dendroclimatic Records? A Mechanistic Model of the Climatic Control on Conifer Tree-Ring Growth Dynamics," in Dendroclimatology. Developments in Paleoenvironmental Research (Springer, Dordrecht), pp 37-75. doi:https://doi.org/10.1007/978-1-4020-5725-0_3.

Vaganov, E. A., Hughes, M. K., Kirdyanov, A. V., Schweingruber, F. H., and Silkin, P. P. (1999). Influence of snowfall and melt timing on tree growth in subarctic Eurasia. Nature 400, 149–151. doi:10.1038/22087.

Waldron, K., Ruel, J. C., and Gauthier, S. (2013). The effects of site characteristics on the landscape-level windthrow regime in the North Shore region of Quebec, Canada. Forestry 86, 159–171. doi:10.1093/forestry/cps061.

Walker, X., and Johnstone, J. F. (2014). Widespread negative correlations between black spruce growth and temperature across topographic moisture gradients in the boreal forest. Environ. Res. Lett. 9, 064016. doi:10.1088/1748-9326/9/6/064016.

Wingler, A. (2015). Comparison of signaling interactions determining annual and perennial plant growth in response to low temperature. Front. Plant Sci. 5, 1–9. doi:10.3389/fpls.2014.00794.

Yang, B., He, M., Shishov, V., Tychkov, I., Vaganov, E., Rossi, S., et al. (2017). New perspective on spring vegetation phenology and global climate change based on Tibetan Plateau tree-ring data. Proc. Natl. Acad. Sci. U. S. A. 114, 6966–6971. doi:10.1073/pnas.1616608114.

Zhang, J., Gou, X., Zhang, Y., Lu, M., Xu, X., Zhang, F., et al. (2016). Forward modeling analyses of Qilian Juniper (Sabina przewalskii) growth in response to climate factors in different regions of the Qilian Mountains, northwestern China. Trees - Struct. Funct. 30, 175–188. doi:10.1007/s00468-015-1286-0.

Ziaco, E. (2020). A phenology-based approach to the analysis of conifers intra-annual xylem anatomy in water-limited environments. Dendrochronologia 59, 125662. doi:10.1016/j.dendro.2019.125662.

Ziaco, E., Truettner, C., Biondi, F., and Bullock, S. (2018). Moisture-driven xylogenesis in Pinus ponderosa from a Mojave Desert mountain reveals high phenological plasticity. Plant Cell Environ. 41, 823–836. doi:10.1111/pce.13152.

5.10 Acknowledgements

This work was funded by the NSERC Industrial Research Chair on Black Spruce Growth and the Influence of Spruce Budworm on Landscape Variability in Boreal Forests, the Canada Foundation for Innovation, le Consortium de Recherche sur la Forêt Boréale Commerciale, les Fonds de Recherche sur la Nature et les Technologies du Québec, and la Forêt d'Enseignement et de Recherche Simoncouche. VS, MP and IT were supported by the Russian Ministry of Science and Higher Education (projects #FSRZ-2020-0010 and #FSRZ-2020-0014) Special thanks are extended to D. McKenney and P. Papadopol for sharing their data set with the temperature and precipitation chronologies and to Murray Hay for verifying the English of the text.

5.11 Contribution statement

VB, SR, and VS conceived and planned the study. VB carried out the analysis and wrote the manuscript. MP provided the initial version of the script to compute the timing of wood formation with the VS model. MP, IT, and VS provided technical support for the analyses. VB, VS, MP, IT, SR, AD, MH, and HM contributed to the interpretation of the results. All authors commented and contributed to improve the initial draft of the manuscript

GENERAL CONCLUSIONS

To study the intra-annual patterns of tree-ring formation and their influence on tree-ring features, cell traits and micro-density were measured along with their underlying bud and wood formation dynamics through the observation of bud and wood phenology. The main objectives of this thesis were: 1) to investigate how bud and wood formation dynamics depend on the timing of carbon allocation patterns within trees, and how this timing affects cell anatomy and micro-density variations within the tree-ring, in addition to environmental factors influencing cell differentiation; 2) comparing wood formation dynamics and cell trait patterns observed in the field and as predicted by available modelling tools. The results of this thesis provide new insights on seasonal carbon allocation patterns within the C-sinks responsible of structural growth, and on their influence on wood formation and tree-ring features over a wide geographical scale. These results rely on an exceptionally long xylogenesis monitoring period (15 years) performed on black spruce (*Picea mariana* Mill. B.S.P.), a species of huge economic interest in North America (Rossi 2015).

6.1 Timing of bud and wood formation jointly modulate tree-ring intra-annual development

Through NDVI time-series and field observations of xylogenesis monitoring, we assessed the timing of photosynthetic and meristem activity. We observed a time-lag between the different phenological events, mirroring the different time periods for carbon allocation to bud and woody tissues growth (Chapter I). The onset of photosynthetic activity was estimated at the beginning of May, three weeks before the onset of bud development. In order to avoir early frorts, black spruce delays meristems resumption (Silvestro et al., 2019; Marquis et al., 2020), at the same time cumulating starch reseaves that will be used during bud burst (Heinrich et al.,2015). During spring, the increasing temperature enhances indeed the use of carbon reserves in plants, and a dose-dependent response modulate bud phenology according to carbon availability (Dhuli et al., 2014, Deslauriers et al.,2019).Latewood formation started in July, when shoot elongation was complete. Mean annual temperature was correlated with the onset of bud and wood phenology, but no correlation was observed with the phenological events in summer and autumn. In agreement with our hypothesis, shoot elongation and latewood formation occurred at different times during the growing season, thereby resulting in a delay between the onset of the photosynthetic activity and the peak of biomass allocation to the stem.

These results have important implications for carbon sequestration models that assess carbon storage in terrestrial ecosystems. Knowledge about the separation of the carbon fraction allocated into the canopy and into the stem are very important to estimate carbon storage and carbon turn-over in forest ecosystems (Friend et al. 2019). Furthermore, according to my results, it would be possible to estimate wood formation dynamics by observing bud phenology, since the first stage of bud development matches with the onset of earlywood formation. The ending of shoot elongation matches the start of latewood formation, whith large impacts on wood quality and carbon sequestration of the tree at that time of the year.

6.2 Wood formation dynamics are key drivers of the tree-ring features

Carbon signalling is a modulator of wood formation, whose dynamics affect the tree-ring cells' spatial pattern, thereby leading to the earlywood-latewood transition (Deslauriers et al. 2016, Cartenì et al. 2018, Buttò et al. 2019). Our results demonstrated that longer durations of cell enlargement and secondary wall deposition determine or influence cell traits in a non-linear fashion (Buttò et al. 2019) (Chapter II). Cell diameter and cell wall thickness linearly increase with the duration of their differentiation until reaching a plateau, after which they remain unchanged regardless of the duration of enlargement and cell wall thickening (Buttò et al. 2019).

Similar relationships between cell trait and their duration of differentiation were observed among the five study sites, indicating shared xylem formation dynamics across the entire latitudinal distribution of the species. The conservative nature of the relationship between tree-ring features and wood formation dynamics suggests that cell anatomy i.e. cell lumen and cell wall thickness could be more reliably predicted by their developmental dynamics than by their relationship with environmental factors.

The effects of environmental stimuli on tree growth and tree-ring features are usually studied at the margins of a species range, in sites characterized by extreme climatic conditions, where climatic signal is enphatized. Only few have studied sites located within the core of a species distribution (Gricar et al. 2015), where endogenous signalling could prevail the influence of external factors. Black spruce is a widespread species in North America, whose growth responses are characterized by complex patterns engendered by converging responses to environmental variables, thereby allowing this species to grow in different locations (Rossi 2015). The reliability of predictions about growth and wood production in black spruce could then greatly benefit from these results, and wood formation dynamics could be studied in other regions of Canada to map wood phenology in order to obtain a more

complete understanding of the mechanisms underlying wood production for this important species in the boreal forest.

6.3 Towards predictive and explanatory models of black spruce tree-ring growth

Our results point to endogenous signals as indispensable tools to explain both cell production and cell trait variation across the black spruce tree-ring. Under both controlled and natural conditions, we observed little variability in the xylem-related traits in black spruce wood. Relative to other species, black spruce adopts a very conservative growth strategy, resulting in an unexpected inertia in wood anatomy vis-à-vis induced or natural environmental change (Belien et al. 2012; Rossi et al., 2015; Balducci et al., 2016). However, in black spruce saplings growing under controlled condition, Balducci et al., 2016 demonstrated that the lack of change in xylem-cell traits after an imposed water stress was due to a counterbalancing effect between the duration and rate of cell differentiation. When exposed to treatments of water stress or temperature increase, black spruce saplings has been observed to counterbalancing the duration and rate of cell differentiation, finally resulting in similar anatomical features than control (Balducci *et al.*, 2016). We propose that black spruce trees, regardless of latitude, are capable of showing a highly plastic developmental response, achieving conservative cell traits by promptly modulating cell

differentiation at the intra-annual scale (Chapter III). By means of our analytical approach, we found that micro-density and cell traits display distinctive ecological correlations, furthering our understanding of the complex network underlying wood trait variation within the tree-ring (Chapter III). Black spruce micro-density was directly influenced by cell anatomy, especially cell wall thickness. Within the tree-ring, the increasing proportion of cell wall thickness over cell diameter determines the general pattern of tree-ring density that culminates in latewood (Preston et al. 2006, Björklund et al. 2017). Wood formation dynamics, i.e. the duration of cell enlargement and cell wall thickening, directly influence cell anatomy (Buttò et al. 2019, Ziaco 2020), and thus indirectly influence micro-density. Endogenous and exogenous signals explain the spatial pattern of cell anatomy within the tree-ring, leading to differences in micro-density (Rathgeber 2017). The effects of environmental factors on cell anatomy and micro-density were not additive, in agreement with Preston *et al.* (2006). This observation supports the assumption that wood density and cell anatomy display distinct patterns of ecological correlations, which explains how similar densities can be reached with different wall/lumen ratios. Based on a complete and detailed framework, we demonstrated the diverse effects of environmental factors on the xylem cell-traits and micro-density, that were so far only described on the basis of fragmented experimental approaches (Björklund et al. 2017, Rathgeber 2017). We observed that during wood formation, decreasing photoperiod

entails increasing micro-density, which was in turn positively affected by soil water content and temperature. All correlations between micro-density, cell anatomy and environmental factors have their specific ecological meaning, by influencing different aspects of cell differentiation, cell wall biosynthesis and metabolic activities (Chapter III).

6.4 Persectives for VS model as a predictive model of black spruce intra-annual growth dynamics

The opportunity to disentangle the effects of the main environmental factors on black spruce tree-ring growth makes very attractive the use of Vaganov–Shashkin (VS) model. Nonetheless, the results of this thesis demonstrate that realistic predictions of black spruce tree-ring growth dynamics entail the integration of endogenous signalling in the modelling framework (Chapter I,II,III). Such integration is not obvious when we consider that all algorithms underlying VS model are the based on the assumption that intra-annual growth dynamics are the result of the current environmental conditions (Vaganov, 2006). Furthermore, the mistmatch between simulated and observed soil water content (Chapter IV) indicates that VS model parameterization poorly suits the wet sites of the eastern Canada, when a massive quantive of water is released in spring due to snow melting (Rossi et al 2011).

We observed that simulated and observed tree-ring chronologies were well correlated, indicating that VS model could be used to predict black spruce cell production (Chapter IV). Being tree-ring width and number of tracheids functionally correlated (Camarero et al 1998), the application of the recent implementation of the cambial model block (Vaganov et al , 2011), recently proposed by Anchukaitis et al, (2020) could provide useful insights about climate change impacts on black spruce cell production.

6.5 Limits and perspectives of the thesis

With this thesis, I aimed to assess the general patterns of cell traits and wood density variation within the tree-ring under developmental and environmental control. These results strongly suggest that the integration of endogenous signals i.e. sugars allocation (Cartení et al 2018), and wood formation developmental dynamics are needed not only to reconstruct ealywood-latewood dynamics (Cuny et al., 2016), but also to simulate changes in wood density. Part of the variability in cell production and cell traits is indeed independent from environmental conditions, but depends on a foundamental signal that could be catched by integrating the basic physiological and development processes occurring within the tree. Finding this basic growth signal is necessary to obtain mechanistic tree-growth models that could be find a more general applicability.

Further studies are needed to investigate how the inter-annual variability, i.e. between tree-rings, of these variables affect cell traits and micro-density patterns. Indeed, I characterized black spruce wood formation dynamics in the eastern part of Canada, but there are elements suggesting that these responses could be different in western Canada. Indeed, wood formation dynamics in western regions are prone to the effect of drought, as suggested by Girardin et al. (2016), possibly entailing different responses and sensitivity to climate change in the future. Further studies are needed to map wood formation dynamics over the entire latitudinal and longitudinal distribution of black spruce, potentially providing new and reliable tools to predict present and future growth responses of this very important species.

Moreover, due to our experimental design, the detected tree growth–environment relationships are limited to the stand-level scale, preventing any interpretation of the importance of within or between individual variability. Indeed, trees sampled during the 15 years of xylogenesis monitoring changed, on average, each 5 years, in order to prevent trees damages linked to a long time period for sampling.

6.6 References

Anchukaitis, K.J., Evans, M.N., Hughes, M.K. and Vaganov, E.A., 2020. An interpreted language implementation of the Vaganov–Shashkin tree-ring proxy system model. Dendrochronologia, 60, p.125677.

Belien E, Rossi S, Morin H, Deslauriers A. 2012. Xylogenesis in black spruce subjected to rain exclusion in the field. Canadian Journal of Forest Research 42: 1306–1315.

Björklund J, Seftigen K, Schweingruber F, Fonti P, Arx G, Bryukhanova M V, Cuny HE, Carrer M, Castagneri D, Frank DC (2017) Cell size and wall dimensions drive distinct variability of earlywood and latewood density in Northern Hemisphere conifers. New Phytol 216:728–740.

Buttò V, Rossi S, Deslauriers A, Morin H (2019) Is size an issue of time? Relationship between the duration of xylem development and cell traits. Ann Bot 123:1257–1265. https://academic.oup.com/aob/advance-article/doi/10.1093/aob/mcz032/5381073 (22 May 2019, date last accessed).

Cartenì F, Deslauriers A, Rossi S, Morin H, De Micco V, Mazzoleni S, Giannino F (2018) The physiological mechanisms behind the earlywood-to-latewood transition: a process-based modelling approach. Front Plant Sci 9:1053.

Cuny HE, Rathgeber CBKK, Kiessé TS, Hartmann FP, Barbeito I, Fournier M (2013) Generalized additive models reveal the intrinsic complexity of wood formation dynamics. J Exp Bot 64:1983–94. http://www.ncbi.nlm.nih.gov/pubmed/23530132 (12 December 2016, date last accessed).

Deslauriers, A., Fournier, M.P., Cartenì, F. and Mackay, J., 2019. Phenological shifts in conifer species stressed by spruce budworm defoliation. Tree physiology, 39(4), pp.590-605.

Deslauriers A, Huang J-G, Balducci L, Beaulieu M, Rossi S (2016) The contribution of carbon and water in modulating wood formation in black spruce saplings. Plant Physiol:pp--01525.

Dhuli, P., Rohloff, J. and Strimbeck, G.R., 2014. Metabolite changes in conifer buds and needles during forced bud break in Norway spruce (Picea abies) and European silver fir (Abies alba). Frontiers in plant science, 5, p.706.

Friend AD, Eckes-Shephard AH, Fonti P, Rademacher TT, Rathgeber CBK, Richardson AD, Turton RH (2019) On the need to consider wood formation processes in global vegetation models and a suggested approach. Ann For Sci 76:49.

Girardin MP, Hogg EH, Bernier PY, Kurz WA, Guo XJ, Cyr G (2016) Negative impacts of high temperatures on growth of black spruce forests intensify with the anticipated climate warming. Glob Chang Biol 22:627–643.

Gricar, Jozica, Peter Prislan, Martin De Luis, Vladimir Gryc, Jana Hacurová, Hanuš Vavrčík, and Katarina Čufar (2015) Plasticity in variation of xylem and phloem cell characteristics of Norway spruce under different local conditions. Front Plant Sci 6:730.

Kong D, Zhang Y, Wang D, Chen J, Gu X (2020) Photoperiod explains the asynchronization between vegetation carbon phenology and vegetation greenness phenology. J Geophys Res Biogeosciences

Heinrich, S., Dippold, M.A., Werner, C., Wiesenberg, G.L., Kuzyakov, Y. and Glaser, B., 2015. Allocation of freshly assimilated carbon into primary and secondary metabolites after in situ 13C pulse labelling of Norway spruce (Picea abies). Tree physiology, 35(11), pp.1176-1191.

Camarero, J.J., Guerrero-Campo, J. and Gutiérrez, E., 1998. Tree-ring growth and structure of Pinus uncinata and Pinus sylvestris in the Central Spanish Pyrenees. Arctic and Alpine Research, 30(1), pp.1-10.

Preston KA, Cornwell WK, DeNoyer JL (2006) Wood density and vessel traits as distinct correlates of ecological strategy in 51 California coast range angiosperms. New Phytol 170:807–818.

Rathgeber CBK (2017) Conifer tree-ring density inter-annual variability - anatomical, physiological and environmental determinants. New Phytol 216:621–625. http://doi.wiley.com/10.1111/nph.14763

Rossi S (2015) Local adaptations and climate change: converging sensitivity of bud break in black spruce provenances. Int J Biometeorol 59:827–835. http://link.springer.com/10.1007/s00484-014-0900-y (11 July 2019, date last accessed).

Rossi, S., Morin, H. and Deslauriers, A., 2011. Multi-scale influence of snowmelt on xylogenesis of black spruce. Arctic, Antarctic, and Alpine Research, 43(3), pp.457-464.

Rossi S, Deslauriers A, Morin H (2003) Application of the Gompertz equation for the study of xylem cell development. Dendrochronologia 21:33–39.

Zhao M, He Z, Du J, Chen L, Lin P, Fang S (2019) Assessing the effects of ecological engineering on carbon storage by linking the CA-Markov and InVEST models. Ecol Indic 98:29–38.

Ziaco E (2020) A phenology-based approach to the analysis of conifers intra-annual xylem anatomy in water-limited environments. Dendrochronologia 59:125662. https://doi.org/10.1016/j.dendro